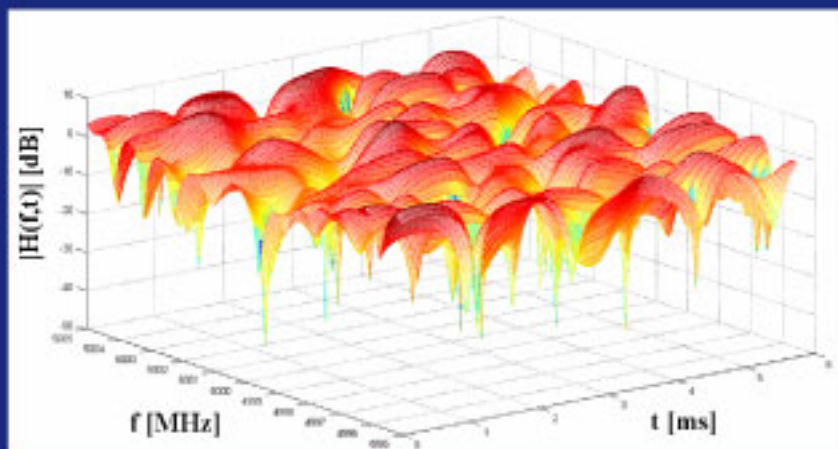


Benigno Rodríguez

# Differential STBC for OFDM based Wireless Systems



# Differential STBC for OFDM based Wireless Systems

Vom Promotionsausschuss der  
**Technischen Universität Hamburg-Harburg**  
zur Erlangung des akademischen Grades  
**Doktor-Ingenieur (Dr.-Ing.)**  
genehmigte Dissertation

von

**Benigno Rodríguez Díaz**

aus

**Montevideo, Uruguay**

2007

### **Bibliografische Information der Deutschen Nationalbibliothek**

Die Deutsche Nationalbibliothek verzeichnet diese Publikation in der Deutschen Nationalbibliografie; detaillierte bibliografische Daten sind im Internet über <http://dnb.ddb.de> abrufbar.

1. Aufl. - Göttingen : Cuvillier, 2007

Zugl.: (TU) Hamburg-Harburg, Univ., Diss., 2007

978-3-86727-459-3

1. Gutachter: Prof. Dr. rer. nat. Dr. h.c. Hermann Rohling

2. Gutachter: Prof. Dr.-Ing. Wolfgang Meyer

Tag der mündlichen Prüfung: 26. November 2007

© CUVILLIER VERLAG, Göttingen 2007

Nonnenstieg 8, 37075 Göttingen

Telefon: 0551-54724-0

Telefax: 0551-54724-21

[www.cuvillier.de](http://www.cuvillier.de)

Alle Rechte vorbehalten. Ohne ausdrückliche Genehmigung des Verlages ist es nicht gestattet, das Buch oder Teile daraus auf fotomechanischem Weg (Fotokopie, Mikrokopie) zu vervielfältigen.

1. Auflage, 2007

Gedruckt auf säurefreiem Papier

978-3-86727-459-3

**Benigno Rodríguez Díaz**

**Differential STBC for OFDM based  
Wireless Systems**



# Acknowledgements

I would like to express my sincere gratitude to Prof. Dr. Hermann Rohling for supervising my work during this time. I have enjoyed very much the possibility of discussing my ideas with him, receiving always very good advices. I have also appreciated very much his leadership qualities going far beyond of pure technical issues. I also thank Prof. Dr.-Ing. Wolfgang Meyer for serving as my external examiner and Prof. Dr. Herbert Werner for chairing the oral examination.

This thesis was written in the first 2.5 years of a 3 years doctorate program supported by the Programme Alban, the European Union Programme of High Level Scholarships for Latin America, scholarship No. (E04D036122UY). This support is also gratefully acknowledged.

I thank all my colleagues and the permanent staff in the department, specially to Rainer Grünheid, Lars Wischhof, Sonom Olonbayar and Christian Stimming for very interesting discussions and lot of support to start living in Germany. The integration in this group was something very simple and enjoyable.

I want to thank also Prof. Juan Mártony and Prof. Fernando Silveira from IIE, Faculty of Engineering, UDELAR for their support and direction in the realization of my postgraduate studies.

I am quite happy of having a large list of new friends in Hamburg to thank for their friendliness as Rodolfo, Sabrina, Paulina and Mateo, Pablo, Lara and Ethan, Andreas, Claudia and Clara, Richard and Claudia, Doris, Axel and Nadja, Max, etc.

Finally I thank my family for its permanent support and comprehension.

Hamburg, December 2007

Benigno Rodríguez Díaz

# Dedication

*To my family*

# Contents

<b>Abstract</b>	<b>VII</b>
<b>1 Introduction</b>	<b>1</b>
1.1 Wireless System Model . . . . .	2
1.2 Contributions and Structure of this Thesis . . . . .	3
<b>2 Mobile Radio Channel</b>	<b>7</b>
2.1 Introduction . . . . .	7
2.2 Propagation . . . . .	8
2.2.1 Propagation Mechanisms . . . . .	8
2.2.2 Propagation Models . . . . .	9
2.3 Additive White Gaussian Noise . . . . .	10
2.4 Path Loss and Shadowing . . . . .	11
2.5 Multipath Propagation . . . . .	13
2.5.1 Narrow Band (Frequency Nonselective Channel) . . . . .	16
2.5.2 Broadband (Frequency Selective Channel) . . . . .	18
2.5.3 Stochastic Models (WSSUS) . . . . .	20
<b>3 OFDM Based System Concepts</b>	<b>27</b>
3.1 Fundamentals . . . . .	27
3.1.1 Continuous Time Model . . . . .	29
3.1.2 Discrete Time Model . . . . .	34
3.2 OFDM System Applications . . . . .	36
3.2.1 Wi-Fi . . . . .	36
3.2.2 WiMAX . . . . .	38
<b>4 Channel Estimation in OFDM based Systems</b>	<b>41</b>
4.1 Pilot Aided Channel Estimation . . . . .	41
4.1.1 Scattered Pilots . . . . .	42
4.1.2 Training Symbols . . . . .	42
4.2 Decision Directed Channel Estimation . . . . .	45

4.2.1	Comparison between DDCE and PACE . . . . .	47
4.3	Differential Modulation, Incoherent Demodulation . . . . .	47
4.3.1	Differential Modulation in Time Direction for an OFDM System . . . . .	48
4.3.2	Differential Modulation in Frequency Direction for an OFDM System . . . . .	48
4.3.3	Comparison between Coherent and Incoherent Demodulation Schemes . . . . .	50
<b>5</b>	<b>Link Adaptation and Diversity</b>	<b>53</b>
5.1	Link Adaptation in OFDM Systems . . . . .	53
5.1.1	Selection of Best Subcarriers . . . . .	53
5.1.2	PHY Mode Selection . . . . .	54
5.1.3	Dynamic Fragmentation . . . . .	54
5.1.4	Subcarrier Specific Adaptive Modulation . . . . .	55
5.1.5	Joint Optimization DLC and PHY Layers . . . . .	55
5.1.6	Water-Filling . . . . .	55
5.2	Diversities . . . . .	59
5.2.1	Delay Diversity . . . . .	59
5.2.2	Frequency Diversity . . . . .	59
5.2.3	Spatial Diversity . . . . .	60
5.2.4	Time Diversity . . . . .	62
5.2.5	Multiuser Diversity . . . . .	63
5.2.6	Polarization Diversity . . . . .	63
<b>6</b>	<b>MIMO Systems</b>	<b>65</b>
6.1	MIMO Channel Models . . . . .	66
6.2	MIMO Channel Capacity . . . . .	68
6.3	MIMO-OFDM Systems . . . . .	72
<b>7</b>	<b>Differential Space Time Block Codes</b>	<b>75</b>
7.1	A New Class of DSTBC . . . . .	78
7.2	Influence of the PCM in this New Class of DSTBCs . . . . .	94
7.2.1	Analysis of a New PCM Scheme (PCM2) . . . . .	95
7.2.2	Conclusion about the Influence of Different PCMs . . . . .	98
7.3	System Performance in WSSUS Channels . . . . .	101
7.4	Proposed Technique with Receive Diversity . . . . .	112
7.5	Summary . . . . .	116

<b>8 Proposed Technique in a Coded System</b>	<b>117</b>
8.1 Convolutional Encoding . . . . .	117
8.2 Viterbi Decoder . . . . .	121
8.3 Performance of the Technique in a Coded System . . . . .	123
8.4 DSTBC, DSFBC and DSTFBC . . . . .	126
<b>9 Summary and Conclusions</b>	<b>129</b>
<b>A Doppler Profile</b>	<b>133</b>
<b>B Channel Model Based on COST 207 Project</b>	<b>137</b>
<b>C Viterbi Decoder Considerations</b>	<b>139</b>
List of Figures	148
List of Tables	149
List of Abbreviations	151
Bibliography	154
Index	163



# Abstract

Broadband wireless mobile data networks are an extremely important technical topic nowadays. These networks are probably the most convenient alternative for achieving the objective of providing and increasing connectivity and Internet access. For underdeveloped countries, these networks are an excellent alternative to diminish the so-called digital gap. For developed countries, they represent an opportunity to increase services, security and comfort.

Broadband wireless networks have been studied, considering their component modules, algorithms and also possibilities of interaction between them. This study was necessary to compare different technical alternatives and earn some knowledge about the related advantages and disadvantages. From this study the dominance of the Orthogonal Frequency Division Multiplexing (OFDM) transmission techniques became clear. It was also clear that multiple antenna (MIMO) systems are needed to guarantee high data rate transmission schemes. The combination between the OFDM transmission technique and multiple antenna MIMO systems is the key focus of this thesis. Robustness and bandwidth efficiency of new differential transmission techniques, improved by the use of diversities, in particular spatial diversity and the related advantages have been studied. Then the attention was focused in these areas, OFDM transmission technique in combination with a subcarrier wise processed differential and spatial diversity technique.

Differential modulation schemes have the advantage that any radio channel estimation procedure can be avoided which reduces the computation complexity dramatically. As a result of this work a new class of Differential Space Time Block Codes (DSTBCs) with high performance (lower bit error rate compared to some previously published techniques) has been proposed. The introduced technique is quite flexible and has still some potential for possible improvements (new modulation schemes, new power control mechanisms, etc.). The proposed technique was extensively tested in different

radio channel conditions, like AWGN, uncorrelated Rayleigh fading and WSSUS, showing always very good performance and system robustness. When it was tested in WSSUS channels, it was found that the relative improvement (compared with the use of a pure M-PSK modulation technique or another previously published technique) is still increased when the mobile terminal velocity is increased. This suggests that the proposed technique could be particularly attractive for high mobility scenarios.

In order to increase the system performance, higher spatial diversity order has been analyzed by using receive diversity. In this case a combining technique for DSTBCs has been proposed, equivalent to Maximum Ratio Combining (MRC) for coherent systems. Observe that the conventional MRC for coherent systems cannot be directly applied to DSTBCs, since an incoherent demodulation is considered, thus there is no direct channel information available at the receiver. Consequently, this new combining technique for DSTBCs has been developed within this work.

Finally the performance of the proposed technique in a channel coded system was analyzed, showing that in this case its use is also convenient. In this study also some information about time delay and complexity, associated with the use of convolutional channel coding, was provided, in order to judge the convenience of its use for a particular application.

# Chapter 1

## Introduction

Mobile communication systems have become a large importance for everyone in our society, which can be observed by the worldwide use of mobile phones for voice communication. New services like video streaming and web browsing will require large data rates for future systems and applications.

Therefore the objective of this thesis is to contribute with new modules or techniques for broadband wireless networks based on the Orthogonal Frequency Division Multiplexing (OFDM) transmission technique, Multiple Input Multiple Output (MIMO) antenna systems and Spatial Time Block Codes (STBCs) modulation schemes. For achieving this purpose a deep study of related wireless systems was carried out. Also the wireless channel was studied, considering different available models and channel estimation techniques usually used in this kind of systems. Several techniques, extremely important for wireless broadband communication systems have been also considered.

The thesis content considers systems with extremely high data rate and Bandwidth Efficiency (BE). Therefore a system with multiple transmit and multiple receive antennas (MIMO) is analyzed. To increase the data rate performance, Amplitude and Phase Shift Keying (APSK) modulation techniques will be considered instead of pure PSK schemes. Due to the radio channel and the multipath propagation inside the radio channel, the OFDM transmission technique will be used. The particular good performance of OFDM systems in multipath fading environments was one important reason for this decision. Once the combination MIMO-OFDM between transmission and antenna systems was selected, the next step was to cope with the complexity of channel estimation in MIMO systems. Due to the computation complexity of all radio channel estimation procedures a differential

modulation technique was considered. Then it was proposed to study a new Differential Space Time Block Code (DSTBC) technique, which offers very good performance at high BE, keeping the system complexity at low level.

## 1.1 Wireless System Model

Here the basic wireless scheme considered in this thesis is introduced. It is well known that wireless communication systems have a large range of different applications, they are present in Personal Area Network (PAN), where the distances between transmitter (Tx) and receiver (Rx) are only few meters and also in satellite systems, where the distances are tens of thousands km. But basically, the majority of them can be described in some way similar to the block diagram shown in Fig. 1.1.

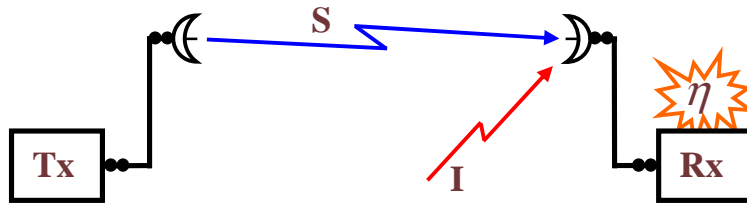


Figure 1.1: Scheme of a wireless system.

In this figure, several of the main components of a general wireless system can be seen. Tx, is the transmitter device, commonly each telecommunication device has integrated one or several transmitters and receivers. A single transmitter (Tx) is connected in this case to a single receiver (Rx).

Tx takes the data to transmit and applies over them a number of procedures in order to improve the transmission quality over the corresponding radio channel. For example in a wireless system some typical modules are the channel encoder, the interleaver, the modulator, and the amplifier.

Connectors, cables and antennas are very important topics in wireless systems, but their analysis is out of the scope of this thesis. In particular a good knowledge of antenna parameters is extremely important for a good radio link design. Antenna design is one very active research topic and the variety of existent devices is incredibly big, going from very small patch antennas to antennas of tens of meters (as the ones used in radio astronomy) [1].

The *radio channel* is probably the main challenge in wireless system design and specially in mobile wireless systems, because of its great variations with time and frequency. Due to these variations, special techniques have to be used, in other case the performance will not be acceptable. Several channel models are presented in Chapter 2. In this thesis the frequency bands Ultra High Frequency (UHF) (0.3-3 GHz) and Super High Frequency (SHF) (3-30 GHz) are mainly considered.

The *receiver* processes the received signal coping with the *noise* ( $\eta$ ) and the *interference* ( $I$ ) if it exists. Basically the Rx performs the reverse operations of those made in the Tx.  $S$  in Fig. 1.1 represents the signal (message) sent from the transmitter to the receiver.

In the following chapters, the elements presented here will be analyzed in more detail.

## 1.2 Contributions and Structure of this Thesis

Several possible new techniques for broadband wireless systems have been studied and rigorously tested. One new approach for the use of DSTBC systems was considered and a new class of DSTBCs was proposed. The performance and the robustness of this technique is very good, among the best reported up to now -as far as the author knows- and it is still quite simple to be implemented (see Section 7.1). The performance of this technique was verified over different channel models, showing always an excellent performance and system robustness. Then a possible improvement was proposed (see Section 7.2.1). When the proposed technique was tested in WSSUS channels, it was found that the relative improvement (relative to some previously published techniques) is increased, when the mobile terminal velocity is increased. Later the increment of spatial diversity by increasing the number of receive antennas has been considered. In this case, a technique equivalent to Maximum Ratio Combining in coherent systems, was developed for DSTBCs. Finally the performance of the proposed technique in a channel coded system was evaluated.

This thesis is structured into 9 chapters as follows:

*Chapter 1.* In this chapter the main goals and the description of the considered wireless system model were introduced.

*Chapter 2.* Wireless channel concepts and models are discussed in this chapter. It is essential because the wireless channel is probably the most important challenge to cope with in wireless systems. In particular the *AWGN*, *uncorrelated Rayleigh fading* and *WSSUS* channel models used for analyzing the proposed technique are presented.

*Chapter 3.* OFDM, the transmission technique behind the most successful Wi-Fi and WiMAX standards, is the area where the contributions of this thesis were focused. OFDM is a particularly promising technique due to robust behavior in frequency selective channels. In this chapter a description of the technique and its models is presented.

*Chapter 4.* An analysis of different channel estimation techniques is presented in this chapter. Normally this is the way to cope with wireless channels when coherent demodulation schemes are used. This chapter makes a review of some well known channel estimation techniques and their complexities; also allows to appreciate the saved complexity by using differential modulation schemes, where channel estimation is not necessary.

*Chapter 5.* Usually the wireless channel is so variable, that only by being very flexible and well adapted to the channel conditions, the best performance that they allow can be achieved. For this reason this chapter is dedicated to the analysis of some well known techniques as link adaptation and diversity. The proposed technique is a space diversity technique, kind of diversity carefully explained in this chapter. The other presented techniques allow a comparison of advantages, disadvantages and also of complexity level.

*Chapter 6.* Multiple Input Multiple Output (MIMO) systems allow a very important improvement of performance by exploiting space diversity. Some aspects of MIMO techniques are discussed in this chapter in order to show the potential of these techniques, which is shared by the proposed technique.

*Chapter 7.* The DSTBCs are presented and also a new class of them is proposed, which is the main contribution of this thesis. In this chapter is explained and evaluated in a detailed way the proposed technique.

*Chapter 8.* In this chapter the convolutional channel coding technique is described and later used to evaluate the proposed technique in a channel coded system.

*Chapter 9, Summary and Conclusions.* Here the main contributions of this work are summarized and discussed.



# Chapter 2

## Mobile Radio Channel

### 2.1 Introduction

The main challenge of wireless channels is their high degree of variability in the direction of time and in the direction of frequency (frequency selectivity). This degree of variability is highly increased when mobility is considered. In this case, a big effort is done to achieve an acceptable performance over variable channels. These efforts are not for free, they have an important cost in redundancy and signal processing. For example, in Global System for Mobile communication (GSM) systems, approximately 20 % overhead is spent for channel estimation purposes [2]. In this case the channel is estimated approx. 250 times per  $s$ ; that means that if a car is moving at 100  $km/h$  while somebody is using a mobile phone inside, the channel is being evaluated approximately each 11  $cm$  of displacement. That is necessary for being able of using a variable channel.

A lot of effort is made to improve all the techniques associated with a better use of frequency resources, what makes that those topics as channel estimation, channel correction, channel coding, link adaptation, etc. are in continuous development.

For any wireless system, the reception of the signal through different paths usually causes some inconveniences known as *multipath fading*. For mobile radio channel is also added the extra difficulty of having shifts in the frequencies due to the relative movement between transmitter and receiver; that shifts are due to *Doppler effect*. The analysis of the mobile radio channel will be started by considering the main propagation mechanisms and the most common channel models.

## 2.2 Propagation

A good basis for the comprehension of the mobile radio channel is the knowledge of the main propagation mechanisms in wireless communications.

### 2.2.1 Propagation Mechanisms

Basically can be distinguished four *propagation mechanisms*: *reflection, transmission, diffraction and scattering*.

*Reflection* happens when an electromagnetic wave coming from a media 1 impacts over a surface dividing this media from a media 2; then appears a reflected wave (in media 1) and a transmitted (or also called refracted) wave (in media 2). For having a reflection of a wave in a given surface, the dimensions of the surface has to be larger than the wavelength. It is also necessary to have a smooth surface, in other case a scattering mechanism would occur. Under certain conditions, the reflected or the transmitted wave can be null. Considering a wireless communication system as the one described in Fig. 1.1, generally the reflected waves generated by this procedure (reflection in different surfaces) constitute an important percentage of the signal power received by a Rx antenna.

Being the main path for the transmitted signal the segment of straight line between the Tx and Rx antennas (line of sight path), the reflection of the transmitted signal in different surfaces provides to the radio link of alternative paths (no line of sight paths) to reach the Rx antenna. That causes a well known effect in wireless communications called multipath fading, which will be discussed later.

*Transmission* mechanism allows that an electromagnetic wave (the transmitted signal) can reach the Rx antenna after passing through some objects. Usually in this passage through the objects the signal loses a certain level of energy, but in some cases it can even reach the Rx antenna with a considerable good level of energy.

*Diffraction* appears when between the Tx and Rx there is an object with edges or sharp irregularities. Typical in an urban scenario the edges of buildings cause diffraction. This mechanism allows a “bending” of the wave around the obstructor building making it possible to reach a Rx antenna behind it in a situation where no line of sight exists.

The diffraction can be explained by Huygen’s principle, that basically states that: “all points on a wavefront can be considered as point sources for the production of secondary wavelets, and that these wavelets combine to produce a new wavefront in the direction of propagation” [3]. The electromagnetic field resulting of the diffracted wave can be obtained as the sum of the field components of all the secondary wavelets around the object. This mechanism is particularly interesting by allowing for example the propagation of waves around the curved surface of the earth and reaching Rx antennas out of the line of sight. For sure the received power is very small in these cases but often it is still useful to receive the message.

*Scattering* appears when a wave impacts over a rough surface, then the reflected energy is spread in several directions. In Fig. 2.1, a representation of these four propagation mechanisms is shown.

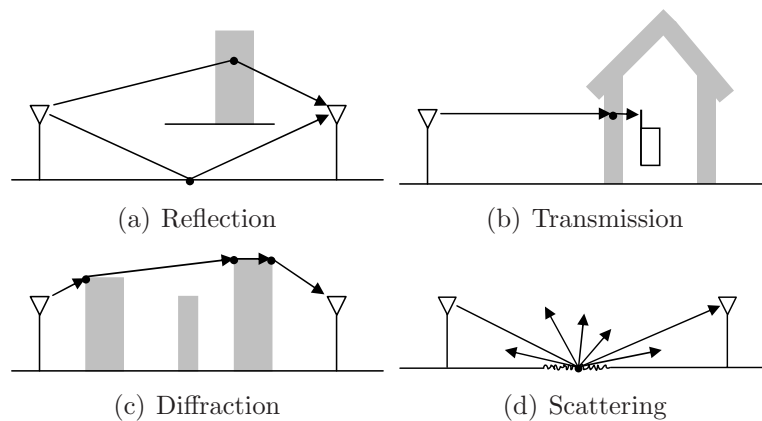


Figure 2.1: Propagation Mechanisms.

### 2.2.2 Propagation Models

Concerning fading models, two quite different kinds of models can be distinguished: “*large scale*” and “*small scale*” fading models which have a very different behavior. They are also referred as slow and fast fading respectively.

“*Large scale*” fading models are those which predicts the mean signal strength for a given distance (usually large, several hundreds or thousands meters) between the transmitter (Tx) and the receiver (Rx).

“*Small scale*” fading models are those which characterize the rapid fluctuations of the received signal strength over short distances (some wavelengths) or short time durations (some seconds). The signal arrives by several ways, since the phases are random the sum of the contributions varies widely. In small scale fading the received signal power may vary by as much as three or four orders of magnitude (30 or 40 dB) when the Rx is moved only a fraction of wavelength [3].

These propagation models can be explained in function of the propagation mechanisms described in Section 2.2.1 and the *Free Space Loss* (see Section 2.4).

## 2.3 Additive White Gaussian Noise

The noise in telecommunications can be classified basically in two classes: *man made noise* and *natural noise*. *Man made noise* has many sources, e.g. spark-plug ignition of vehicles, radiated electromagnetic waves, etc. *Natural noise* is caused for natural elements as the atmosphere, the sun, etc., but also for electrical components in the telecommunication equipment. This source of *natural noise* is known as *thermal noise* or *Johnson noise*.

The *thermal noise* is caused by thermal motion of electrons in dissipative element [4], [5]. Considering that a normal receiver has several dissipative components as resistors and wires, it is always present in normal receivers and it is one cause of performance degradation.

The adjective *additive* means that the noise signal  $n(t)$  is superimposed or added to the signal  $s(t)$ . There are not multiplicative mechanisms for example. Then the received signal  $r(t)$  will be

$$r(t) = s(t) + n(t) \quad (2.1)$$

That the thermal noise is “*white*” means that it has the same spectral characteristics for all the frequencies, it has a flat spectrum. The idea of “white” comes from the light, where the “white” light contains all the frequencies in the visible range with the same amount of power.

Thermal noise can be described as a zero mean Gaussian random process  $n(t)$ . Then the probability density function (pdf) of the random noise vari-

able  $n$  for any arbitrary time  $t$  is

$$pdf(n) = \frac{1}{\sigma\sqrt{2\pi}} e^{-\frac{1}{2}\left(\frac{n}{\sigma}\right)^2} \quad (2.2)$$

where  $\sigma^2$  is the variance of  $n$ .

The *Gaussian* distribution is usually used as the system noise model because of the *central limit theorem*. This theorem basically states that the probability distribution of the sum of  $N$  statistically independent random variables approaches to the Gaussian distribution when  $N \rightarrow \infty$ , independently of the individual distribution functions [6].

Considering this result, no matter that individual noise mechanisms can have a different distribution than the Gaussian one, the sum of several of them will have a probability distribution approximately equal to a Gaussian distribution [7].

In this way can be understood the physical origin and mathematical approach for the well known and extensively used Additive White Gaussian Noise (AWGN) model. Considering that thermal noise is present in all telecommunication systems and usually it is the most important source of noise on them, it is reasonable to use the characteristics of thermal noise (additive, white, Gaussian) to model the noise in telecommunications.

## 2.4 Path Loss and Shadowing

*Path loss* is the reduction of the power density (attenuation) of an electromagnetic wave along its propagation. One important effect responsible of *large scale* path loss is the natural dispersion of the radiated power due to *Free Space Loss* [1].

*Shadowing* is caused by obstacles between the transmitter and the receiver that attenuate the power through *absorption* of energy during the *transmission* through the object, *reflection*, *diffraction* and *scattering*.

While significant variations in attenuation for *large scale path loss* occurs over large distances (100-1000 m) the variations due to *shadowing* occurs for intermediate distances (10-100 m) which are related to the length of the obstructing object.

## Path Loss

The *path loss* of the channel can be defined [8] as the ratio between the transmit ( $P_t$ ) and receive ( $P_r$ ) power, it is

$$L = \frac{P_t}{P_r} \quad (2.3)$$

in *decibels*

$$L_{dB} = 10 \log_{10} \left( \frac{P_t}{P_r} \right) \quad (2.4)$$

Theory and practical measurements show that *path loss* can be expressed as

$$\bar{L}(d) = \bar{L}(d_0) \cdot \left( \frac{d}{d_0} \right)^n \quad (2.5)$$

where  $\bar{L}(d)$  is the average value of the attenuation around a certain distance  $d$  between transmit and receive antenna. In order to remove the influence of *small scale* factors (multipath), the empirical measurements to average are taken at a given distance  $d$  over several wavelengths.  $d_0$  is a reference distance where the attenuation is  $\bar{L}(d_0)$ . This attenuation is calculated with the same technique previously explained to make the average.  $n$  is known as *path loss exponent*. It depends on the environment and usually varies in  $2 \leq n \leq 6$  according to Table 2.1.  $\bar{L}(d)$  in *decibels* is

$$\overline{L_{dB}}(d) = \overline{L_{dB}}(d_0) + 10 \cdot n \cdot \log_{10} \left( \frac{d}{d_0} \right) \quad (2.6)$$

## Path Loss plus Shadowing

To integrate the effect of *shadowing* in (2.6), the term  $X_\sigma$  is added.

$$L_{dB}(d) = \overline{L_{dB}}(d) + X_\sigma = \overline{L_{dB}}(d_0) + 10 \cdot n \cdot \log_{10} \left( \frac{d}{d_0} \right) + X_\sigma \quad (2.7)$$

$X_\sigma$  is a zero-mean Gaussian distributed random variable (in dB) with standard deviation  $\sigma$  (also in dB). Then  $X_\sigma$  introduces a normal (Gaussian) variation around the value given by pure *path loss*. In a linear scale the *path loss* ( $L(d)$ ) is

$$L(d) = 10^{\frac{\overline{L_{dB}}(d_0)}{10}} \cdot \left( \frac{d}{d_0} \right)^n \cdot 10^{\frac{X_\sigma}{10}} \quad (2.8)$$

Table 2.1: Path Loss Exponents for different Environments [3].

Environment	Path Loss Exponent (n)
Free Space	2
Urban area cellular radio	2.7 to 3.5
Shadowed urban cellular radio	3 to 5
In building line of sight	1.6 to 1.8
Obstructed in building	4 to 6
Obstructed in factories	2 to 3

Where the term  $10^{\frac{x\sigma}{10}}$  (with *log-normal distribution*) shows the influence of *shadowing* in the *path loss*.

Fig. 2.2 illustrates the influences of *path loss*, *shadowing* and *multipath propagation* over the ratio between receive and transmit power in dB. There are several empirical *path loss* models to have in account the attenuations discussed in this section. In outdoor environments can be mentioned: Okumura model [9] for signal prediction in large urban macrocells, Hata model [10] which is an empirical formulation of the graphical data provided by Okumura, what simplifies the *path loss* calculation, COST 231 [11] which is an extension of Hata model, etc. Also can be mentioned specific contributions as a model developed by Walfish and Bertoni for diffraction from rooftops and buildings in cellular systems [12].

In indoor environments, [13], [14], [15] and [16] can be mentioned; there studies and measurements about attenuation in indoor propagation are provided.

## 2.5 Multipath Propagation

In this section, a classification of different models for the mobile radio channel is done in order to show some of the generally used scenarios.

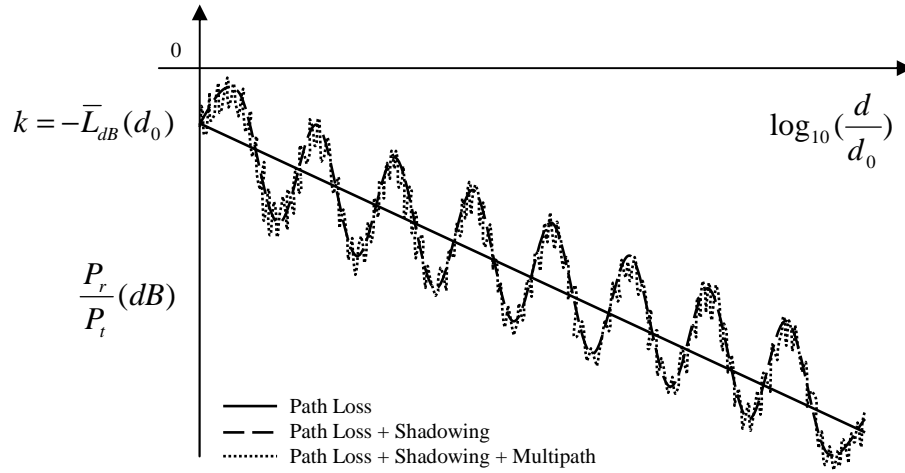


Figure 2.2:  $(\frac{P_r}{P_t})_{dB}$  versus  $d$  for “*path loss*”, “*path loss+shadowing*” and “*path loss+shadowing+multipath propagation*”.

### Multipath Fading Channels

*Multipath fading* is the signal fading caused by multipath propagation. In Fig. 2.3 can be observed a stationary terminal and several different path through which the signal reaches the terminal. Given that each path has a particular length and the propagation velocity is the same for all the paths (in the same media) the arrival time for each path is different. It means that one transmitted signal is going to arrive to the receiver with different time delays. It produces a kind of interference known as *Multipath fading*.

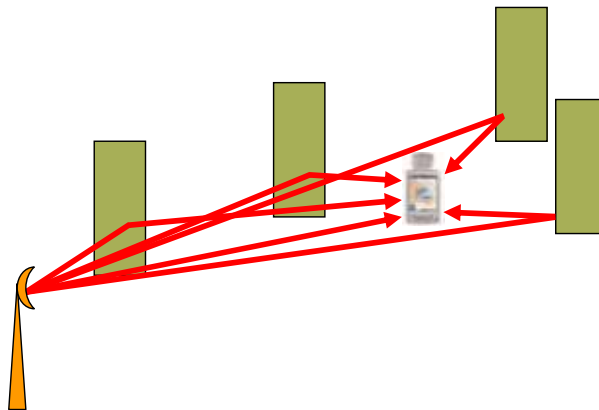


Figure 2.3: Multipath fading for a stationary terminal.

For *Time-invariant* channels with multipath fading the channel impulse response  $h(t)$  at a certain location can be written as:

$$h(t) = \sum_{p=1}^P h_p \cdot \delta(t - \tau_p) \quad (2.9)$$

where:  $h_p$  depends on path length, reflection coefficient, etc. and  $\tau_p$  is the time delay associated to the path  $p$ .

In *Time-variant* channels, for a given time  $t$  we will have a given *time-variant impulse response*  $h(\tau, t)$  as a function of  $\tau$ . Due to the fact that in a Time-variant Channel, the paths and its influence change with  $t$ , we will have different impulse response functions for each different time  $t$ ; as shown in Fig. 2.4.

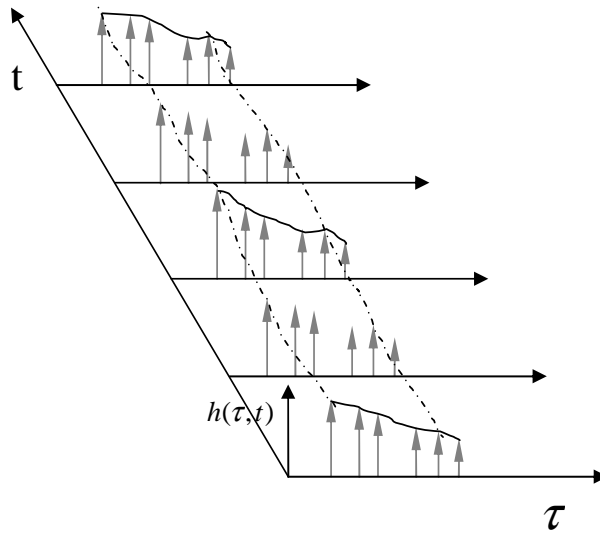


Figure 2.4: Representation of  $h(\tau, t)$ .

One parameter to characterize these channels is the Power Delay Profile (PDP), it is the expected value of the received power at a certain delay  $P(\tau) = E_t[|h(\tau, t)|^2]$ .

These variations in  $h(\tau, t)$ , very well known in mobile scenarios, are observed in the envelop of the received signal as two effects: *fast fading* and *slow fading*. *Fast fading* is mostly due to the quick variations on the phases

of the different paths and looks like very quick and important variations in the envelope of the received signal. While *slow fading* is related with the variations in the set of reflection points that determine the more important paths and produce a slow variation in the envelope of the received signal.

Quite often, *multipath fading* channels are modelled as a WSSUS process (see Section 2.5.3.1 on page 23).

## 2.5.1 Narrow Band (Frequency Nonselective Channel)

### 2.5.1.1 Multipath Propagation Deterministic Models

Considering a fixed multipath scenario, (2.10) can be used to explain how the received signal  $r(t)$  results from the superposition of several “versions” of the signal, received through different paths. Each path ( $p$ ) produces a different attenuation, phase shift and time delay ( $\tau_p$ ) over the transmitted signal when it arrives to the receiver.

$$r(t) = \sum_{p=1}^P h_p \cdot s(t - \tau_p) \quad (2.10)$$

This model can be used for a fixed multipath scenario in order of having a deterministic calculation of the received signal.

Considering a mobile scenario, for using (2.10) it should be necessary to actualize the information for each path in an almost continuous way, due to the variation that they experiment when the relative position between Tx and Rx is modified and the Doppler effect (see Appendix A). This could be possible but extremely complicated and inefficient. More than that, if this was done, the obtained results will be only valid for the particular considered scenario. For these reasons when mobile scenarios are considered a better approach is to use stochastic models. The stochastic models offer samples of the channel between Tx and Rx as a random variable, what assures that not one particular scenario is considered, but more than that all the possible particular scenarios with their probabilities are considered. That is a much better way of evaluating the performance of systems which are going to operate in different scenarios.

### 2.5.1.2 Multipath Propagation Stochastic Models

Basically we can distinguish between two situations, one where there is “*No Line Of Sight*” (NLOS) and another one where there is “*Line Of Sight*”

(LOS). The first situation happens when there is no direct view between Tx and Rx and the communications between them exist only through indirect paths. In this case we can say that we are in presence of a *NLOS* or *Rayleigh* channel. The second one happens when the Tx and Rx can see each other directly in presence of a *LOS* or *Ricean* channel. These two models are discussed in the following section.

### Rayleigh Fading Channels

For channels with *NLOS* the “*Rayleigh distribution*” is used; it has the following “*probability density function*” (PDF):

$$p(r) = \begin{cases} \frac{r}{\sigma^2} \cdot e^{-\frac{r^2}{2\sigma^2}} & (0 \leq r \leq \infty) \\ 0 & (r < 0) \end{cases} \quad (2.11)$$

Where:  $r$  is the received signal envelope voltage.  $\sigma$  is the rms value of the received voltage signal before envelope detection [3].  $\sigma^2$  is the time average power of the received signal before envelope detection.

The envelope of the sum of two quadrature zero mean Gaussian noise signals obeys a Rayleigh Distribution.

### Ricean Fading Channels

For channels with *LOS* the “*Ricean distribution*” is used, it has the following PDF:

$$p(r) = \begin{cases} \frac{r}{\sigma^2} \cdot e^{-\frac{(r^2+A^2)}{2\sigma^2}} \cdot I_0\left(\frac{A \cdot r}{\sigma^2}\right) & (A \geq 0, r \geq 0) \\ 0 & (r < 0) \end{cases} \quad (2.12)$$

Where:  $A$  is the “peak amplitude” of the “dominant signal” (direct path).  $I_0(x)$  is the “modified Bessel function of the first kind and zero order”.  $\sigma^2$  is the average power of all *NLOS* paths.

One parameter to characterize the Rice distribution is the “*Ricean factor*” defined as:  $k = \frac{A^2}{2\sigma^2}$  or  $k(\text{dB}) = 10 \log\left(\frac{A^2}{2\sigma^2}\right)$  in dB. Observe that when  $A \rightarrow 0$  then Ricean factor tends to 0 (or  $-\infty$  dB) and the Ricean distribution turns into a Rayleigh one.

## 2.5.2 Broadband (Frequency Selective Channel)

### 2.5.2.1 Time-invariant Systems

One channel is said *time invariant* if its channel frequency response  $H(f)$  does not change over the time.

For a broadband channel in the context of multipath propagation, the model described in (2.9) can be used if the movement of the mobile station and the environment (e.g., vehicles) can be neglected (assuming also a fixed base station). This situation is rarely found in reality but such a channel model can be used as an approximation for a WLAN in an office environment or in a Wireless Local Loop (WLL) application in which mobility is not required.

Then for a *time invariant* channel, the channel impulse response (as it was written in (2.9)) is

$$h(t) = \sum_{p=1}^P h_p \cdot \delta(t - \tau_p) \quad (2.13)$$

Where  $h_p$  is the channel gain coefficient affecting the path  $p$  and  $\tau_p$  is the time delay associated to the path  $p$ .

and the channel frequency response will be

$$H(f) = F\{h(t)\} = \sum_{p=1}^P h_p \cdot e^{-j2\pi f\tau_p} \quad (2.14)$$

But as it was said this model is only applicable to very few real situation, a much more general model is the one for time-variant systems.

### 2.5.2.2 Time-variant Radio Channel

This kind of radio channel assumes that there are variations in the *channel impulse response*. As a first approach these channels can be described as Linear Time Variant (LTV) systems. A LTV system can be represented as it is shown in Fig. 2.5.

Usually these systems are characterized by one of the following functions  $h(\tau, t)$ ,  $H(f, t)$ ,  $V(\tau, f_D)$  and  $U(f, f_D)$  (*system functions*). Where  $h(\tau, t)$  is the *Time-variant Impulse Response*, this is the response of the system in time  $t$  corresponding to a Dirac impulse in time  $t - \tau$ .

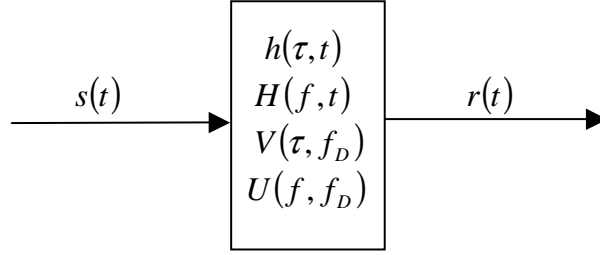


Figure 2.5: Linear Time-variant systems.

$H(f, t)$  is the *Time-variant Transfer function* which can be obtained by applying the *Fourier Transform* to  $h(\tau, t)$ , that is

$$H(f, t) = \int_{-\infty}^{+\infty} h(\tau, t) e^{-j2\pi f\tau} d\tau = F_{\tau}(h(\tau, t)) \quad (2.15)$$

$V(\tau, f_D)$  is the *Delay-Doppler function* which can be obtained as

$$V(\tau, f_D) = \int_{-\infty}^{+\infty} h(\tau, t) e^{-j2\pi f_D t} dt = F_t(h(\tau, t)) \quad (2.16)$$

$U(f, f_D)$  is the *Frequency-Doppler function* which can be obtained as

$$U(f, f_D) = \int_{-\infty}^{+\infty} H(f, t) e^{-j2\pi f_D t} dt = F_t(H(f, t)) \quad (2.17)$$

these last two functions are not so much used as the first two, but they are also a way of characterizing a LTV system. The relation between these four functions is summarized in Fig. 2.6, there it can be seen how to obtain these functions from the others, just by applying the *Fourier Transform* or the *Inverse Fourier Transform*.

For obtaining the received signal  $r(t)$  by working with  $h(\tau, t)$  we make the *convolutional product* of the transmitted signal  $s(t)$  with the *Time-variant Impulse Response* over the variable  $\tau$ .

$$r(t) = s(t) * h(\tau, t) \quad (2.18)$$

what is

$$r(t) = \int_{-\infty}^{+\infty} s(t - \tau) h(\tau, t) d\tau \quad (2.19)$$

Another common example of the use of these functions is to obtain the spectrum  $R(f, t)$  of the received signal. It can be simply obtained by making

$$R(f, t) = S(f, t) \cdot H(f, t) \quad (2.20)$$

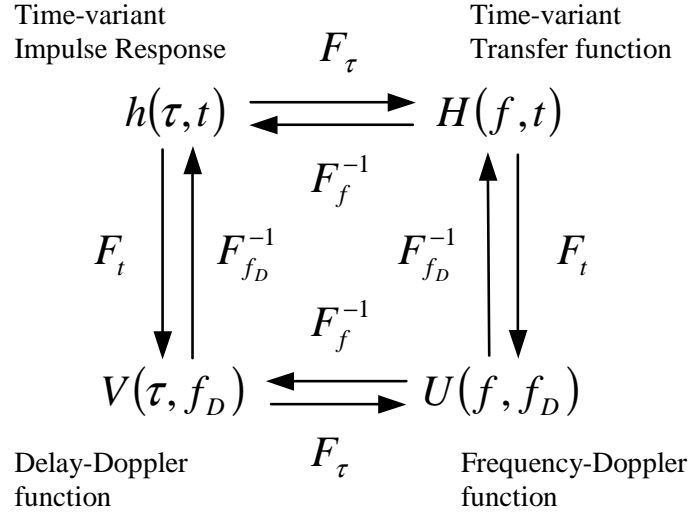


Figure 2.6: Linear Time-variant functions.

Considering the natural complexity of a real environment plus the very high variation in the channel behavior due to mobility, usually this description as a LTV system is not adequate. None deterministic description is adequate in these cases, then a stochastic model can be used to describe the channel behavior.

### 2.5.3 Stochastic Models (WSSUS)

When Channel Impulse Response cannot be predicted in a deterministic way (e.g., in mobile radio channels) stochastic models are used. In this case the radio channel is described by its statistical properties. More precisely the channel is defined by the *autocorrelation function of the channel impulse response* ( $\Phi_h$ ), where the channel impulse response is  $h(\tau, t)$ .

$$\Phi_h(\tau_1, \tau_2, t_1, t_2) = E[h(\tau_1, t_1)h^*(\tau_2, t_2)] \quad (2.21)$$

We can look for a simplification of this description by using the following two assumptions:

1.- The channel can be categorized as Stationary in the Wide Sense (WSS). That means that  $h(\tau, t)$  is invariant under short time translations. More precisely the autocorrelation function (ACF) of the channel impulse

response depends on the difference between  $t_1$  and  $t_2$  ( $\Delta t = t_2 - t_1$ ). Then (2.21) can be expressed as:

$$\Phi_h(\tau_1, \tau_2, \Delta t) = E[h(\tau_1, t)h^*(\tau_2, t + \Delta t)] \quad (2.22)$$

2.- The amplitudes and phases of the different paths should be uncorrelated, it is called “uncorrelated scattering” (US). Then the ACF of the impulse response disappears when  $\tau_1 \neq \tau_2$  and the radio channel is defined by

$$\Phi_h(\tau, \Delta t) = E[h(\tau, t)h^*(\tau, t + \Delta t)] \quad (2.23)$$

When a radio channel fulfils these conditions we can say that the channel is a Wide Sense Stationary Uncorrelated Scattering (WSSUS) channel.

The WSSUS channel can also be described by the ACFs of other functions of the system as it is shown in Fig. 2.7.

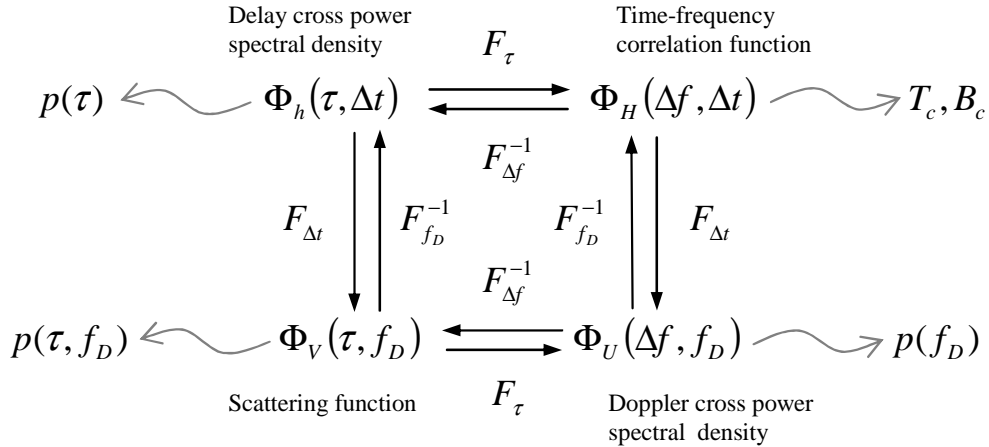


Figure 2.7: Relation between ACFs for a WSSUS channel model.

By using the ACFs of the *system functions* some statistical values can be derived in order to describe the characteristic properties of the channel in a summarized way. Even a more summarized and rough description of the channel can be given by calculating the *coherence time*  $T_c$  and the *coherence bandwidth*  $B_c$  by using the ACF of the *Transfer function* ( $H$ ) as we will see later.

By calculating the ACF of the *impulse response*  $\Phi_h(\tau, \Delta t)$  in  $\Delta t = 0$  is

obtained the *delay-power spectral density*  $\Phi_h(\tau) \equiv \Phi_h(\tau, 0)$ .  $\Phi_h(\tau)$  defines the power associated to the echoes with delay  $\tau$  received by the receiver. Then it is proportional to the *probability density function*  $p(\tau)$  of the signal delay  $\tau$

$$p(\tau) = \frac{\Phi_h(\tau)}{\int_{-\infty}^{+\infty} \Phi_h(\tau) d\tau} \quad (2.24)$$

The expectation value for the random variable  $\tau$  is

$$\bar{\tau} = E(\tau) = \int_{-\infty}^{+\infty} \tau p(\tau) d\tau \quad (2.25)$$

and the *standard deviation* of  $\tau$  is

$$\sigma_\tau = \sqrt{\int_{-\infty}^{+\infty} (\tau - \bar{\tau})^2 p(\tau) d\tau} \quad (2.26)$$

Analogously to this, by calculating the ACF of the *frequency Doppler function*  $\Phi_U(\Delta f, f_D)$  in  $\Delta f = 0$  is obtained the *Doppler-power spectral density*  $\Phi_U(f_D) \equiv \Phi_U(0, f_D)$ .  $\Phi_U(f_D)$  defines the power associated to the echoes with Doppler shift  $f_D$  received by the receiver. Then it is proportional to the *probability density function*  $p(f_D)$  of the Doppler frequency shift  $f_D$ .

$$p(f_D) = \frac{\Phi_U(f_D)}{\int_{-\infty}^{+\infty} \Phi_U(f_D) df_D} \quad (2.27)$$

Then the expected value of  $f_D$  (mean Doppler frequency) in the received signal is

$$\bar{f}_D = E(f_D) = \int_{-\infty}^{+\infty} f_D p(f_D) df_D \quad (2.28)$$

and the *standard deviation* of  $f_D$  is

$$\sigma_{f_D} = \sqrt{\int_{-\infty}^{+\infty} (f_D - \bar{f}_D)^2 p(f_D) df_D} \quad (2.29)$$

The *Scattering function*  $\Phi_V(\tau, f_D)$  has an important meaning, it is proportional to the probability of finding a given delay  $\tau$  and a given Doppler shift  $f_D$  in a propagation path [17], this is

$$\Phi_V(\tau, f_D) \propto p(\tau, f_D) \quad (2.30)$$

To give a full stochastic description of a channel it is necessary to provide both *probability density functions*,  $p(\tau)$  and  $p(f_D)$ . Both can be obtained by channel estimation procedures.

A stochastic description of the channel can be given by using the ACF of the *transfer function*  $\Phi_H(\Delta f, \Delta t)$ , which is called *spaced time spaced frequency correlation function*. Particularly  $\Phi_H(0, \Delta t)$  is known as *time correlation function* and  $\Phi_H(\Delta f, 0)$  as *frequency correlation function*. They express how much the transmission characteristics of the channel varies with time and frequency respectively. These variations can be expressed by the following two parameters respectively, *coherence time*  $T_c$  and *coherence bandwidth*  $B_c$ ; these parameters can be used as a rough description of the channel.

The *coherence time*  $T_c$  for a given channel, is the period of time in which the *time correlation function* has a magnitude equal or greater than the half of its maximum value (see Fig. 2.8), this is

$$|\Phi_H(0, \frac{T_c}{2})| = \frac{1}{2}|\Phi_H(0, 0)| \quad (2.31)$$

For  $T_c$  the following approximation is generally used

$$T_c \approx \frac{1}{f_{Dmax}} \quad (2.32)$$

The *coherence bandwidth*  $B_c$  for a given channel, is the bandwidth in which the *frequency correlation function* has a magnitude equal or greater than the half of its maximum value (see Fig. 2.8), this is

$$|\Phi_H(\frac{B_c}{2}, 0)| = \frac{1}{2}|\Phi_H(0, 0)| \quad (2.33)$$

For  $B_c$  the following approximation is generally used

$$B_c \approx \frac{1}{\tau_{max}} \quad (2.34)$$

### 2.5.3.1 Wide Sense Stationary with Uncorrelated Scattering

When a channel can be categorized as stationary in wide sense in the direction of time and also can be assumed that the propagation in the different

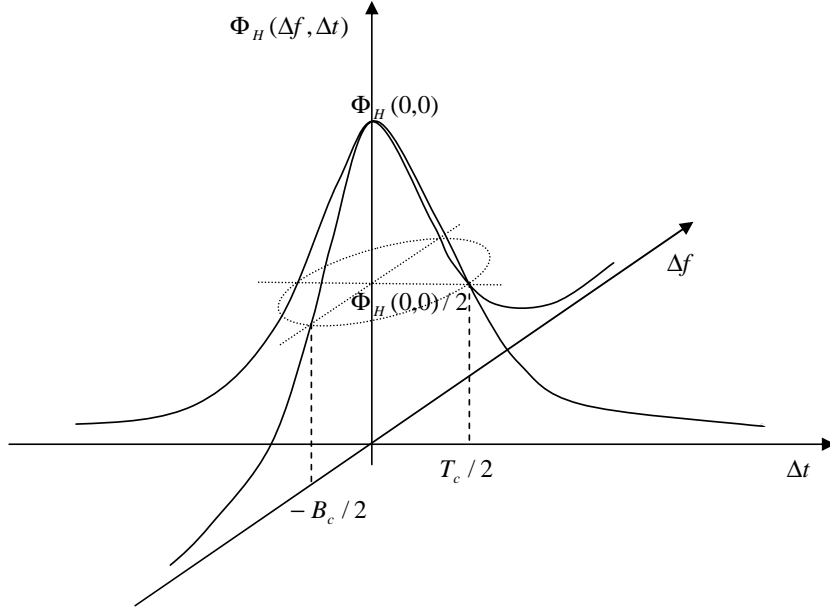


Figure 2.8: Definition of  $T_c$  and  $B_c$  by using  $\Phi_H(\Delta f, \Delta t)$ .

paths is uncorrelated (uncorrelated amplitudes and phases between different paths) then it is said that the channel is a Wide Sense Stationary with Uncorrelated Scattering (WSSUS) channel.

A WSSUS channel with  $P$  propagation paths (echoes) is described -in baseband- by the following *time-variant channel impulse response*:

$$h(\tau, t) = \frac{1}{\sqrt{P}} \sum_{p=1}^P \delta(\tau - \tau_p) e^{j(2\pi f_{D,p}t + \theta_p)} \quad (2.35)$$

Where  $P$  is the number of propagation paths,  $\tau_p$  is the delay associated with each individual path,  $f_{D,p}$  is the Doppler shift in frequency for each path and  $\theta_p$  is the initial phase for each path [18]. If it is true that (2.35) is valid for the limit, when  $P \rightarrow \infty$ , it is also true that it is generally used for  $P = 20$  or  $P = 30$ .

The frequency selective behavior of the channel is due to different time delays  $\tau_p$  for the different paths. The time variant behavior of the channel is due to the movement of the mobile station and it is described by  $f_{D,p}$  (see Fig. 2.9).

For simulation purposes  $P$  is a fixed number of paths assumed in the simulation, the variables  $\theta_p$ ,  $f_{D,p}$  and  $\tau_p$  are defined by their “probability density functions” (PDFs). The variable  $\theta_p$  has uniform distribution in  $[0, 2\pi)$ , this is

$$p(\theta) = \begin{cases} \frac{1}{2\pi} & \text{for } \theta \in [0, 2\pi) \\ 0 & \text{in other case} \end{cases} \quad (2.36)$$

The “joint probability density function”  $p(\tau, f_D)$  is directly proportional to the “scattering function”  $\Phi_V(\tau, f_D)$  ( $p(\tau, f_D) \propto \Phi_V(\tau, f_D)$ ).

For many applications the statistic independence of both random variables  $\tau$  and  $f_D$  of the “scattering function”  $\Phi_V(\tau, f_D)$  is assumed. That means that also for the “joint probability density function”  $p(\tau, f_D)$  the variables  $\tau$  and  $f_D$  are statistically independent and then  $p(\tau, f_D)$  can be expressed as

$$p(\tau, f_D) = p(\tau)p(f_D) \quad (2.37)$$

Some typical examples used in simulations as  $p(\tau)$  and  $p(f_D)$  (PDFs of  $\tau$  and  $f_D$  respectively) are:

$$p(\tau) = \begin{cases} ae^{-\frac{\tau}{b}} & \text{for } \tau \in [0, \tau_{max}] \\ 0 & \text{in other case} \end{cases} \quad (2.38)$$

$$p(f_D) = \begin{cases} \frac{1}{\pi f_{Dmax} \sqrt{1 - (\frac{f_D}{f_{Dmax}})^2}} & \text{for } |f_D| \in [0, f_{Dmax}) \\ 0 & \text{in other case} \end{cases} \quad (2.39)$$

Where  $a$ ,  $b$  and  $\tau_{max}$  in (2.38) are parameters determined by the environment (e.g., see Table B.1 in Appendix B). From these three parameters, only two are free parameters, the third one has to be set in order to fulfill  $\int_{-\infty}^{+\infty} p(\tau) d\tau = 1$ . In (2.39)  $f_{Dmax}$  is the maximum value for the Doppler shift  $f_D$  in the *Jakes Doppler Profile*. Different examples of  $p(f_D)$  (*Jakes Doppler Profile*, *Rectangular Doppler Profile* and *Gauss Doppler Profile*) can be seen in Appendix A.

Then, once we have the PDFs for  $\theta$ ,  $\tau$  and  $f_D$  ( $p(\theta)$ ,  $p(\tau)$  and  $p(f_D)$ ) it is only needed to obtain samples of  $\theta$ ,  $\tau$  and  $f_D$  with these PDFs and by using these values in (2.35) we can obtain samples of the “time-variant channel impulse response”  $h(\tau, t)$  of our WSSUS channel.

In Fig. 2.9 are shown some examples of WSSUS channels. This figure shows clearly the influence of the maximum delay  $\tau_{max}$  and the speed of the mobile station  $v$  (which is directly proportional to the maximum Doppler shift

$f_{Dmax}$ ) in the behavior of the channel. When  $\tau_{max}$  is increased, the *frequency selectivity* of the channel is increased. While the speed of the mobile station is increased, the *time selectivity* of the channel is increased. The relation between  $v$  and  $f_{Dmax}$  is given by  $f_{Dmax} = v \cdot \frac{f_c}{c}$ , where  $f_c$  is the carrier frequency and  $c$  is the speed of light.

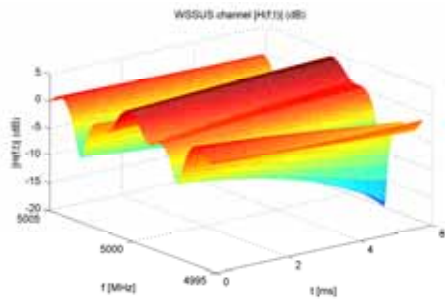
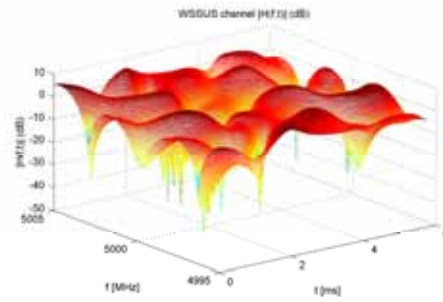
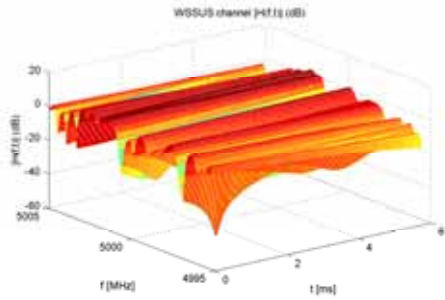
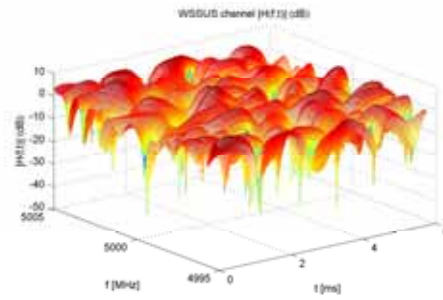
(a)  $\tau_{max} = 0.7 \mu s$  and  $v = 5 km/h$ (b)  $\tau_{max} = 0.7 \mu s$  and  $v = 120 km/h$ (c)  $\tau_{max} = 3.2 \mu s$  and  $v = 5 km/h$ (d)  $\tau_{max} = 3.2 \mu s$  and  $v = 120 km/h$ 

Figure 2.9: Examples of WSSUS channels.

# Chapter 3

## OFDM Based System Concepts

The OFDM transmission technique is a special case of Multi Carrier Modulation (MCM), which relies on dividing the data sequence in several parallel bit sequences and modulating each one in individual subcarriers. MCM dates from the 50s (1950), with military radio links of high frequency (HF). By the middle of 60s R. W. Chang published an article [19] demonstrating those concepts that today are used in OFDM. What Chang demonstrated was the principle of transmission of multiple messages simultaneously, through a linear channel of limited bandwidth without Inter Channel Interference (ICI) neither Inter Symbol Interference (ISI). The great advantage with respect to the well known MCM systems, was that Chang allowed the spectral overlapping of subcarriers under the restriction of being mutually orthogonal between them.

Later in 1971 Weinstein and Ebert [20] suggested the use of the Discrete Fourier Transform (DFT) and the Inverse Discrete Fourier Transform (IDFT) to carry out the modulation and demodulation in base band. Those are essential modules in today's OFDM systems.

### 3.1 Fundamentals

One very basic representation of an OFDM system can be seen in Fig. 3.1, there a transmitter, a channel and a receiver are represented.

In this figure, *IDFT* is the *Inverse Discrete Fourier Transform*, which is applied to the vector of *constellation points*  $(x_{0,l}, x_{1,l}, \dots, x_{N-1,l})$  (produced by one modulation process) that are going to be transmitted. *Cyclic Prefix* (*CP*) represents a module, where the *Cyclic Prefix* is added. The *CP* is

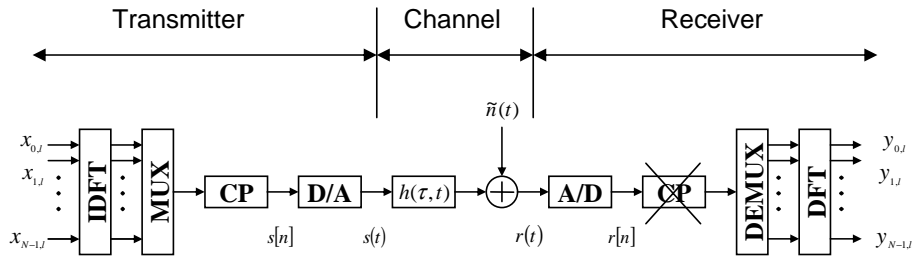


Figure 3.1: Basic representation of an OFDM system [21].

only the last part of the *OFDM symbol* which is pre-appended to it. This *CP* plays an important role to avoid *Inter Symbol Interference* because it avoids the influence of adjacent symbols. The *D/A* module is a *Digital to Analog converter* to have a continuous signal to transmit. Later the channel is applied to the signal and then all the process done in the Tx are undone in the Rx in order to recover the transmitted message.  $\tilde{n}(t)$  is the noise added in the Rx (see Section 2.3).

An arbitrary bit sequence is mapped to a sequence of modulation symbols  $(x_{0,l}, x_{1,l}, \dots, x_{N-1,l})$  described as discrete points in the constellation diagram (see Fig. 3.2 (a) as an example). Then these constellation points will be transmitted. The estimation of these constellation points  $(y_{0,l}, y_{1,l}, \dots, y_{N-1,l})$  will be obtained in the receiver. These estimations will be affected by the channel as it is represented in (b). Then, the maximum likelihood decision will be the constellation point closest to the obtained estimation ( $y_{k,l}$  with  $0 \leq k \leq N - 1$ ).

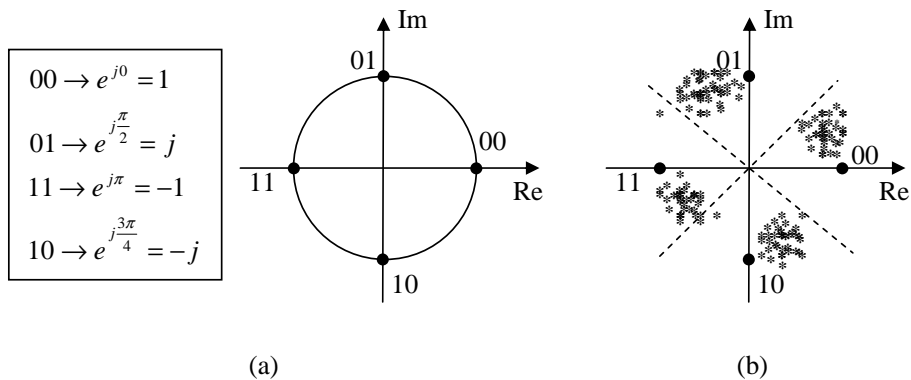


Figure 3.2: QPSK constellation.

### 3.1.1 Continuous Time Model

It is quite common to see continuous time models for OFDM systems, in Fig. 3.3 a very basic one (in base band) is shown.

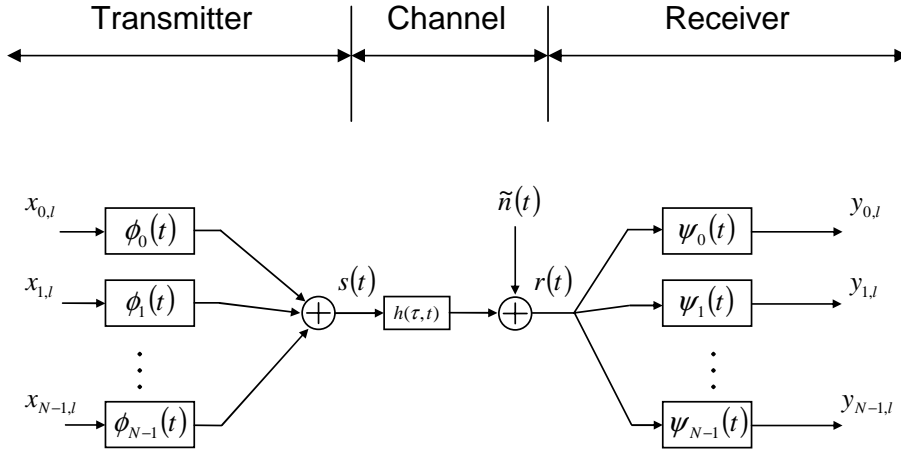


Figure 3.3: Continuous time model for an OFDM system [21].

Based on this figure, we can analyze an OFDM based system, step by step. The first element is the transmitter, where the OFDM signal is generated.

#### Transmitter

In the transmitter, the elements of the OFDM symbol are multiplied by rectangular pulses modulated by different subcarriers. These elements ( $x_{k,l}$ ) are complex values from the set of constellation points corresponding to the used modulation.  $\phi_k(t)$  is the subcarrier “ $k$ ” inside the interval  $[0, T]$ . After that all these signals are added as shown in Fig. 3.4.

Figure 3.5 shows in a graphic way how each one of these  $\phi_k(t - lT)$  becomes in one of the shifted *sinc* functions of the OFDM spectrum. Considering that the Fourier Transform (FT) of a rectangular pulse is a *sinc* signal and the FT of a sinusoidal signal is a delta ( $\delta$ ), it is clear that the FT of the rectangular pulse modulated by the subcarrier “ $k$ ” is a *sinc* signal convolved with the respective  $\delta$  (the FT of the sinusoidal signal corresponding to the subcarrier “ $k$ ”).

The spectrum of the OFDM signal results from the superposition of all these *sinc* functions as it is shown in Fig. 3.6.

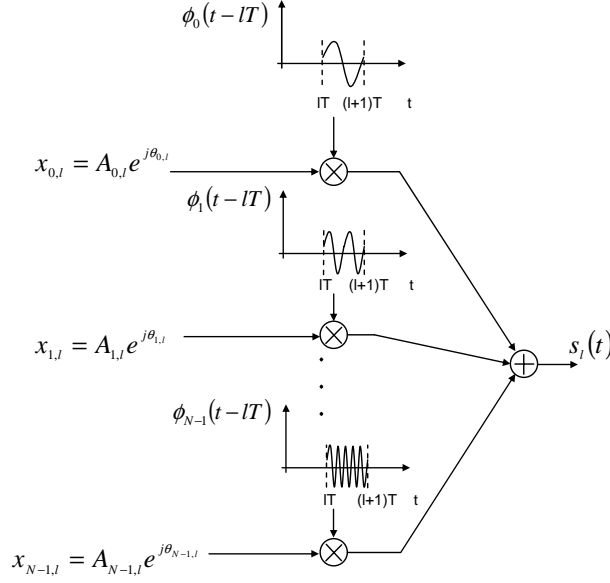


Figure 3.4: Continuous time model for an OFDM transmitter.

This process is mathematically described by (3.1)

$$\phi_k(t) = \begin{cases} \frac{1}{\sqrt{T-T_{CP}}} \cdot e^{j2\pi k \Delta f (t-T_{CP})} & \text{if } t \in [0, T] \\ 0 & \text{in other case} \end{cases} \quad (3.1)$$

Where  $T_{CP}$  is the time length of the *CP*,  $T$  is the time length of the symbol (including the *CP*) and  $\sqrt{(T-T_{CP})}$  is a normalization factor.  $\Delta f = \frac{B}{N} = \frac{1}{T-T_{CP}}$ , where  $B$  is the bandwidth of the OFDM system and  $N$  the number of subcarriers of it. The index  $k$  indicates the subcarrier.

Then the transmitted signal for symbol  $l$  can be written as

$$s_l(t) = \sum_{k=0}^{N-1} x_{k,l} \cdot \phi_k(t-lT) \quad (3.2)$$

When an infinite sequence of OFDM symbols are transmitted, then this signal  $s(t)$  can be represented as

$$s(t) = \sum_{l=-\infty}^{+\infty} s_l(t) = \sum_{l=-\infty}^{+\infty} \sum_{k=0}^{N-1} x_{k,l} \cdot \phi_k(t-lT) \quad (3.3)$$

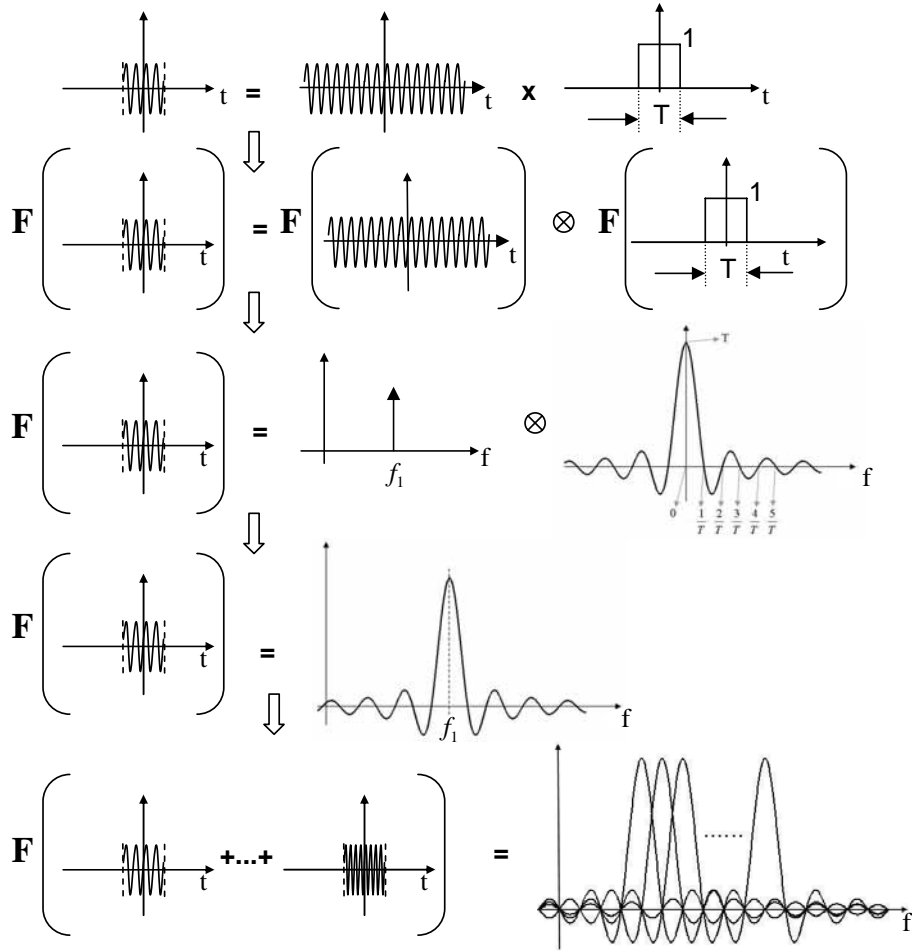


Figure 3.5: Spectrum of  $\phi_k(t - lT)$ .

## Channel

By assuming that the *time impulse response* of the physical channel is restricted to the interval  $\tau \in [0, T_{CP}]$ , i.e. it is smaller than the CP time length, the received signal is

$$r(t) = (h * s)(t) + \tilde{n}(t) = \int_0^{T_{CP}} h(\tau, t) s(t - \tau) d\tau + \tilde{n}(t) \quad (3.4)$$

Where  $\tilde{n}(t)$  is AWGN mainly added in the receiver.

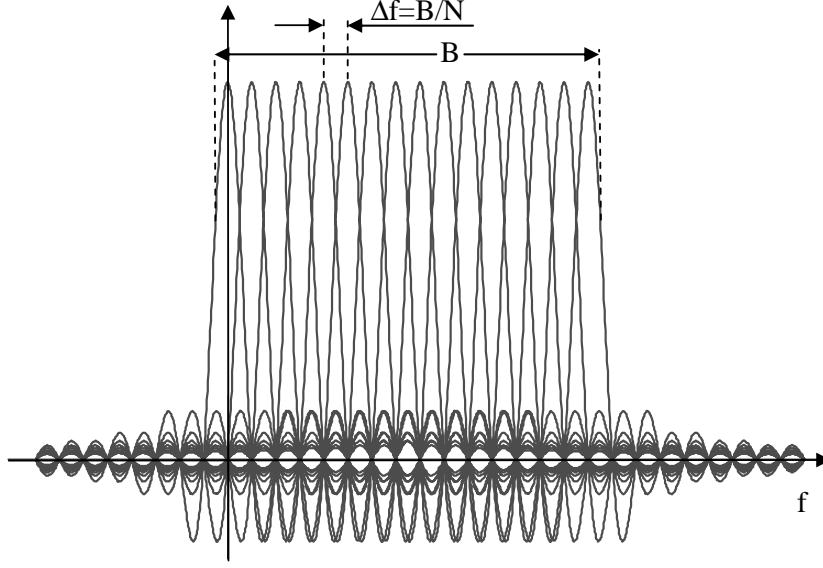


Figure 3.6: Overlapping subcarrier spectra.

## Receiver

The OFDM receiver consists of a filter bank, matched to the last part  $[T_{CP}, T]$  of the subcarrier signal  $\phi_k(t)$  [21].

$$\psi_k(t) = \begin{cases} \phi_k^*(T-t) & \text{if } t \in [0, T - T_{CP}] \\ 0 & \text{in other case} \end{cases} \quad (3.5)$$

That means that the CP will be removed in the receiver. Since the CP contains all the ISI from the previous symbol, the sampled output from the receiver filter bank will not contain ISI.

Ignoring the symbol (time) index “ $l$ ” when calculating the sampled output at the  $k_{th}$  matched filter (subcarrier), using (3.3), (3.4) and (3.5) we obtain:

$$\begin{aligned} y_k &= (r * \psi_k)(t) |_{t=T} = \int_{-\infty}^{+\infty} r(t) \psi_k(T-t) dt \\ &= \int_{T_{CP}}^T \left( \int_0^{T_{CP}} h(\tau, t) \left[ \sum_{k'=0}^{N-1} x_{k'} \phi_{k'}(t-\tau) \right] d\tau \right) \phi_k^*(t) dt + \\ &\quad \int_{T_{CP}}^T \tilde{n}(T-t) \phi_k^*(t) dt \end{aligned} \quad (3.6)$$

Observe that this convolution  $((r * \psi_k)(t))$  evaluated in  $t = T$  gives the scalar product between  $\phi_{k'}(t)$  and  $\phi_k(t)$  which (due to these two functions are or-

thonormal among them) will be “0”  $\forall k' \neq k$  and “1” for  $k' = k$ . Allowing in this way extracting the data  $x_{k,l}$  which came in the subcarrier  $k$ , in the symbol  $l \forall l$ . For sure the data is affected by the channel impulse response and the noise acquired in the receiver.

Also observe that when performing this convolution, the CP is suppressed. Due to all the ISI caused by the previous symbol (convolved with the channel impulse response) is contained in this CP, by removing it, it will be removed all the ISI.

By assuming a fixed channel over the OFDM symbol interval and by denoting the channel as  $h(\tau)$ , it is obtained:

$$y_k = \sum_{k'=0}^{N-1} x_{k'} \int_{T_{CP}}^T \left( \int_0^{T_{CP}} h(\tau) \phi_{k'}(t-\tau) d\tau \right) \phi_k^*(t) dt + \int_{T_{CP}}^T \tilde{n}(T-t) \phi_k^*(t) dt \quad (3.7)$$

The integration intervals are  $T_{CP} < t < T$  and  $0 < \tau < T_{CP}$  which implies that  $0 < t - \tau < T$  and the inner integral can be written as:

$$\begin{aligned} \int_0^{T_{CP}} h(\tau) \phi_{k'}(t-\tau) d\tau &= \int_0^{T_{CP}} h(\tau) \left[ \frac{e^{j2\pi k' \Delta f (t-\tau-T_{CP})}}{\sqrt{T-T_{CP}}} \right] d\tau \\ &= \frac{e^{j2\pi k' \Delta f (t-T_{CP})}}{\sqrt{T-T_{CP}}} \int_0^{T_{CP}} h(\tau) e^{-j2\pi k' \Delta f \tau} d\tau, \quad T_{CP} < t < T \end{aligned}$$

The latter part of the expression is the sampled frequency response of the channel at frequency  $f = k' \Delta f$ , at the  $k'^{th}$  subcarrier frequency:

$$H_{k'} = H(k' \Delta f) = \int_0^{T_{CP}} h(\tau) e^{-j2\pi k' \Delta f \tau} d\tau \quad (3.8)$$

Where  $H(f)$  is the Fourier Transform of the channel impulse response  $h(\tau)$ . Using this notation, the output from the receiver filter bank can be simplified to:

$$\begin{aligned} y_k &= \sum_{k'=0}^{N-1} x_{k'} \int_{T_{CP}}^T \frac{e^{j2\pi k' \Delta f (t-T_{CP})}}{\sqrt{T-T_{CP}}} H_{k'} \phi_k^*(t) dt + \int_{T_{CP}}^T \tilde{n}(T-t) \phi_k^*(t) dt \\ &= \sum_{k'=0}^{N-1} x_{k'} H_{k'} \int_{T_{CP}}^T \phi_{k'}(t) \phi_k^*(t) dt + n_k \quad (3.9) \end{aligned}$$

where  $n_k = \int_{T_{CP}}^T \tilde{n}(T-t)\phi_k^*(t)dt$ . Since the subcarrier signals  $\phi_k(t)$  are orthogonal,

$$\int_{T_{CP}}^T \phi_{k'}(t)\phi_k^*(t)dt = \int_{T_{CP}}^T \frac{e^{j2\pi k'\Delta f(t-T_{CP})}}{\sqrt{T-T_{CP}}} \frac{e^{-j2\pi k\Delta f(t-T_{CP})}}{\sqrt{T-T_{CP}}} dt = \delta[k-k'] \quad (3.10)$$

Where  $\delta[k]$  is the Kronecker delta function, therefore the expression (3.9) can be written as:

$$y_k = H_k x_k + n_k \quad (3.11)$$

Where  $n_k$  is AWGN.

### 3.1.2 Discrete Time Model

In Fig. 3.7 a fully discrete time model for an OFDM system is shown, where a discrete description for the channel is used.

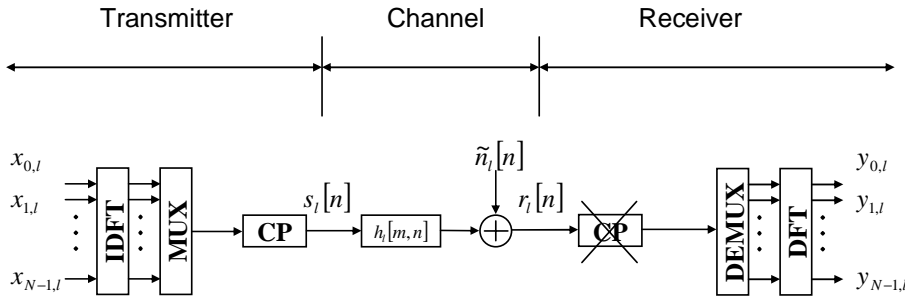


Figure 3.7: Discrete time model for an OFDM system [21].

With the help of Fig. 3.8 the advantages of using the CP can be observed. There in (a) if someone looks the signal received for different values of  $\tau$  inside of the *FFT window*, that clearly do not correspond to a periodic signal. Also can be seen that data corresponding to *Symbol 1* are considered in the *FFT window* corresponding to *Symbol 2*, that is ISI.

A much more convenient situation we have when CP is used as in Fig. 3.8 case (b). Then two important effects are achieved by using the CP. The first one is that now, there are no more data corresponding to *Symbol 1* being considered in the *FFT window* corresponding to *Symbol 2*. That means that the ISI has been cancelled. The other important effect is that now, for different values of  $\tau$ , inside of the *FFT window*, are seen different shifted versions

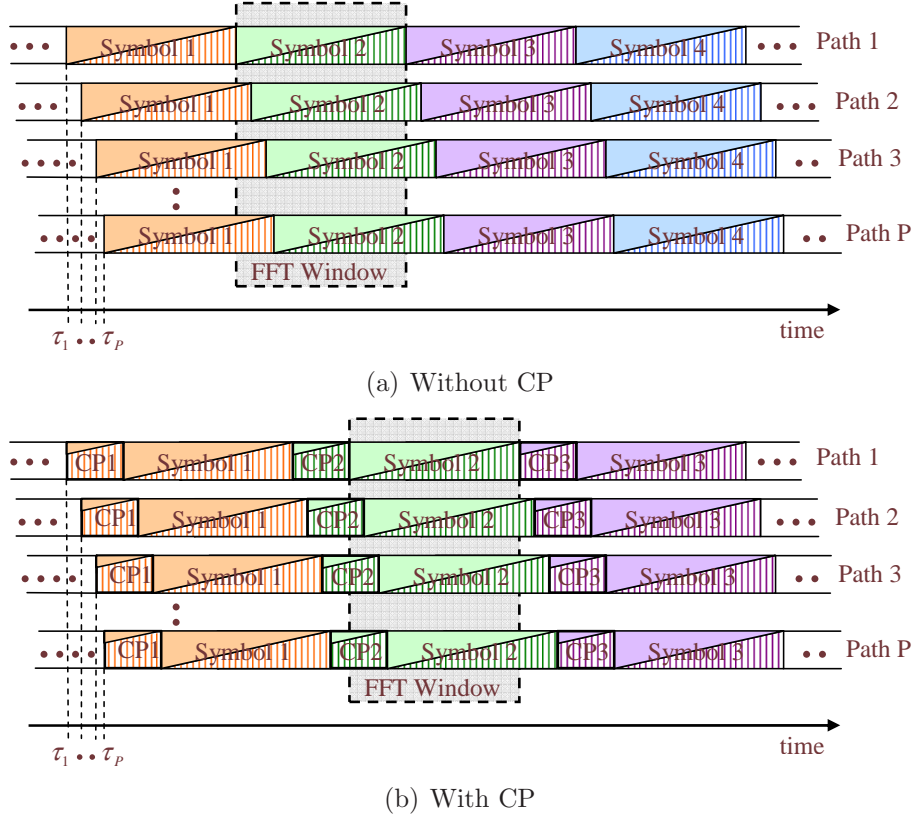


Figure 3.8: CP and FFT window in an OFDM system.

of one periodic signal.

The use of the CP makes the signal periodic -inside the *FFT window*- that transforms the *linear convolution* in a *cyclic* or *circular convolution* [22] between the transmitted signal and the channel. Then we have

$$y_l = DFT(IDFT(x_l) \circledast h_l + \tilde{n}_l) = DFT(IDFT(x_l) \circledast h_l) + n_l \quad (3.12)$$

Where “ $\circledast$ ” represents the *cyclic convolution*,  $x_l$  is the signal -containing the  $N$  transmitted *constellation points*-,  $h_l$  is the channel impulse response of the channel (remember that it has to be padded with zeros in order to have a length of  $N$ ) and  $n_l = DFT(\tilde{n}_l)$  is uncorrelated Gaussian noise (due to  $\tilde{n}_l$  was assumed AWGN).

Using that the DFT of two *cyclic convolved* terms is equal to the product of

their respective DFTs, it is obtained

$$\boxed{y_l = x_l \cdot DFT(h_l) + n_l = H_l \cdot x_l + n_l} \quad (3.13)$$

Where  $y_l$  is the vector containing the  $N$  received data points (see Fig. 3.7),  $x_l$  is the vector containing the  $N$  transmitted constellation points (data), “ $\cdot$ ” denotes a component by component multiplication between vectors,  $H_l = DFT(h_l)$  is the frequency response of the channel and  $n_l = DFT(\tilde{n}_l)$  is the channel noise vector in the space of frequency.

## 3.2 OFDM System Applications

### 3.2.1 Wi-Fi

*Wireless Fidelity* (Wi-Fi) is the commercial name for a set of Wireless Local Area Networks WLAN which provides Wireless access in the indoor context. Some of the most successful options (standards) are based in OFDM transmission technique. To know, IEEE802.11a and g standards consider OFDM as the transmission technique. IEEE802.11b and g are the more common standards used in notebooks to provide indoor Wireless Access. As an example Fig. 3.9 shows a simplified block diagram of a transmitter based on the standard IEEE802.11a [23].

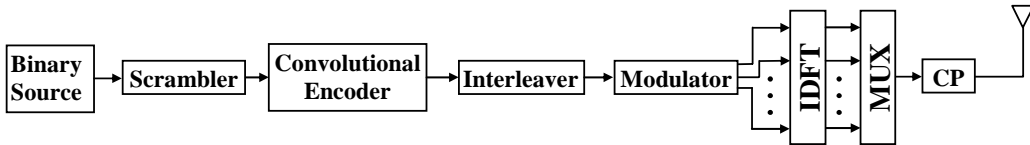


Figure 3.9: Simplified block diagram of a IEEE802.11a OFDM based transmitter.

There can be observed the following modules:

“*Scrambling*”. This procedure avoids large sequences of “1” or “0” which provides not enough bit temporization in the receiver and could cause synchronization degradation. For making that, one alternative is to compose the data sequence with a *pseudo random binary sequence* generated by a known circuit (scrambler encoder). Later the original data can be recovered in the receiver by using an “inverse” circuit (scrambler decoder).

The scrambler process also produces a spreading of energy in the spectrum by avoiding periodic sequences which have the power concentrated in few harmonics.

“*Channel Coding and Decoding*”. This procedure makes the data transmission more robust. There are several alternatives to perform channel coding. In the standard IEEE802.11a and also in this work a *Convolutional* channel coding process is considered. *Convolutional* coding and decoding (Viterbi decoder) is discussed in more details in Section 8.1 and Appendix C. An idea of the improvement in the performance produced by these techniques can be obtained by analyzing the results in Section 8.3.

“*Interleaving*”. The interleaving process essentially looks for separating in the transmission the bits of one same data word. By doing this, a burst of interference is going to damage less bits in each word and then the corrector algorithms have a high chance to recover the correct words. One alternative to do this (Block interleaving) is to save the data words in the columns of a matrix and then read the matrix, row by row and transmit this information. In this way the bits of one word are separated. The number of bits temporally stored in the matrix is known as the *interleaving depth* and this is a parameter to tune considering the used modulation. There are also other way of making this process in a more effective way, from the point of view of the use of memory in the system, it is by using the *convolutional interleaving*. In this way can be achieved the same depth with approximately the half of memory.

The storage of this information in the matrix and its posterior reading introduce a delay, it has to be verified that this delay is tolerable for the system in consideration.

“*Modulator*”. This is the block responsible for converting the bits in constellation points to be transmitted. The “*IDFT*” and “*CP*” modules have already been explained in Section 3.1.

Later in the receiver, the reverse operations than the ones performed in the transmitter are done in order to obtain the message. If the system is working with a coherent demodulation, then the receiver has also to provide some *channel estimation* and *channel correction* techniques.

These standards were thought originally for indoor environments with low

mobility, but later scientific research and normal practice has demonstrated that these standards are still useful in other environments.

In the city of Philadelphia has been started a project by the year 2004, known as Philadelphia project<sup>1</sup>, to provide the city with public wireless access. In this project has been developed an outdoor wireless network. This Wireless Metropolitan Area Network (WMAN), was developed using the standard IEEE802.11b which is originally an indoor standard. The reasons to do this can be several, the prices of devices using this standard, the maturity of the technology in the moment that the project was started, the simplicity and good results of this standard. This is a good example of the use of a Wi-Fi standard in a different environment than the indoor one.

Several researchers have considered the use of IEEE802.11a, b and g standards in the context of vehicular ad hoc networks for Car to Car<sup>2</sup> or Car to infrastructure communications [24], [25]. These kind of networks are developed with the purpose of improving the security and the comfort for motorists and pedestrians. Thanks to these researches today exists a good knowledge about the performance of these standards in this context. Some interesting figures reported in [25] show that by using the standard IEEE802.11g, 70 MB files can be transmitted between two cars at a velocity of 50 km/h, achieving a range of coverage of more than 1 km. For these applications again the price, simplicity and the maturity of these standards make them a very convenient alternative.

Also these standards have been considered for the surveillance of airport mobiles [26]. All these different applications, added to the original one, indoor wireless networks for offices and home applications, show the potential, flexibility and simplicity of these standards. Those are the reasons for the success of these standards, two of them (IEEE802.11a and g) based on the OFDM transmission technique.

### 3.2.2 WiMAX

*Worldwide Interoperability for Microwave Access* WiMAX is the commercial name for the IEEE802.16 specification conducted by the IEEE802.16 working group. This specification has the objective to provide a technology platform for developing low cost broadband wireless systems. As an strategy to obtain

---

<sup>1</sup><http://www.phila.gov/wireless/faqs.html>.

<sup>2</sup><http://www.car-2-car.org>.

low cost, the competence and the scale are assured by avoiding proprietary solutions. The definition of this technology platform is quite open and participatory<sup>3</sup>.

The first IEEE802.16 standard was approved at the end of 2001, after that there were some revisions and amendments. Basically this standard defines several options for WMANs operating between 2 and 66 GHz. Concerning to the Physical layer, in [27] were considered basically three options. The first option is “*WirelessMAN-SCa PHY*”, it is based on a single carrier technology. The second one is “*WirelessMAN-OFDM PHY*”, it is based on OFDM. The third option is “*WirelessMAN-OFDMA PHY*”, also based in OFDM modulation. The three options were designed for *NLOS* conditions and thought for operating in frequency bands below 11 GHz.

Fig. 3.10 describes the WiMAX transmitter by a block diagram. In [27] and [28] the modules of this figure are explained.

---

<sup>3</sup>See WiMAX Forum in <http://www.wimaxforum.org/home/>.

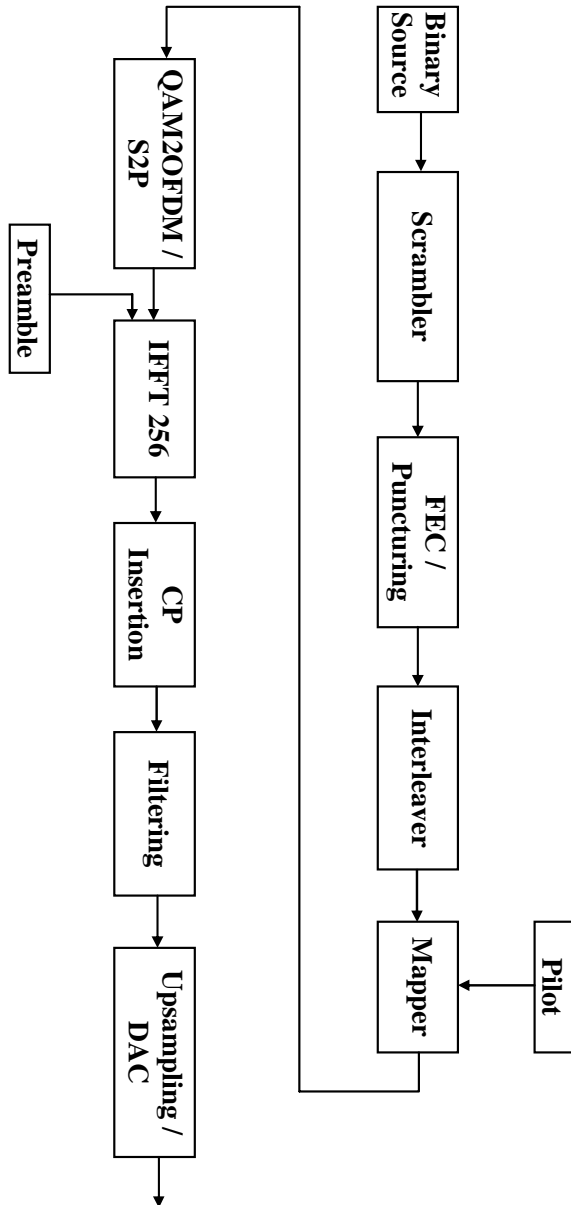


Figure 3.10: Simplified block diagram of a IEEE802.16 OFDM based transmitter.

# Chapter 4

## Channel Estimation in OFDM based Systems

For coherent systems it is necessary to estimate the channel and using this information to correct the received data. In differential modulation schemes the channel state information is not necessary but it can help to improve the performance. Considering that wireless channels, especially mobile radio channels are very time variant, the task of estimating and maintaining and actualized knowledge of the channel is not a simple task. For this reason several different techniques have been proposed; in this section some of them will be presented.

Channel estimation is quite demanding and also a very important task in order to achieve a good use of the channel. Basically can be distinguished two approaches for channel estimation techniques, a “*frequency domain approach*” and a “*time domain approach*”. In the “*frequency domain approach*” the channel estimation is performed after the DFT (see Fig. 3.1), the *channel frequency response* is estimated. In the “*time domain approach*” the estimation is performed before the DFT, the *channel impulse response* is estimated in this case.

### 4.1 Pilot Aided Channel Estimation

*Pilot Aided Channel Estimation* (PACE) is a channel estimation technique based in the insertion of pilots in some subcarriers (instead of data). In PACE can be distinguished basically two ways of using the pilots to perform channel estimation. One of them is the use of *scattered pilots* and the other is the use of *training symbols*, these methods are discussed in Sections 4.1.1

and 4.1.2 respectively.

### 4.1.1 Scattered Pilots

The *scattered pilots* technique is a frequency domain channel estimation technique based in the insertion of pilots in some subcarriers (instead of data). By interpolating the effect of the channel over these pilots, the effect of the channel over the subcarriers used for transmitting data can be estimated. These pilots allow to estimate the effect caused by the channel over the data, in counter part not all the subcarriers can be used for transmitting data (some of them are used for these pilots). This technique is particularly common in broadcast OFDM systems (e.g., Digital Video Broadcasting-Terrestrial (DVB-T)), where the subcarrier spacing is very small. In these cases, when the subcarrier spacing is much less than the *coherence bandwidth*, the channel effect over neighbor subcarriers is practically identical. Then the error in the interpolation (to estimate the influence of the channel over those subcarriers which do not have pilots) is acceptable.

### 4.1.2 Training Symbols

The use of *training symbols* is quite extended among WLAN systems and it consists in using pilots in all subcarriers of the preamble symbols for channel estimation purposes. *Training symbols* can be used in PACE in the frequency domain or in the time domain. In the first case the training symbols in the system preamble are used for *channel frequency response* estimation. In the second case *channel estimation* is performed before the DFT process. After having calculated the *channel impulse response*, the *channel frequency response* can be obtained by applying a DFT to the first one. Both approaches are commented in this section.

Fig. 4.1 gives an example of a possible pilot pattern for channel estimation in an OFDM system. There, black circles were used to represent pilot symbols and white circles for payload data symbols. The first column of black circles at the left represents a training symbol in the direction of the frequency. The rest of black circles represent scattered pilots.

## Frequency Domain Approach for Channel Estimation, using Training Symbols

For WLAN applications, is generally assumed a *quasistationary* channel, that means that the channel do not vary during the *data packet*. Then the channel

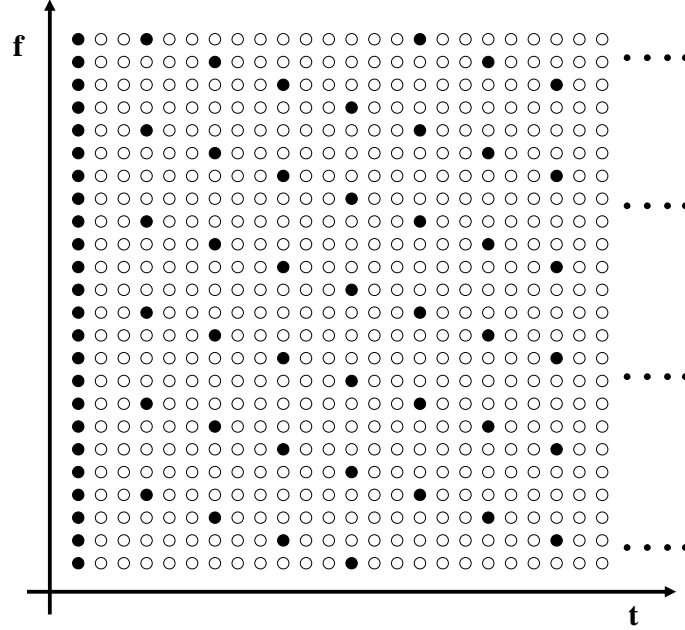


Figure 4.1: Example of a possible pilot pattern for channel estimation in an OFDM system.

for a given subcarrier  $k$  in a data packet can be represented by the channel transfer factor as  $H_k$ . If the training symbol  $X_k$  is used for a subcarrier  $k$  in the data packet, the received training symbol  $R_{k,1}$  will be

$$R_{k,1} = H_k \cdot X_k + N_{k,1} \quad (4.1)$$

Where  $N_{k,1}$  is the AWGN added to the subcarrier  $k$  in time symbol 1 (corresponding to the training symbol) and  $X_k$  (the training symbol) is a complex value with amplitude equal to one. Then the channel estimator can be calculated as

$$\hat{H}_k = R_{k,1} \cdot X_k^* \quad (4.2)$$

Where  $X_k^*$  denotes the complex conjugate of  $X_k$ , then

$$\begin{aligned} \hat{H}_k &= (H_k \cdot X_k + N_{k,1}) X_k^* \\ &= H_k \cdot |X_k|^2 + N_{k,1} \cdot X_k^* \end{aligned} \quad (4.3)$$

Considering that the amplitude of  $X_k$  is one, the channel estimator will be

$$\hat{H}_k = H_k + N_{k,1} \cdot X_k^* \quad (4.4)$$

This will be the channel estimator for the subcarrier  $k$  for all the symbols contained in the considered data packet, when a frequency domain approach is used in combination with training symbols. For some WLAN applications the training symbol is transmitted two times and  $\hat{H}_k = \frac{1}{2}(R_{k,1} + R_{k,2})X_k^*$  is used as channel estimator instead of (4.2) in order to improve the quality of the channel estimation.

## Time Domain Approach for Channel Estimation, using Training Symbols

In the time domain approach the training symbols will be processed before the DFT, then the channel impulse response, instead of the channel frequency response will be estimated. Later the estimator of the last one can be obtained from the first one just by making  $\hat{H} = DFT\{\hat{h}\}$ . As an example, here is described the derivation of the time domain channel estimator, using training symbols, for a WLAN application.

Being  $h[n]$  the channel impulse response,  $x[n]$  the time domain training symbol and  $n_1[n]$  the AWGN vector added in the receiver in the time symbol 1 (the corresponding to the training symbol), the received training symbol  $r_1$ , in time domain, will be

$$r_1 = h \circledast x + n_1 \quad (4.5)$$

Where “ $\circledast$ ” denotes the *cyclic* or *circular convolution*. Remembering that the discrete *circular convolution* can be expressed as

$$h[n] \circledast x[n] = \sum_{m=0}^{N-1} h[m] \cdot x[(n-m)_{\text{mod}N}] \quad (4.6)$$

where “ $(n-m)_{\text{mod}N}$ ” is the *modulo N* value of  $(n-m)$  [22]. Then it can be derived that the convolution product of (4.5) can be expressed as the product of a  $X$  matrix by a  $h$  vector as follows

$$r_1 = X \cdot h + n_1 \quad (4.7)$$

Considering an OFDM system with 64 subcarriers, which means 64 time samples after IDFT (in time domain),  $X$  would be

$$X = \begin{bmatrix} x_1 & x_{64} & x_{63} & \cdot & \cdot & \cdot & x_{64-L+2} \\ x_2 & x_1 & x_{64} & \cdot & \cdot & \cdot & x_{64-L+3} \\ \cdot & \cdot & \cdot & \cdot & \cdot & \cdot & \cdot \\ x_{63} & x_{62} & x_{61} & \cdot & \cdot & \cdot & x_{64-L} \\ x_{64} & x_{63} & x_{62} & \cdot & \cdot & \cdot & x_{64-L+1} \end{bmatrix} \quad (4.8)$$

and  $h$  is

$$h = \begin{bmatrix} h_1 \\ h_2 \\ h_3 \\ \vdots \\ \vdots \\ h_L \end{bmatrix} \quad (4.9)$$

$L$  is the length of the impulse response.

Considering (4.7) the channel impulse response estimator is

$$\begin{aligned} \hat{h} &= X^+ \cdot r_1 \\ &= X^+(X \cdot h + n_1) \\ &= h + X^+ \cdot n_1 \end{aligned} \quad (4.10)$$

Where  $X^+$  denotes de Moore-Penrose<sup>1</sup> generalized inverse matrix of  $X$  [29].

The time domain approach for channel estimation has better performance than the frequency domain approach when the maximum length of the impulse response is significantly less than the number of subcarriers. A possible explanation for this behavior could be that the signal energy used to estimate each channel coefficient would be more for the time domain approach, where the coefficients to estimate in this case are less than for the frequency domain approach, being the transmitted signal to make the estimation (training symbols) the same [30]. In counter part the time domain approach is computationally more complex.

Additional considerations about PACE can be found in [31], [32], [33].

## 4.2 Decision Directed Channel Estimation

*Decision Directed Channel Estimation* (DDCE) is a technique for channel estimation which does not need specific pilot signals for channel estimation. This technique is based in the update of the channel state knowledge performed symbol by symbol. For these updates the transmitted data are used. The process applied symbol by symbol can be described in two steps.

---

<sup>1</sup><http://mathworld.wolfram.com/Moore-PenroseMatrixInverse.html>.

1.- Using the channel information corresponding to time  $n - 1$  ( $\tilde{H}_{k,n-1}$ ), the symbol  $n$  is calculated.

$$\hat{S}_{k,n} = \frac{R_{k,n}}{\tilde{H}_{k,n-1}} \quad (4.11)$$

Where  $\hat{S}_{k,n}$  is the component for subcarrier  $k$  in time  $n$  of the “equalized estimator” of the transmitted symbol  $n$ .  $\tilde{H}_{k,n-1}$  is the “corrected estimator” of channel transfer factor for subcarrier  $k$  in time  $n - 1$  and  $R_{k,n}$  is the component for subcarrier  $k$  in time  $n$  of the received symbol  $n$ .

2.- Using the “corrected estimator” of the transmitted symbol  $S_{k,n}$  and the received symbol  $R_{k,n}$ , the channel state knowledge is updated.

$$\hat{H}_{k,n} = \frac{R_{k,n}}{\tilde{S}_{k,n}} \quad (4.12)$$

Where  $\hat{H}_{k,n}$  is the component for subcarrier  $k$  in time  $n$  of the “estimator” of the channel transfer factor.  $R_{k,n}$  is the component for subcarrier  $k$  in time  $n$  of the received symbol  $n$  and  $\tilde{S}_{k,n}$  is the component for subcarrier  $k$  in time  $n$  of the “corrected estimator” of the transmitted symbol  $n$ .

This process is repeated for each symbol (in each subcarrier) and in this way the channel state knowledge is maintained updated and received symbols are corrected.

The relation between  $\tilde{H}_{k,n}$  and  $\hat{H}_{k,n}$  can be given, e.g., for an  $\alpha$ ,  $\beta$  filter as it is indicated in (4.13) and (4.14).

$$\tilde{H}_{k,n} = (1 - \alpha)(\tilde{H}_{k,n-1} + \tilde{\Delta}_{k,n-1}) + \alpha\hat{H}_{k,n} \quad (4.13)$$

$$\tilde{\Delta}_{k,n} = (1 - \beta)\tilde{\Delta}_{k,n-1} + \beta(\hat{H}_{k,n} - \tilde{H}_{k,n-1}) \quad (4.14)$$

For obtaining  $\tilde{S}_{k,n}$  starting from  $\hat{S}_{k,n}$  we have to take  $\hat{S}_{k,n}$ , make a demodulation (making a “Hard Decision” [8]) and another modulation. In this way we obtain the “corrected estimator” of the transmitted symbol  $n$  starting from the “equalized estimator” of the transmitted symbol  $n$ , further information can be seen [34]. The followed sequence for each time  $n$  is

$$\tilde{H}_{k,n-1} \rightarrow \hat{S}_{k,n} \rightarrow \tilde{S}_{k,n} \rightarrow \hat{H}_{k,n} \rightarrow \tilde{H}_{k,n}$$

More information about *decision directed channel estimation* can be found in [35], [36], [37] and [38].

### 4.2.1 Comparison between DDCE and PACE

DDCE and PACE are both coherent demodulation techniques, in both cases the received signal ( $R_{k,n}$ ) is

$$R_{k,n} = H_{k,n} \cdot S_{k,n} + N_{k,n} \quad (4.15)$$

and the transmitted signal ( $S_{k,n}$ ) can be estimated as

$$\hat{S}_{k,n} = \frac{R_{k,n}}{\hat{H}_{k,n}} \approx S_{k,n} \quad (4.16)$$

which means that both techniques need channel estimation ( $\hat{H}_{k,n}$ ).

The performance for DDCE is affected by the performance of the particular error correction code applied by the system, some works have found that PACE outperforms the results for DDCE under all fading conditions [39]. In [39] were considered Space Time Block Codes (STBC) and Space Frequency Block Codes (SFBC) OFDM systems, which are a particular class of MIMO systems explained later in Chapter 7, see also [40]. It is clear that for DDCE the performance depends on the number of errors in the decided or decoded symbols used to estimate the channel and then it is susceptible of error propagation [34], [39]. Only in some particular cases where the number of decision errors is very low, DDCE outperforms PACE [41].

## 4.3 Differential Modulation, Incoherent Demodulation

In this chapter have been discussed some techniques for channel estimation. Channel estimation is completely necessary when coherent demodulation is used, in this case the channel must be estimated and the received signals corrected before demodulating and decoding.

When differential modulation and incoherent demodulation is used channel estimation is not necessary. It is because the signal is sent in the quotient between two successive transmitted elements (successive in the direction of time or frequency); that means that the effect of the channel over these two successive elements is the same and then it is going to be cancelled when the quotient at the receiver is performed. That makes the system more simple and also less overhead is needed. For these reasons in this thesis a particular differential modulation with incoherent demodulation will be proposed.

### 4.3.1 Differential Modulation in Time Direction for an OFDM System

Considering an OFDM system with a differential modulation in the direction of time, the transmitted value in subcarrier  $k$  and time symbol  $l$  will be  $C_{k,l}$

$$C_{k,l} = S_{k,l} \cdot C_{k,l-1} \quad (4.17)$$

where  $S_{k,l}$  is the constellation point containing the user information after the modulation and  $C_{k,l-1}$  is the previous transmitted value in subcarrier  $k$  (time symbol  $l-1$ ).  $C_{k,l}$ ,  $S_{k,l}$  and  $C_{k,l-1}$  are complex values, the use of capital letters here denotes that the equations are written in the space of frequency.

At the receiver it will be received

$$R_{k,l} = C_{k,l} \cdot H_{k,l} + N_{k,l} \quad (4.18)$$

The previous received value is

$$R_{k,l-1} = C_{k,l-1} \cdot H_{k,l-1} + N_{k,l-1} \quad (4.19)$$

Assuming

$$H_{k,l} = H_{k,l-1} \quad (4.20)$$

by neglecting the noise, it can be obtained

$$D_{k,l} = \frac{R_{k,l}}{R_{k,l-1}} \simeq \frac{C_{k,l}}{C_{k,l-1}} = S_{k,l} \quad (4.21)$$

Observe that (4.21) is also valid when  $H_{k,l} \simeq H_{k,l-1}$ , which is valid unless the channel is a very time variant channel.

From (4.21) it is clear that with this differential procedure, no channel estimation is needed to be able of recovering the transmitted information.

Fig. 4.2 shows a block diagram of the differential modulator and incoherent demodulator described previously.

### 4.3.2 Differential Modulation in Frequency Direction for an OFDM System

For an OFDM system with a differential modulation in the direction of frequency, the transmitted value in subcarrier  $k$  and time symbol  $l$  will be  $C_{k,l}$

$$C_{k,l} = S_{k,l} \cdot C_{k-1,l} \quad (4.22)$$

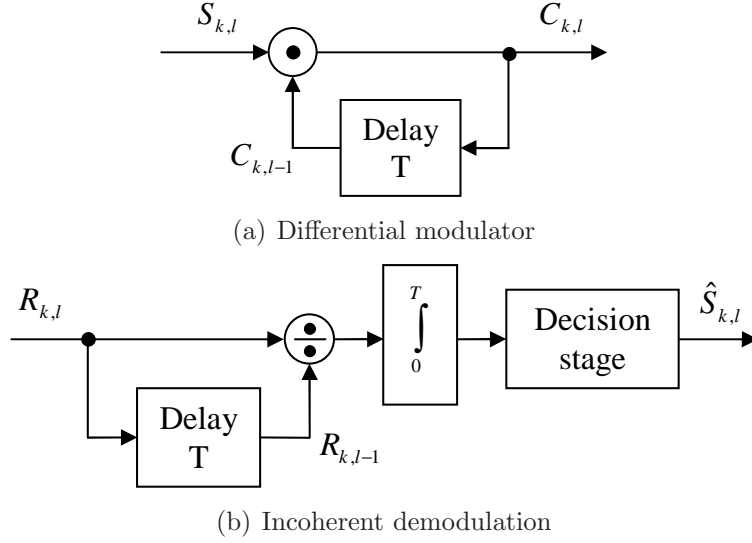


Figure 4.2: Block diagram of differential modulation and incoherent demodulation in time direction.

where  $C_{k-1,l}$  is the transmitted value in subcarrier  $k - 1$  (for the same time symbol  $l$ ).

The received signal in subcarrier  $k$  will be

$$R_{k,l} = C_{k,l} \cdot H_{k,l} + N_{k,l} \quad (4.23)$$

While the received signal in subcarrier  $k - 1$  will be

$$R_{k-1,l} = C_{k-1,l} \cdot H_{k-1,l} + N_{k-1,l} \quad (4.24)$$

Assuming

$$H_{k,l} = H_{k-1,l} \quad (4.25)$$

by neglecting the noise, it can be obtained

$$D_{k,l} = \frac{R_{k,l}}{R_{k-1,l}} \simeq \frac{C_{k,l}}{C_{k-1,l}} = S_{k,l} \quad (4.26)$$

Observe that (4.26) is also valid when  $H_{k,l} \simeq H_{k-1,l}$ , which is valid unless the channel was a very frequency selective channel.

Eq. (4.26) shows that it is also possible to transmit information with a differential modulation in the direction of frequency.

Fig. 4.3 shows different alternatives to select the reference values (first transmitted values) in differential modulations. In (a) the modulation is carried out in the direction of time, starting from one reference value ( $R$ ) for each subcarrier. In (b) it is carried out in the direction of frequency starting from one reference value for each time slot. For avoiding the performance degradation due to the transmission of so many reference values, strategy (c) can be used where only one reference value is transmitted.

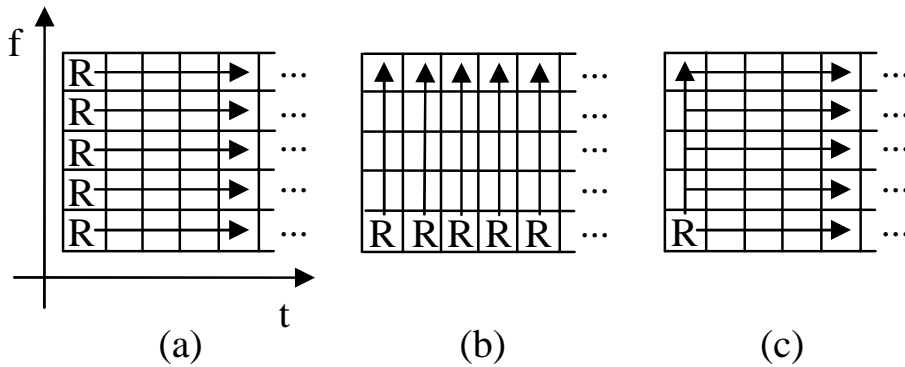


Figure 4.3: Alternatives for the use of reference values in differential modulations for OFDM systems.

### 4.3.3 Comparison between Coherent and Incoherent Demodulation Schemes

As it was discussed previously, differential modulation schemes have the advantages of simplicity and less overhead needed given that channel estimation is not necessary.

In counter part, the performance of a coherent system with ideal channel knowledge is around 3 dB better than the corresponding one for the differential system (see Section 5.1 in [42]). When the hypothesis of ideal channel knowledge is changed by a more realistic one, as obtaining the channel estimation by a linear interpolation of certain pilots (approximately 3% of the total subcarriers), this improvement is reduced to approx. 1.5 dB [43]. If it is also considered that in coherent systems the useful bandwidth is reduced because of pilots, then the effective performance of coherent system is not so different than the corresponding to differential systems. This is a good

motivation to invest effort in optimizing differential systems which is one of the main contributions of this thesis.

Fig. 4.4 shows the difference in performance between a 64-PSK coherent demodulation with ideal *Channel State Information* (CSI) and the corresponding incoherent one for a single carrier Single Input Single Output (SISO) system, in an uncorrelated Rayleigh fading channel.

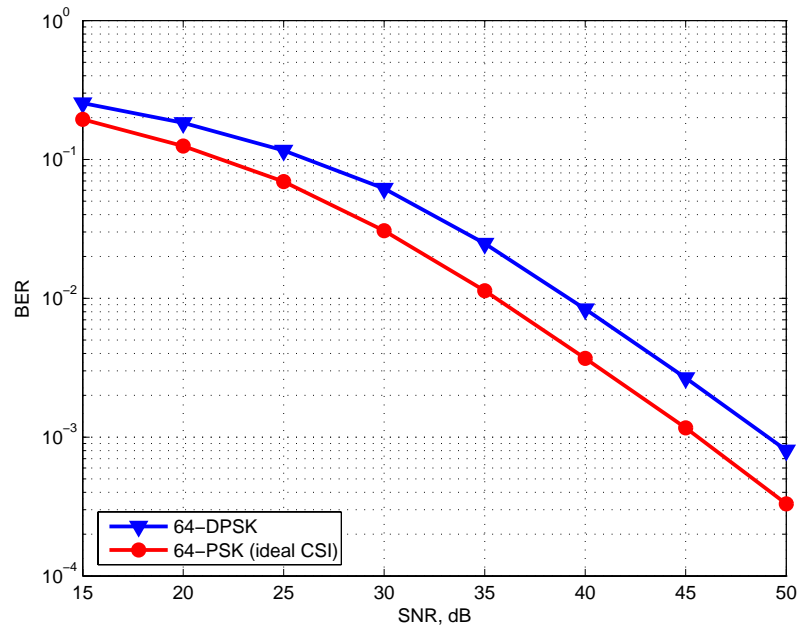


Figure 4.4: Comparison between coherent (ideal CSI) and incoherent 64-PSK demodulations in an uncorrelated Rayleigh fading channel.



# Chapter 5

## Link Adaptation and Diversity

### 5.1 Link Adaptation in OFDM Systems

The Link Adaptation (LA) topic is composed of all those techniques developed to allow the adaptation of the communication to the conditions of the particular link. For this reason it is a very important topic in any wireless communication system.

This topic could be divided into two categories, one composed by those LA techniques used in a “single cell environment” and those used in a “cellular environment” (several cells) -some times identified as Self Organizing Radio Resources Management (SORRM)-.

The techniques discussed in this section can be applied for OFDM systems, but they are not exclusive for this technique. Some of them are extensively used with other transmission techniques also.

#### 5.1.1 Selection of Best Subcarriers

In OFDM systems some subcarriers may suffer a deep degradation. When the *Channel State Information* (CSI) is available at the transmitter some adaptive techniques can be applied in order to mitigate the performance degradation due to this situation. For example, in [44] is discussed an “*Adaptive Subcarrier Selection*” technique, where the idea is to exclude subcarriers affected by deep fading and only use those subcarriers with high channel gain factors.

In the context of cellular systems, the assignation of its best subcarrier to

each user produces a general improvement of the performance for the whole system.

### 5.1.2 PHY Mode Selection

Considering an OFDM system, the idea is to select one modulation scheme and code rate from a set of allowed combinations of them (*PHY modes*). The selection is made considering the channel conditions and then applied to all subcarriers. This selection determines the Bandwidth Efficiency (BE) of the transmission. Usually the criterion is to use the best combination that the channel allows; with a very bad channel is not reasonable to use a “high *PHY mode*” (*PHY mode* of high BE) because it would produce a high BER, degrading the transmission instead of improving it.

Some results for *PHY mode* selection in the OFDM based WLAN standards HyperLAN/2 and IEEE802.11a can be found in [45] and [46] respectively.

### 5.1.3 Dynamic Fragmentation

The idea of this technique is varying the packet length in order to diminish the probability of having a packet error (it diminishes when the length of the packet is reduced). A packet is considered to be erroneous when at least one of its data bits is erroneous.

*Packet Error Rate* (PER) directly affects the effective throughput of the system and assuming uncorrelated bit errors can be estimated by means of the BER as follows:

$$PER = 1 - (1 - BER)^{N_{bpp}} \quad (5.1)$$

Where  $N_{bpp}$  is the number of data bits per packet. This result is quite easy to be obtained from  $(1 - PER) = (1 - BER)^{N_{bpp}}$ , where  $(1 - PER)$  is the probability of having a not erroneous packet and  $(1 - BER)^{N_{bpp}}$  is the probability of having  $N_{bpp}$  not erroneous bits (all of them in the packet).

From (5.1) it is clear that reducing  $N_{bpp}$ ,  $PER$  is reduced; but by reducing the packet length, the protocol overhead is increased which reduces the performance. For this reason the goal in this LA technique is to find an optimum length for the packet in order to diminish the PER without increasing too much the protocol overhead.

### 5.1.4 Subcarrier Specific Adaptive Modulation

Previously *PHY mode* selection was discussed where one combination of modulation scheme and code rate are applied to all subcarriers. But it is also feasible to apply different modulation schemes to different subcarriers. In a frequency selective channel, in the same instant, one subcarrier can have a good SNR while another can have a bad one; then in order to optimize the use of resources, the first one can use a high order modulation scheme (modulation scheme of high BE) and the second one a low one. That is *Adaptive modulation*, selecting a specific modulation scheme for each subcarrier considering its specific channel transfer factor; observe that when independent identically distributed noise is considered, it is the same that considering its specific SNR.

This technique of selecting a specific modulation scheme for each subcarrier is also named *bit loading* because by determining the specific modulation scheme to use for a given subcarrier is directly determined the number of data bits to be transmitted in that subcarrier in one OFDM symbol. Some examples of this technique can be found in [47], [48].

### 5.1.5 Joint Optimization DLC and PHY Layers

The joint optimization of the *Data Link Control* (DLC) and *Physical* (PHY) layers has some advantages with respect to the independent optimization of them. Improved results can be obtained by considering simultaneously the conditions in both layers.

The main goal of these proposals is to be able of considering simultaneously the statistics of the data sources and the statistics of the time variant and frequency selective radio channels. With these two sources of information is possible to make a highly efficient management of resources. Some work has been developed in this area and in some cases some “*cross layer oriented protocols*” has been proposed, further information can be found in [49].

### 5.1.6 Water-Filling

The *Water-Filling* approach also called *Water-Pouring* [50] allows an optimization by using a power allocation technique. It consists in giving more power and using higher order modulation schemes to those subcarriers with higher SNRs and less power and using lower order modulation schemes to those with lower SNRs. The subcarriers with strong attenuation are not

used. The idea is to maximize the data rate for a given average transmit power, in this way the use of resources is optimized. For applying water-filling, channel knowledge at the transmitter side is needed.

Considering a multicarrier system in a frequency selective channel there will be some subcarriers with very bad SNR, because of the great attenuation that some of them can suffer in this kind of channels (Fig. 5.1 shows an example). It is clear that to allocate power in these subcarriers, i.e. trying

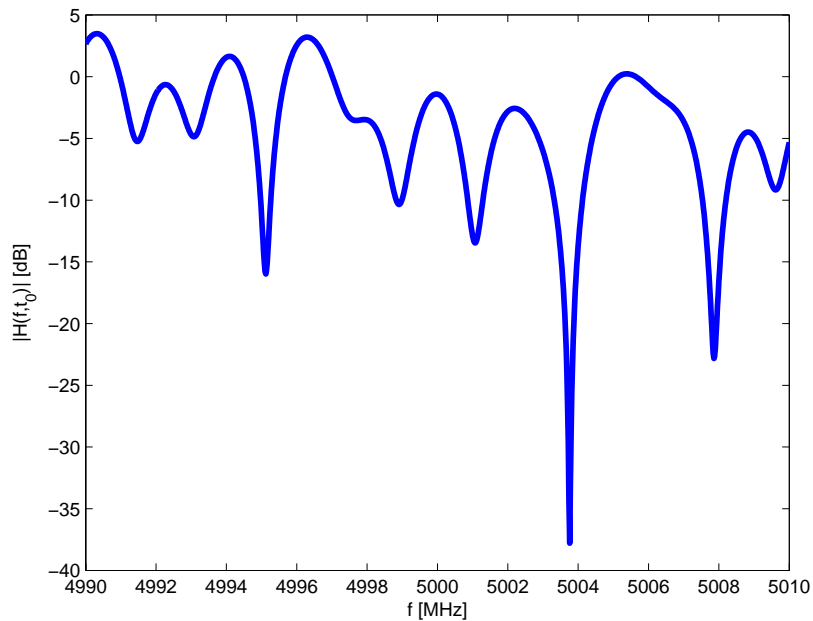


Figure 5.1: Channel *transfer function* ( $H(f, t)$ ) for a given time instant ( $t = t_0$ ).

to transmit information in these subcarriers can be a waste of power. The water-filling approach consists in trying to apply a spectral shaping in order to assign more power to those subcarrier with higher channel gain coefficients to optimize the use of these channels. Assuming a flat spectrum for the noise, to have a good channel gain coefficient for a given subcarrier is equivalent to have a good SNR for it.

Usually water-filling is applied in two steps, the first step is *power allocation*, where the power to allocate to each subcarrier is decided. The second

one is *bit loading*, where the number of bits to use in each subcarrier is calculated considering the allocated power in them.

### Power Allocation

Concerning the power allocation, it can be defined

$$\gamma(f) = \frac{|H(f)|^2}{N(f)} \quad (5.2)$$

where  $\gamma(f)$  is the channel *SNR function*,  $H(f)$  is the channel *transfer function* and  $N(f)$  is the power spectral density of the noise. Considering now  $P(f)$  as the power spectral density of the transmitted signal, can be said that the total capacity in the bandwidth  $B$  is

$$C_{Tot} = \int_B \log_2(1 + P(f)\gamma(f))df \quad (5.3)$$

The idea is to maximize the capacity with respect to  $P(f)$  under the constraint of transmitting a power smaller or equal to  $P$ , it is

$$\int_B P(f)df \leq P \quad (5.4)$$

This maximization can be done by using Lagrange multipliers [30] and the result is

$$P(f) = P_{Alloc}(f) = \left[\mu - \frac{1}{\gamma(f)}\right]^+ \quad f \in B \quad (5.5)$$

where  $P_{Alloc}(f)$  is the power to allocate in order to maximize the total capacity under the constraint of (5.4).  $[\cdot]^+$  means that all the negative values are taken as 0, i.e. there is no power allocated for the negative values.  $\mu$  is taken such that  $P_{Alloc}(f)$  satisfies (5.4) with the equality.

Then by substituting (5.5) in (5.3) the optimized total capacity for the band  $B$  is obtained.

$$C_{Tot-Opt} = \int_B [\log_2(\mu\gamma(f))]^+ df \quad (5.6)$$

Fig. 5.2 shows a graphic representation of the algorithm, where the “water” is the power and the “bottom of the container to fill” is related with the channel *SNR function* by the equation  $\frac{1}{\gamma(f)} = \frac{N(f)}{|H(f)|^2}$ . This figure shows the application of Water-Filling in the direction of the frequency, but this technique can be also applied in two dimensions considering time and frequency [51].

After the power allocation was performed the second step, bit loading, can be performed for the given power allocation.

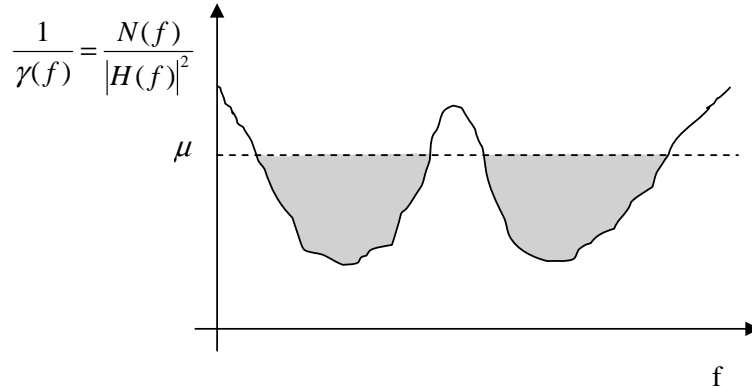


Figure 5.2: Water-Filling representation.

### Bit Loading

The main idea for *Bit loading* is to load the subchannels (subcarriers) with a different number of bits according to their SNR values. In this way the BER is not increased by overloading a subchannel with low SNR value and a subchannel with high SNR value can also be used in a more efficient way. It means that good subchannels will have more load than the bad ones, which results in an effective use of available resources.

Bit loading is extensively used in multicarrier systems over stationary subchannels, where the needed measure of their SNR is not very demanding.

Assuming  $N$  subcarriers in the band  $B$  ( $B = N \cdot \Delta f$ ), by using (5.5) can be calculated  $P_i$ , the power to assign to the subcarrier  $i$  with  $1 \leq i \leq N$ . Bit loading will assign a rate of bits for each subcarrier according to the assigned power  $P_i$  in order to have a reliable transmission over each subcarrier; optimizing in this way the use of the channel.

As shown in this section, there is a big set of techniques under the umbrella of LA. In last years has also been considered the cooperative use of multiple air interface standards for improving a single communication. These techniques could be considered as high level LA techniques to provide improved performances (more robust communications, extended areas of coverage and grater throughputs) [52], [53].

## 5.2 Diversities

To improve the performance some diversity techniques are considered. In this way exists: Delay, Frequency, Space, Time, User and Polarization diversity.

### 5.2.1 Delay Diversity

This is a useful technique for time variant channels, the main idea is to alter the order in the transmission sequence of the symbols, with the intention that the channel affects them in a different way. One particular class of delay diversity is *cyclic delay diversity*, in this case -used with Multiple Input Single Output (MISO) or MIMO systems- a certain number of symbols is taken and transmitted in different order, with different delays, by different antennas. In this way one particular channel state able of corrupting one time symbol is not able of corrupting none symbol due to they are transmitted in other different time symbols (time slot) by the other antennas; further explanations can be seen in [54].

### 5.2.2 Frequency Diversity

This diversity technique is particularly effective in frequency selective channels. Examples of wireless systems that take advantages of this kind of diversity are the spread spectrum systems as Frequency Hopping Spread Spectrum (FHSS) systems or Direct Sequence Spread Spectrum (DSSS) systems. These techniques are successfully used for example for point to point or point to multipoint commercial wireless communications systems covering distances of several kilometers (e.g., BreezeNET DS11 from Alvarion<sup>1</sup>).

In the case of FHSS systems the transmission frequency is changed at regular small time intervals. The original purpose, was a military purpose, the idea was trying to change the transmission frequency after small intervals of transmission in order that the enemy was not able to retune his system to obtain the full transmission. The reception is made with a receiver which knows the Frequency Hopping pattern (sequence in which the different frequencies are used). These systems are also useful in commercial applications to cope with frequency selective channels. As they use different frequencies for the transmission, then they do not suffer too much when a range of frequencies is deeply faded.

---

<sup>1</sup>[http://www.alvarion.com/upload/contents/291/ds11outdoor\\_rev.e.pdf](http://www.alvarion.com/upload/contents/291/ds11outdoor_rev.e.pdf).

In the case of DSSS systems the approach is different, here the signal is passed through a spreading function and in this way it is distributed over all the band. Then the influence of a strongly faded range of frequencies has not so big impact over the transmission as it had been located in this particular range. The spreading function simply consists in multiplying the sequence of data for a pseudorandom sequence of 1 and -1 of higher frequency. Then the energy of the data sequence is spread in a wider band. In the receiver the sequence of data is recovered just by multiplying the received signal by the same pseudorandom sequence used in the transmitter.

This idea of distributing the signal over all the band in order to cope with particularly attenuated ranges of frequencies is also used in Code Division Multiplex Access (CDMA) systems. Here the signal is coded by using orthogonal codes as a way of multiplexing the information over the channel (each subchannel has a particular orthogonal code and due to this it can be separated from other subchannels in the receiver).

### 5.2.3 Spatial Diversity

*Spatial diversity*, some times also called *antenna diversity*, is a way of diversity that involves the use of several antennas in the transmitter and/or in the receiver. These antennas have to have an adequate separation between them in order to minimize the mutual coupling and maximize the spatial diversity effects [1]. That is the kind of diversity that exploit the MIMO systems.

This kind of diversity is subdivided in two types, *receive diversity* when multiple receive antennas are used and *transmit diversity*, when multiple transmit antennas are used. The first type is quite easy to implement and the challenge is how to use the multiple received versions of the transmitted signal in order to obtain the major improvement.

### Multiple Receive Antennas

When multiple receive antennas are used as shown in Fig. 5.3, a combining technique has to be applied in order to combine the information received through these antennas. *Selection Combining*, *Equal Gain Combining* and *Maximum Ration Combining* are some well known combining techniques.

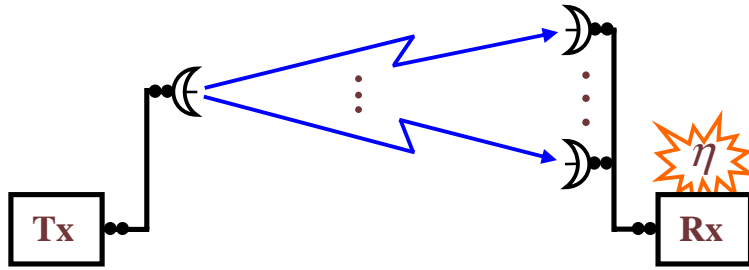


Figure 5.3: Receive diversity technique.

### Selection Combining

*Selection combining* consists in choosing from the signals received by the multiple receive antennas, that one which has the highest SNR. This technique is probably the simplest one and also has the advantage that it does not require additional RF chains [30], what is an interesting saving of complexity and money. These advantages justify the adoption of this technique in the IEEE 802.11b standard.

Selecting the antenna with highest SNR is very simple when the noise is assumed as independent identically distributed Gaussian noise, in this case is only necessary to choose the signal of the receive antennas which has highest power.

### Equal Gain Combining Diversity

This technique consists just in making an average of the decoded signals in the receiver. One example of the application of this technique can be read in Section 7.4.

### Maximum Ratio Combining Diversity

In Maximum Ratio Combining (MRC) the signal obtained through each antenna is combined in order to maximize the instantaneous SNR. In practice, considering that the transmitted signal is the same for all the receive antennas, this maximization is made by considering a weighted average, where the weighting factors are the channel gain coefficients for each branch previously co-phased [8]. In this way the signal in each receive antenna is weighted by its corresponding fading attenuation in order to perform this weighted average [30].

MRC is the optimum solution, having better performance than the two previous ones. In Section 7.4 is proposed an adaptation of this technique for a particular differential system. Also some results to compare the performance of some of these receive diversity techniques over this particular case are provided there.

## Multiple Transmit Antennas

Transmit diversity is achieved when multiple antennas are used at the transmitter side (as shown in Fig. 5.4). This kind of diversity is commonly used in the downlink of a cellular system, due to it is much more convenient to put several antennas in the base station and one in the mobile terminal than the other way around.

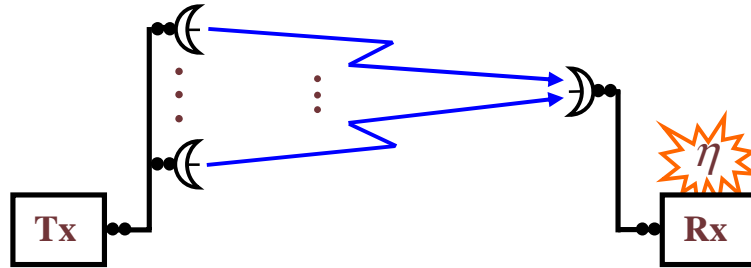


Figure 5.4: Transmit diversity technique.

One very well known example of transmit diversity is Alamouti scheme [40]. An adaptation of Alamouti proposition for the differential case is considered in detail in Chapter 7.

Another topic related with the use of multiple antennas is the mutual coupling between them and the grade of correlation between the subchannels constituting the MIMO channel. In this work the mutual coupling is assumed null and also no correlation between the mentioned subchannels. For checking the influence due to mutual coupling the reader can see [1] and [55].

### 5.2.4 Time Diversity

*Time diversity* exists when signals representing the same information are transmitted in different time intervals. In this way a temporally bad condition of the channel, able to corrupt the received signal, can be overcome because this information is also received in a different time interval hopefully

with better channel conditions. For being effective these retransmissions in different time intervals, they should be spaced by time intervals that exceed the coherent time of the channel (see Section 2.5.3).

One well known technique to achieve *time diversity* without adding any overhead is *bit interleaving* as it was explained in Section 3.2.1. Another way of achieving *time diversity* is by using channel coding (see Chapter 8).

### 5.2.5 Multiuser Diversity

This is one technique belonging to the category of LA techniques used in “cellular environments”. In this case the idea is to assign the subcarriers to that users who has better conditions to use them, as a way of obtaining an optimum use of resources.

One well known method to make this subcarrier allocation is Hungarian method. Each user has a given power of the channel transfer factor for each subcarrier, Hungarian method tries to distribute subcarriers between users in order to maximize the sum of the powers with which they are used.

### 5.2.6 Polarization Diversity

*Polarization diversity* refers to the possibility of using different polarizations in a wireless system. Usually this diversity produces a isolation of several *decibels* between antennas using horizontal and vertical (linear) polarization. The polarization of a transmission is determined by the direction of the Electric field, which is determined by the design of the antenna [1].

In some cases to implement polarization diversity is only needed to rotate  $90^\circ$  the position of the antenna (for some linear polarized antennas). The capacity of an antenna of attenuating the signals received with cross polarization is defined by the antenna parameter *Cross Polarization Discrimination* (CPD). It is quite common to find antennas with a CPD between 6 and 20 dB which allows to make a more effective reuse of frequencies, due to this possibility of using different polarizations.



# Chapter 6

## MIMO Systems

Multiple Input Multiple Output (MIMO) is one of the most active areas in wireless systems. The reason is that MIMO offers an alternative to increase the performance of a wireless system without needing more spectrum; only by increasing the number of antennas (as shown in Fig. 6.1), related components and the complexity of the system. Considering the extremely high cost of the radio electric spectrum and the always falling prices of electronic systems, this is a very attractive option for increasing the channel capacity.

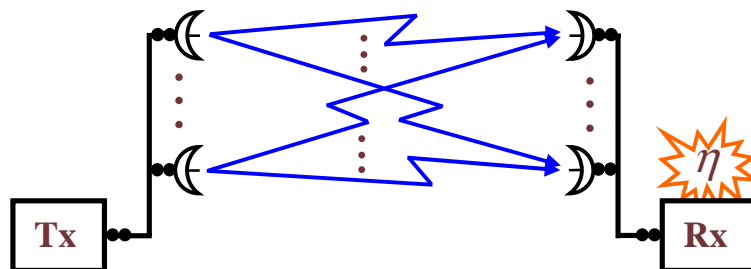


Figure 6.1: Scheme of a MIMO system.

Usually multipath fading is a cause of degradation for wireless systems, but in the case of MIMO, this random fading is used to improve the performance [56], [57], [58]. MIMO can also exploit the multipath delay spread [59], [60]. These are key features of MIMO systems.

MIMO techniques can be classified according to the *channel state information* required in the transmitter and in the receiver. Table 6.1 shows a classification according to this criterion. For a description of the techniques mentioned in Table 6.1 see Chapter 7 and [55], [50]. From this table the simplicity of Differential Space Time Block Code (DSTBC) techniques can be

Table 6.1: Classification of MIMO techniques considering the required CSI.

Rx \ Tx	Full	Partial	None
Full	SVD + bit loading, Eigenbeamforming	Tx selection diversity	STBC, SFBC, Spatial multiplexing
None	Joint transmission		DSTBC

considered, from the point of view that these techniques do not require CSI; this is a good reason to try to improve the performance of these techniques.

## 6.1 MIMO Channel Models

MIMO is a technique which achieves spatial diversity by using more than one antenna in the transmitter and in the receiver, there are several MIMO techniques proposed to take advantage of this spatial diversity. In this section an introduction to this topic will be presented. In general these techniques provide more reliable (less BER for the same SNR) or higher data rate (for the same BER) communications without increasing the used bandwidth, which generally is a limited and very expensive resource.

Considering a system with  $N_T$  transmit antennas and  $N_R$  receive antennas the MIMO channel is composed by a set of individual channels between each transmit antenna and each receive antenna, as it is indicated in Fig. 6.2.

If the channel is frequency-nonselctive, as it is for each subcarrier in an OFDM system, then the MIMO channel can be represented by a  $N_R \times N_T$  matrix  $H$ .

$$H = \begin{bmatrix} h_{1,1} & h_{1,2} & \dots & \dots & \dots & h_{1,N_T} \\ h_{2,1} & h_{2,2} & \dots & \dots & \dots & h_{2,N_T} \\ \dots & \dots & \dots & \dots & \dots & \dots \\ h_{i,1} & h_{i,2} & \dots & h_{i,j} & \dots & h_{i,N_T} \\ \dots & \dots & \dots & \dots & \dots & \dots \\ h_{N_R,1} & h_{N_R,2} & \dots & \dots & \dots & h_{N_R,N_T} \end{bmatrix} \quad (6.1)$$

In this matrix, the element  $h_{i,j}$  represents the channel transfer factor between the transmit antenna  $j$  and the receive antenna  $i$  (arriving to  $i$  coming from  $j$ ). That means e.g. that if only the transmit antenna  $j$  transmit a signal  $c_j$  and all the other transmit antennas keep silence, then the received signal in receive antenna  $i$  ( $r_i$ ) will be  $r_i = h_{i,j} \cdot c_j + n_i$ , where  $n_i$  is channel noise added

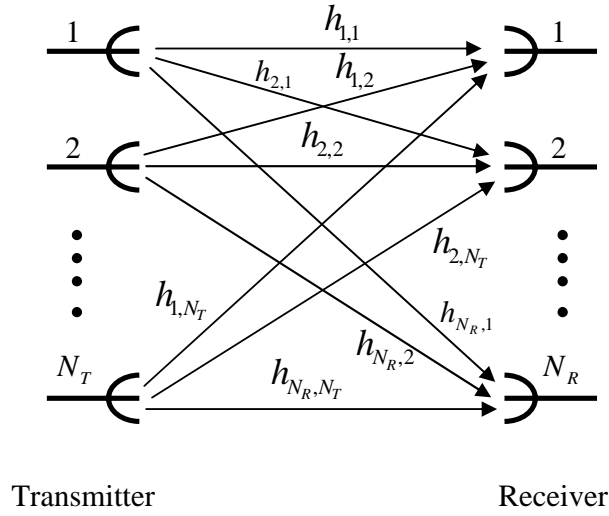


Figure 6.2: MIMO Channel for  $N_T$  transmit antennas and  $N_R$  receive antennas.

in the receiver. In matrix notation we can represent the received signal  $\vec{r}$ , for each time slot, as

$$\vec{r} = H \cdot \vec{c} + \vec{n} \quad (6.2)$$

Where  $\vec{r}$  is the received signal (a  $N_R \times 1$  vector with elements  $r_i$ ),  $\vec{c}$  is the transmitted signal (a  $N_T \times 1$  vector whose elements are  $c_j$ ) and  $\vec{n}$  is the channel noise added in the receiver (a  $N_R \times 1$  vector whose elements are  $n_i$ ).

In a MIMO system it is necessary to specify how the data are sent to the transmit antennas and how they are collected from the receive antennas, these tasks are performed by the *MIMO encoder* and the *MIMO decoder* respectively as it is shown in Fig. 6.3.

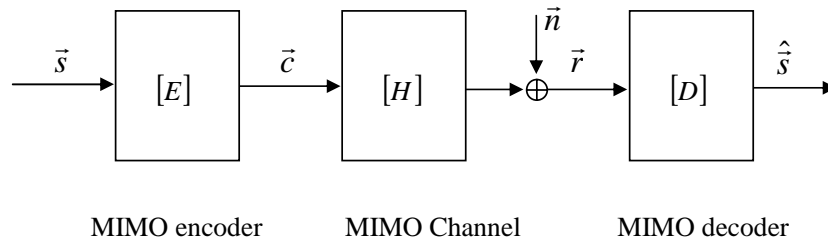


Figure 6.3: Representation of a MIMO system.

Here  $\vec{s}$  is the information signal (also a vector) and  $\hat{\vec{s}}$  is the estimator of

the information signal ( $\vec{s}$ ) obtained in the receiver. The relation between  $\hat{\vec{s}}$  and  $\vec{s}$  is given by

$$\hat{\vec{s}} = D \cdot (H \cdot E \cdot \vec{s} + \vec{n}) \quad (6.3)$$

In Chapter 7 a particular example of a *MIMO encoder* is described. In Section 7.4 two particular examples of *MIMO decoders* are explained. These examples are based in a particular MIMO system  $2 \times n$  with  $n=2$  or  $3$  (2 transmit antennas and 2 or 3 receive antennas) called Differential Space Time Block Codes which will be explained in Chapter 7.

## 6.2 MIMO Channel Capacity

Claude Shannon, based in notions of *mutual information* between the input and the output, in the late 1940s proposed a limit for the channel capacity ( $C$ ) [61], [62], [63]. Shannon defined  $C$  as the maximum value of the mutual information considering all possible input distributions. This postulation was very promising at that time predicting that the existent telephone lines could give 300 times more throughput than the used in that moment [8]. Shannon limit is still today very useful, giving a clear idea of how far is one system from its optimum performance.

For analyzing MIMO channel capacity first we are going to discuss the channel capacity for the SISO case. For the SISO case, for a time-invariant AWGN channel the capacity is given by

$$C = B \cdot \log_2 \left( 1 + \frac{S}{N} \right) \quad (6.4)$$

Where  $C$  is the channel capacity,  $B$  is the bandwidth of the system and  $\frac{S}{N}$  is the signal to noise ratio.

Basically this limit says that it is not possible to transmit information successfully faster than the limit established by  $C$ . If the transmitter transmits at a rate higher than  $C$ , the number of errors in the reception will limit the successful rate to a value smaller or equal to  $C$ .

For proving it Shannon has used the concept of *mutual information* between the input  $x$  and the output  $y$  of a channel. For a system with an input  $x[i]$  at a given time  $i$ , and an output  $y[i]$  in the presence of a discrete time AWGN channel. Where the relation between  $y$  and  $x$  is  $y[i] = x[i] + n[i]$ . By considering a random input  $x$ , a memoryless time invariant channel and a random

output  $y$ , the *mutual information* of the channel can be written [8] as

$$I(X;Y) = \sum_{x,y} p(x,y) \log \left( \frac{p(x,y)}{p(x)p(y)} \right) \quad (6.5)$$

Where  $x$  and  $y$  are taken over all the possible values of  $x$  and  $y$ , being  $X$  and  $Y$  the input and output alphabets respectively. Typically  $\log$  is taken with base 2 and then the units for  $C$  are *bps*. Using this concept Shannon demonstrated that the channel capacity  $C$  is equal to the maximum value of the *mutual information* maximized over all the possible input distributions ( $p(x)$ ), this is

$$C = \max_{p(x)} I(X;Y) = \max_{p(x)} \sum_{x,y} p(x,y) \cdot \log \left( \frac{p(x,y)}{p(x)p(y)} \right) \quad (6.6)$$

*Mutual information* can also be written in terms of *entropy* as follows

$$I(X;Y) = \varepsilon(Y) - \varepsilon(Y | X) \quad (6.7)$$

It can be verified by considering that  $\varepsilon(Y)$  can be written as

$$\begin{aligned} \varepsilon(Y) &= - \sum_{y \in Y} p(y) \cdot \log(p(y)) \\ &= - \sum_{y \in Y} p(y) \cdot \log(p(y)) \cdot \sum_{x \in X} p(x | y) = - \sum_{x \in X, y \in Y} \log(p(y)) \cdot p(x,y) \end{aligned} \quad (6.8)$$

In the previous equation the definition of entropy was used, that  $p(x | y) = \frac{p(x,y)}{p(y)}$  and also that  $\sum_{x \in X} p(x | y) = \sum_{x \in X} \frac{p(x,y)}{p(y)} = \frac{p(y)}{p(y)} = 1$ .

And considering also that  $-\varepsilon(Y | X)$  can be written as follows

$$-\varepsilon(Y | X) = \sum_{x \in X, y \in Y} p(x,y) \cdot \log(p(y | x)) = \sum_{x \in X, y \in Y} p(x,y) \cdot \log \left( \frac{p(x,y)}{p(x)} \right) \quad (6.9)$$

In this case was used the definition of entropy for the conditional process [64] and that  $p(y | x) = \frac{p(x,y)}{p(x)}$ .

Then by using (6.7), (6.8) and (6.9) it is clear that

$$\varepsilon(Y) - \varepsilon(Y | X) = \sum_{x \in X, y \in Y} p(x,y) \cdot \log \left( \frac{p(x,y)}{p(x)p(y)} \right) \quad (6.10)$$

and we can say that *mutual information* can also be written in terms of entropy as it was done in (6.7).

As we have previously said Shannon proved that the capacity of the channel is equal to the maximum value of mutual information, maximized over all the possible input distributions; that, in terms of *entropy* can be written as

$$C = \max_{p(x)} I(X; Y) = \max_{p(x)} (\varepsilon(Y) - \varepsilon(Y | X)) \quad (6.11)$$

This is a general expression for the capacity of the channel.

### Extension of Channel Capacity for MIMO Case

The capacity for a MIMO channel is an extension of the capacity for the SISO case. In this case we can also consider the capacity defined by (6.11).

It can be demonstrated [8] that the channel capacity for the MIMO case can be written as

$$C = \max_{P_i: \sum_i P_i \leq P} \sum_i B \cdot \log_2 \left( 1 + \frac{\sigma_i^2 P_i}{N_0 B} \right) \quad (6.12)$$

Where  $N_0$  is the power spectral density of the noise,  $P_i$  and  $\sigma_i$  are respectively the power allocated to and the channel gain of the  $i_{th}$  parallel channel. These “ $i_{th}$  parallel channels” are the ones that result from a *parallel decomposition* of the MIMO channel (see Sections 10.1 and 10.2 in [8]).

Observing (6.12) it can be said that it is related with (6.4) for the SISO case. The Capacity for the MIMO case would be the maximization of the sum of SISO capacities for each  $i_{th}$  parallel channel. The maximization is made over the power allocation to each  $i_{th}$  parallel channel, fulfilling that  $\sum_i P_i \leq P$ , being  $P$  the total transmit power.

By solving the optimization, the expression for the channel capacity is

$$C = \sum_{i: \gamma_i \geq \gamma_0} B \cdot \log_2 \left( \frac{\gamma_i}{\gamma_0} \right) \quad (6.13)$$

Then with this sum over all the  $i$  that fulfill  $\gamma_i \geq \gamma_0$  the capacity for the MIMO channel is obtained.  $\gamma_0$  is a cutoff value for  $\gamma_i$  which is obtained as it is explained in the following procedure.  $\gamma_i$  is

$$\gamma_i = \sigma_i^2 \left( \frac{P}{N_0 \cdot B} \right) \quad (6.14)$$

Where  $\sigma_i$  is the channel gain of the  $i^{\text{th}}$  parallel channel.

The power allocation (for the maximization of the mutual information of the channel) must fulfill

$$\frac{P_i}{P} = \begin{cases} \frac{1}{\gamma_0} - \frac{1}{\gamma_i} & \gamma_i \geq \gamma_0 \\ 0 & \gamma_i < \gamma_0 \end{cases} \quad (6.15)$$

The procedure to calculate the channel capacity for a MIMO system is described in the following four steps.

- *Step 1:* First, starting from  $P, N_0, B, \sigma_i$  will be calculated all the  $\gamma_i$  values (one for each  $i^{\text{th}}$  parallel channels).
- *Step 2:* Then, assuming that the transmit power ( $P$ ) is completely allocated to all the  $i^{\text{th}}$  parallel channels we have the following condition to fulfill

$$\sum_{i=1}^N \frac{P_i}{P} = 1 \quad (6.16)$$

In order to obtain  $\gamma_0$  we are going to suppose in the first iteration that all the  $i^{\text{th}}$  parallel channels are used ( $\gamma_i \geq \gamma_0$ ). Under this supposition, using (6.16) and (6.15), we are going to calculate  $\gamma_0$ .

- *Step 3:* Now, we are going to check if the value obtained for  $\gamma_0$  fulfills ( $\gamma_i \geq \gamma_0$  for all considered  $\gamma_i$ ); if it is the case we continue in step 4. If it is not the case we must to recalculate  $\gamma_0$  using (6.16) and the corresponding option for  $\frac{P_i}{P}$  in (6.15) (imposing  $P_i = 0 \forall i / \gamma_i < \gamma_0$ ). Then we go again to the beginning of step 3 (to check if this time all considered  $\gamma_i$  -those whose associated  $P_i \neq 0$ - fulfill  $\gamma_i \geq \gamma_0$  or we have to recalculate again  $\gamma_0$ ). This iteration (step 3) is repeated up to all the considered  $\gamma_i$  satisfy  $\gamma_i \geq \gamma_0$ .
- *Step 4:* Once we have obtained a  $\gamma_0$  value which is smaller or equal than all the considered  $\gamma_i$ , we can use the considered  $\gamma_i, \gamma_0$  and  $B$  for using (6.13) to obtain the capacity value. The power allocated to each  $i^{\text{th}}$  parallel channel can be directly obtained from (6.15).

For more clarifications the reader can check the example 10.2 in page 304 of [8].

### 6.3 MIMO-OFDM Systems

Starting from Fig. 6.3 it is clear that a MIMO-OFDM system can be defined just by repeating the structure in this figure for each subcarrier in the OFDM system. This is a very simple way of implementing a MIMO-OFDM system but also a flexible and effective one. The system would be as it is represented in Fig. 6.4.

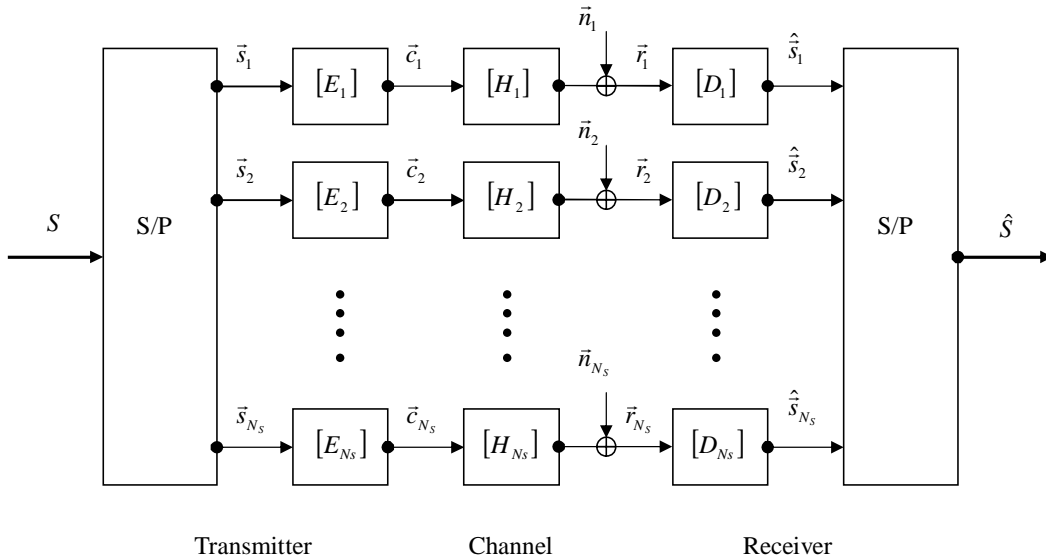


Figure 6.4: Representation of a MIMO-OFDM system.

Where  $[H_i]$  is the channel matrix corresponding to the subcarrier  $i$ ,  $[E_i]$  and  $[D_i]$  are the matrices corresponding to the MIMO encoder  $i$  and MIMO decoder  $i$  respectively.  $N_s$  is the number of subcarriers in the OFDM system.

From Fig. 6.4 is clear that this structure allows the use of different MIMO techniques (encoders-decoders) for each subcarrier, which represents an interesting grade of flexibility.

As it was explained, MIMO techniques increase the capacity of a telecommunication system. Fig. 6.5 shows an example of the difference in performance between a SISO system, using 64DPSK and a MIMO system using a 64PSK modulation scheme in Differential Space Time Block Codes (DSTBCs).

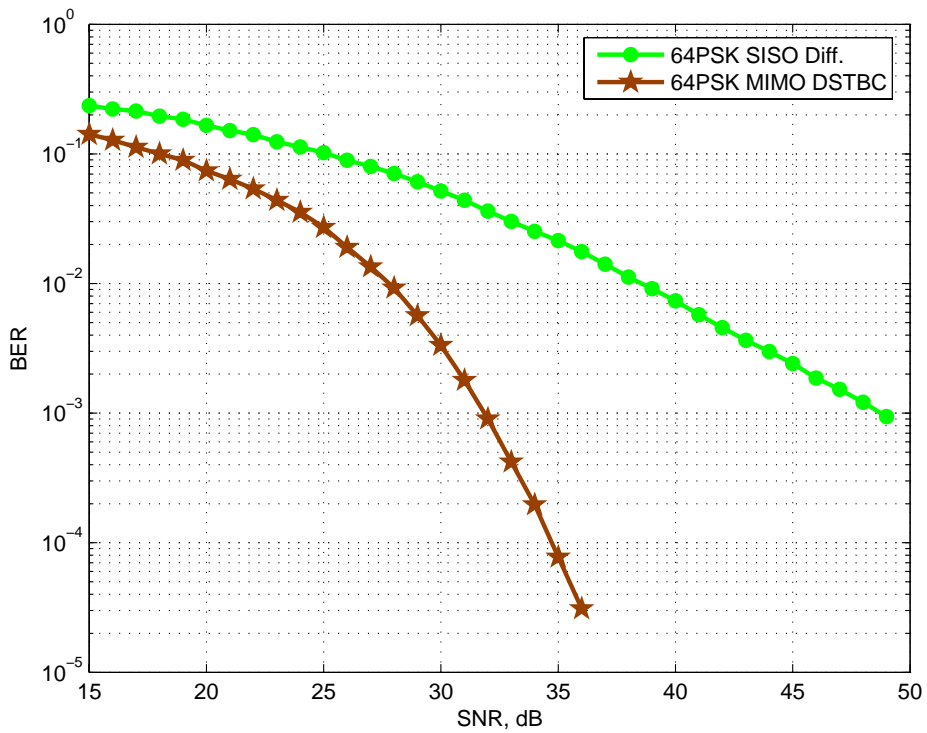


Figure 6.5: Comparison between differential 64PSK modulation in a SISO case and in a 2x3 MIMO case in an uncorrelated Rayleigh fading channel.



# Chapter 7

## Differential Space Time Block Codes

As it was already mentioned the spatial diversity given by MIMO systems is very promising and successful. That is the reason why so many different MIMO techniques have been proposed. In this chapter an improvement for one of these techniques will be discussed.

When we consider coherent transmission systems the radio channel *impulse response* or *transfer function* must be estimated precisely. In MIMO systems the radio channel must be estimated between all transmit and all receive antennas. In this case the test signal overhead and the computation complexity are increased. That is the reason why differential modulation schemes are especially interesting for MIMO systems, because with these systems the radio channel does not need to be estimated. Test signal overhead can be avoided and the computation complexity is significantly reduced.

Differential Space Time Block Codes (DSTBCs) are a very interesting kind of differential MIMO systems. The performance of these systems is quite good and the complexity is not too high. For this reason these systems have been studied in depth in this thesis. To get high channel capacity, higher level modulation schemes are needed. Reason why a new high level modulation technique, based in the use of new Amplitude and Phase Shift Keying (APSK) modulation schemes, will be proposed in this chapter.

### Origin and Evolution of DSTBC Schemes

The origin of DSTBC is in the Space Time Block Codes (STBCs) proposed in [40] and [65]. After that *differential unitary space time modulations* were

proposed [66], [67]. In this case the data bits to be transmitted are mapped in a unitary matrix which is differentially encoded with the previous transmitted matrix for obtaining the present matrix to transmit.

Later some extensions which consider a simultaneous differential phase and amplitude modulation have been proposed [68], [69], [70], [71]. Previous to the development of STBC some Differential Amplitude and Phase Shift Keying (DAPSK) schemes [72] have been proposed for the Single Input Single Output (SISO) system environment.

In this thesis a simultaneous amplitude and phase shift keying modulation technique is proposed for DSTBC schemes [73]. This differential encoding technique is combined with a new receiver structure.

## Description of DSTBC Schemes

A classical DSTBC procedure is described here for a 64-PSK modulation scheme over a 2x1 Multiple Input Single Output (MISO) system as the one in Fig. 7.1.

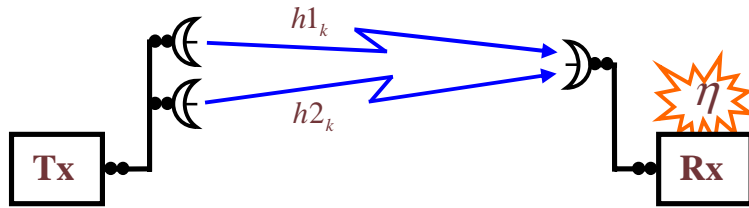


Figure 7.1: General Scheme of the considered MISO system.

The first step in the encoding procedure is to construct the 2x2 Block Code (BC) described by the 2x2 information matrix  $S_k$  which contains the two complex valued modulation symbols  $s1_k$  and  $s2_k$ .

$$S_k = \begin{bmatrix} s1_k & s2_k \\ -s2_k^* & s1_k^* \end{bmatrix} \quad (7.1)$$

By taking the amplitude of the 64-PSK modulation equal to  $\sqrt{0.5}$  the  $S_k$  is a unitary matrix.

For the assumed 64-PSK modulation scheme each matrix  $S_k$  transmits 12 bits by the two constellation points  $s1_k$  and  $s2_k$ .

The differential modulation scheme is described by the 2x2 transmit matrix  $C_k$ , which is recursively calculated by the product of the information matrix  $S_k$  and the previous transmitted matrix ( $C_{k-1}$ ). As first transmitted matrix ( $C_0$ ), the identity matrix can be used. The differential modulation scheme can be described mathematically by the following matrix product

$$C_k = S_k \cdot C_{k-1} = \begin{bmatrix} c1_k & c2_k \\ -c2_k^* & c1_k^* \end{bmatrix} \quad (7.2)$$

These complex valued symbols described in matrix  $C_k$  will be transmitted via two adjacent antennas at the time slot  $k$  ( $ts_k$ ). Time slot  $k$  is composed of two time slots  $ts_{k1}$  and  $ts_{k2}$  as it is shown in Fig. 7.2.

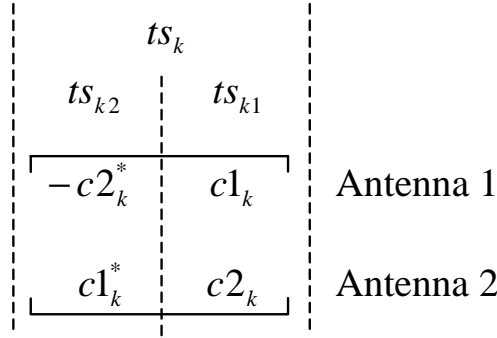


Figure 7.2:  $C_k$  matrix transmitted at time slot  $k$ .

This is the way in which the information is differentially encoded and transmitted.

Concerning the radio channel influence, usually a Rayleigh fading model is used. The noise added in the receiver is considered to be Additive White Gaussian Noise (AWGN). In this way the received signal  $r1_k$  and  $r2_k$  in adjacent time samples of a single receive antenna are corresponding to the two adjacent time slots  $ts_{k1}$  and  $ts_{k2}$ . The received signals can be written in matrix notation as:

$$\begin{bmatrix} r1_k & -r2_k^* \\ r2_k & r1_k^* \end{bmatrix} = \begin{bmatrix} c1_k & c2_k \\ -c2_k^* & c1_k^* \end{bmatrix} \cdot \begin{bmatrix} h1_k & -h2_k^* \\ h2_k & h1_k^* \end{bmatrix} + \begin{bmatrix} n1_k & -n2_k^* \\ n2_k & n1_k^* \end{bmatrix} \quad (7.3)$$

in a summarized form

$$R_k = C_k \cdot H_k + N_k \quad (7.4)$$

Concerning to the classical receiver structure, the received signal matrix  $R_k$  is conventionally processed by a matrix multiplication

$$D_k = R_k \cdot R_{k-1}^H \quad (7.5)$$

where  $R_{k-1}^H$  is the Hermitian matrix of  $R_{k-1}$  (transpose conjugate of  $R_{k-1}$ ).

## 7.1 A New Class of Differential Space Time Block Codes

This new class of DSTBCs allows the use of modulations whose constellations points have different amplitudes. Using modulation schemes that include variations in amplitude (not only in phase) allows to obtain an improved BER. The proposed DSTBC structure is quite similar to the one described previously but with the following differences:

- Given that the modulations to be used have constellation points with different amplitudes, the  $S_k$  matrices will not be unitary matrices. Instead of it, the following normalized matrix  $U$  is a unitary matrix in this case

$$U = \frac{1}{\sqrt{|s1_k|^2 + |s2_k|^2}} \cdot S_k$$

i.e.  $U^H = U^{-1}$ , where  $U^H$  is the Hermitian matrix of  $U$ . This observation is important because DSTBC theory generally is described for unitary matrices but in this case they are not strictly unitary.

- There will be a Power Control Mechanism (PCM) in order to control the power of the transmitted symbols. In previous propositions this PCM usually is implicit in the definition of the modulation scheme. Using an explicit PCM allows the use of a greater and more varied range of modulation schemes.
- The new decoding procedure is mathematically described by the inverse matrix  $R_{k-1}^{-1}$  as follows:

$$\begin{aligned} D_k &= R_k \cdot R_{k-1}^{-1} \simeq C_k \cdot H_k \cdot (C_{k-1} \cdot H_{k-1})^{-1} \\ &= C_k \cdot H_k \cdot H_{k-1}^{-1} \cdot C_{k-1}^{-1} \end{aligned} \quad (7.6)$$

Here the decoding procedure is different compared to Eqn. (7.5) because in this case it is necessary to decode amplitude and phase, not only phase as

for 64-PSK. The noise influence is ignored in the received matrices  $R_k$  and  $R_{k-1}^{-1}$ . If furthermore the two adjacent radio channel matrices do not vary in this short time interval, which means

$$H_k = H_{k-1}$$

and if (7.2) is applied, the following relation is valid

$$D_k \simeq C_k \cdot C_{k-1}^{-1} = S_k \quad (7.7)$$

where  $S_k$  is the information matrix containing the transmitted symbols from the constellation diagram. If the added noise was small, the demodulation matrix  $D_k$  is strongly related to the information matrix  $S_k$  transmitted in the 2x1 MISO system.

## New Modulation Schemes for DSTBCs

Here several amplitude and phase modulation schemes are presented and compared with a 64-PSK modulation (fixed amplitude modulation) used in DSTBC. 64-PSK modulation used in DSTBC is considered here as the refer-

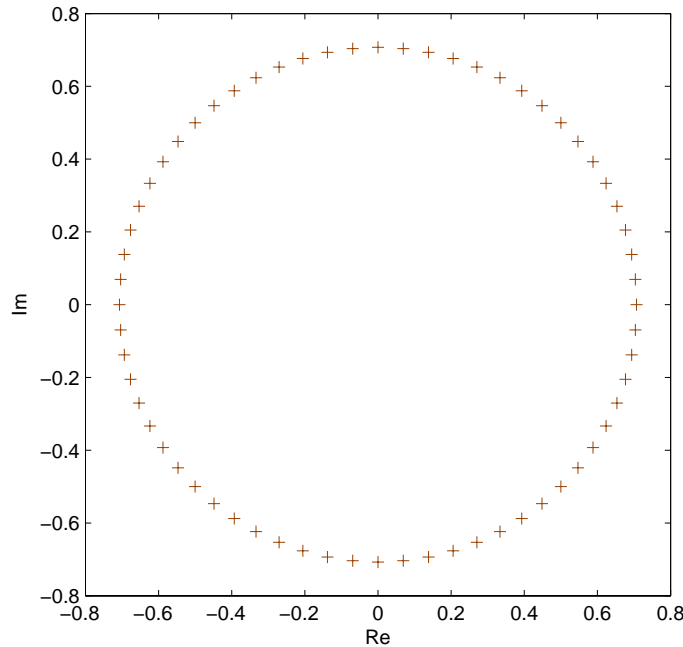


Figure 7.3: 64-PSK modulation applied to DSTBC schemes.

ence modulation scheme, because this modulation does not have amplitude variations and the objective is to show the improvement in performance obtained by using this new technique which make it feasible to use amplitude and phase modulations in DSTBC with quite freedom.

The problem when using amplitude variable modulations is that the transmitted power can be increased or decreased up to  $\infty$  or 0 respectively. For avoiding such a situation, the amplitude of the constellation points in the 64-PSK modulation is normalized to  $a_1 = \sqrt{0.5}$ .

### “4A16PSK”

The first kind of 64-APSK (Amplitude and Phase Shift Keying) modulation that we are going to consider is “4A16PSK”. That is a modulation with 4 amplitude values and 16 phase values for each subconstellation. Each constellation has 2 subconstellations with one amplitude value in common ( $a_1 = \sqrt{0.5}$ ); 7 different amplitudes for the whole constellation (see Fig. 7.4). In the “4A16PSK” modulation scheme the set of possible amplitudes  $A$  is

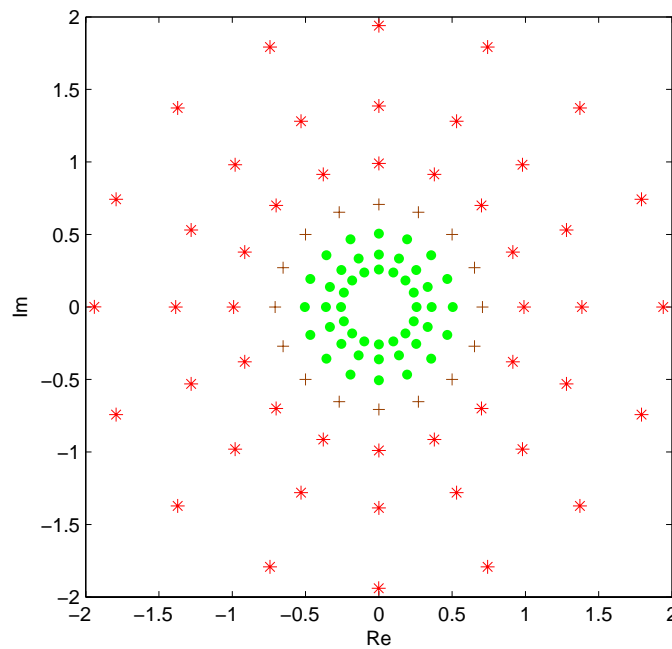


Figure 7.4: “4A16PSK” modulation scheme used in DSTBC.

determined by a parameter  $a$  as follows:

$$A \in \{(\sqrt{0.5}) \cdot [1/a^3, 1/a^2, 1/a, 1, a, a^2, a^3]\}$$

(coding [01, 11, 10, 00, 01, 11, 10] respectively) and the phases are 16 equal spaced phase states starting in  $0^\circ$  (see Fig. 7.4). These phases map 4 bits onto one modulation symbol in a Gray coding way. “4A16PSK” has two subconstellations, the small one composed by those constellation points with amplitude smaller or equal to  $a_1 = \sqrt{0.5}$  (“.” and “+” in Fig. 7.4) and the big one whose constellation points have bigger or equal to  $a_1 = \sqrt{0.5}$  amplitudes (“+” and “\*” in the same figure). The responsible unit for using the small or big subconstellation to modulate the data bits is the transmitter, depending on the *spectral norm* of the previous  $C_k$  matrix ( $C_{k-1}$ ) (definition in page 91); if it is smaller than a predefined value *maxl* the big subconstellation will be used, else the small one will be used. In this way the control of transmitted power is performed. This mechanism to control the power (described in page 91) will be referred as Power Control Mechanism 1 (PCM1).

Due to the fact that all the constellation points of “4A16PSK” are different between them (no matter if they are in the small or big subconstellation) no extra information is needed in the receiver to demodulate these constellation points.

The value of  $a$  which produces acceptable transmitted powers and optimizes the performance of the modulation was estimated by simulations. This value is  $a = 1.4$  and it can be seen in Fig. 7.5 that the performance is approximately 5.5 dB better at a  $BER = 10^{-2}$  than for the corresponding classical PSK modulation (64-PSK, Bandwidth Efficiency (BE) 6 bit/s/Hz).

All the APSK modulation schemes presented here were tested under the PCM named PCM1, described later in this section. This PCM demonstrated to be completely robust and quite effective for all the analyzed modulation schemes.

### “2A32PSK”

Other 64-APSK tested modulation was “2A32PSK”, it consists of 3 circles as it is shown in Fig. 7.6. Here, as in the previous case, the small constellation is composed by the points “.” and “+” in Fig. 7.6 and the big one by the points “+” and “\*” in the same figure. For this modulation, as in previous cases, the central circle has a radius  $a_1 = \sqrt{0.5}$ . An  $a$  parameter which specifies the difference between the circles radii was optimized. The

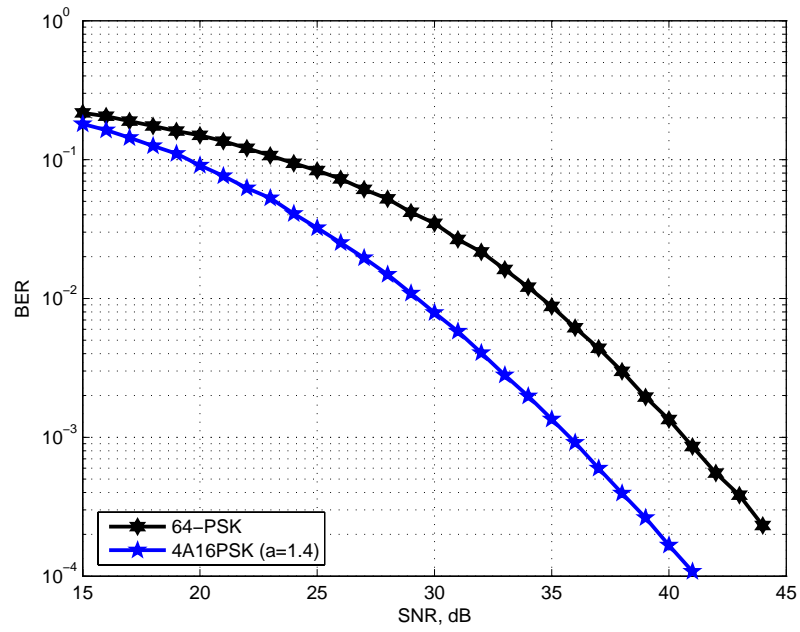


Figure 7.5: Comparison between “4A16PSK PCM1” and 64-PSK for DST-BCs in an uncorrelated Rayleigh fading channel.

optimum value obtained for the parameter  $a$  was  $a = 0.34$ .

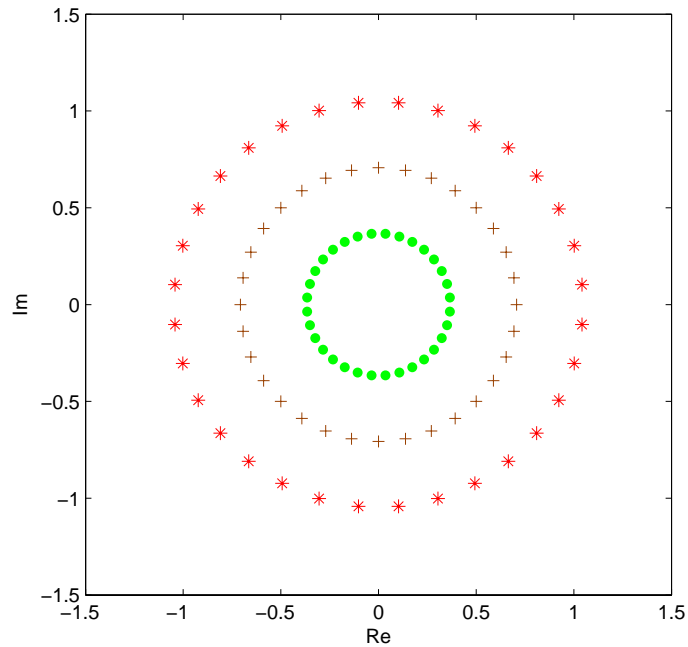


Figure 7.6: “2A32PSK” modulation applied to DSTBC scheme.

As it can be seen in Fig. 7.7 “2A32PSK” is approximately 4.2 dB better at a  $BER = 10^{-2}$  than 64-PSK when they are used in DSTBC. This result is reasonable considering that when 32-PSK is used instead of 64-PSK the BER is improved in 6 dB and the BE is decreased in 1 bit/s/Hz. In this case the BE is maintained by adding a second circle (for each subconstellation) with other 32-PSK set of constellation points. By making this the 6 dB of improvement are reduced to 4.2 dB.

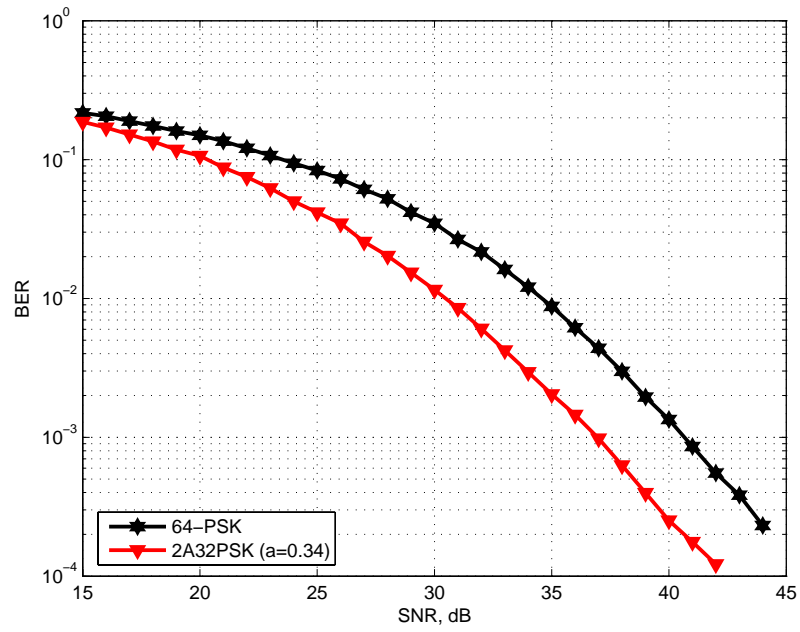


Figure 7.7: Comparison between “2A32PSK PCM1” and 64-PSK for DST-BCs in an uncorrelated Rayleigh fading channel.

**“APSK1”**

This modulation scheme is a variation of “4A16PSK” where an additive rule is used instead of an exponential rule for the radii variations of the circles in the constellation diagram.

For “APSK1” modulation scheme the set of possible amplitudes  $A$  is determined by the parameter  $a$  as follows:

$$A \in \{(\sqrt{0.5}) \cdot [1 - 3a, 1 - 2a, 1 - a, 1, 1 + a, 1 + 2a, 1 + 3a]\}$$

(coding [01, 11, 10, 00, 01, 11, 10] respectively) and the phases are 16 equally spaced, starting in  $0^\circ$  (see Fig. 7.8). The parameter  $a$  was optimized in or-

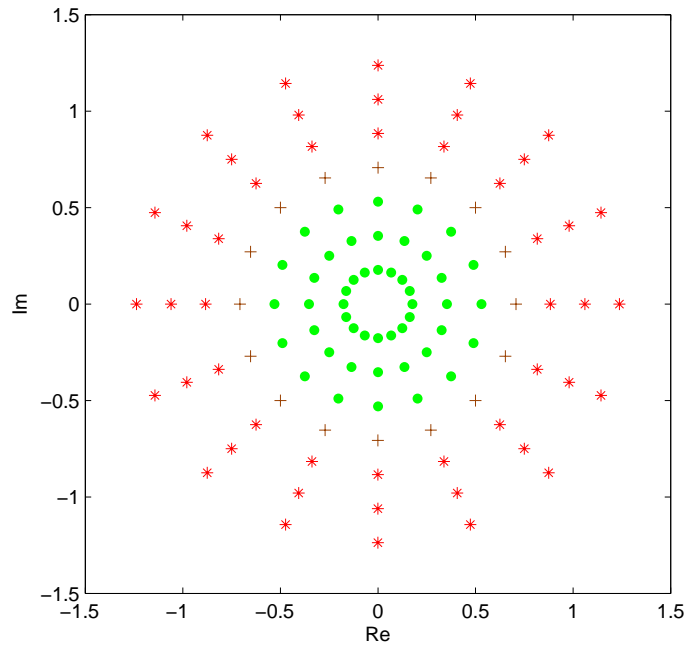


Figure 7.8: “APSK1” modulation scheme used in DSTBC.

der to obtain the best possible performance for this modulation scheme and the optimum value for  $a$  was  $a = 0.25$ . As it can be seen in Fig. 7.9 the performance of this modulation scheme is not as good as the corresponding to “4A16PSK”.

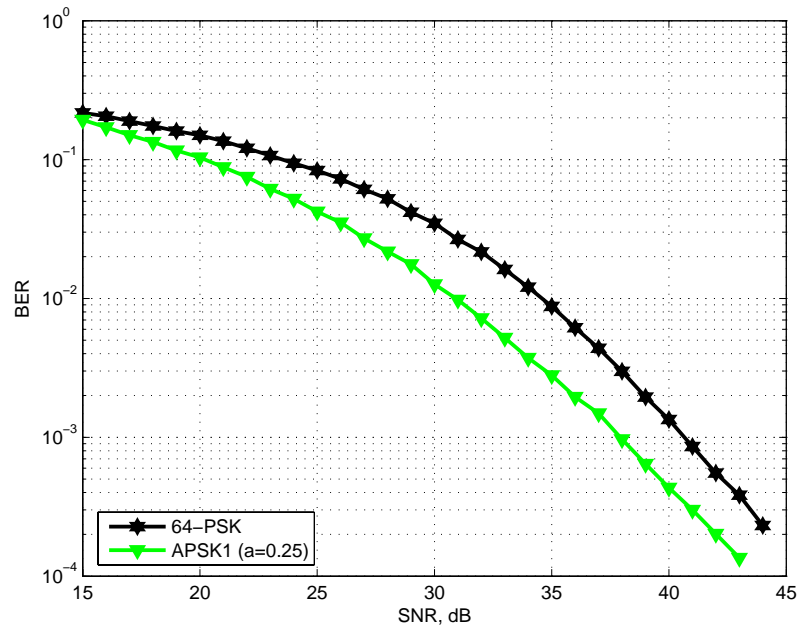


Figure 7.9: Comparison between “APSK1 PCM1” and 64-PSK for DSTBCs in an uncorrelated Rayleigh fading channel.

**“APSK2”**

“APSK2” tests the performance of a modulation scheme with equal spaced constellations points. Here the parameter that determine the distance between points is  $a$ . In this case  $a$  was taken as  $a = \sqrt{\frac{1}{41}}$ , for this value, the points in the common ring has an amplitude of  $\sqrt{0.5}$ . That value ensures that do not mind the sequence of bits in the input, the modulation scheme will be always (for any sequence of bits in the input) able to control the transmitted power. “APSK2” looks like it is shown in Fig. 7.10. If e.g.

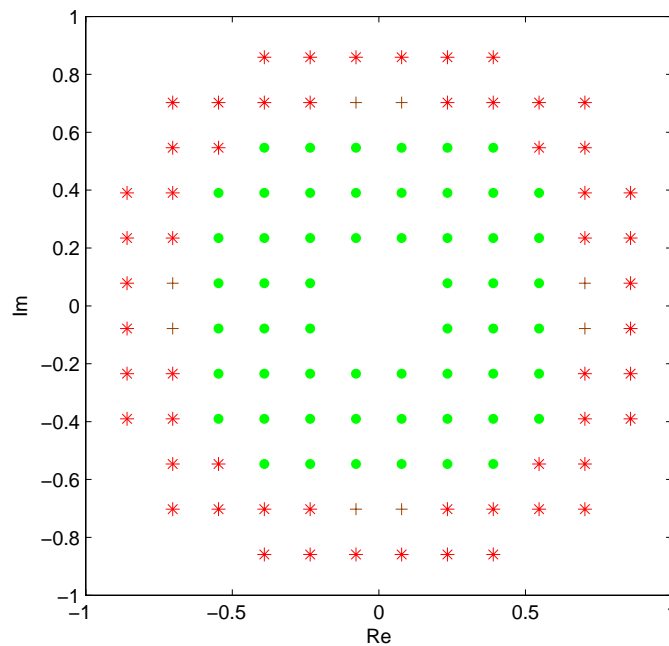


Figure 7.10: “APSK2” modulation scheme used in DSTBC.

$a > \sqrt{\frac{1}{41}}$  is selected, it could happen that while the transmitter is trying to reduce the transmit power by using the small subconstellation, it continues growing. This situation would happen e.g. for a given sequence of bits, whose modulation always repeat one constellation point over the common ring. In this case having this point an amplitude greater than  $\sqrt{0.5}$ , the transmit power would continue growing. For this reason, for ensuring the robustness of the system,  $a$  was selected as  $a = \sqrt{\frac{1}{41}}$ .

It could be considered that such situation has very low probability to appear,

specially due to scrambling process (pseudo randomizing) in the transmitter and that is true. But in any case the proposed value for  $a$ , makes the proposed modulation scheme absolutely robust.

It was also evaluated the performance of this modulation scheme for the optimum value of  $a$  (without consideration about the robustness of the system). The optimum value obtained was  $a = 0.20$ . The difference in performance for  $a = \sqrt{\frac{1}{41}}$  and  $a = 0.20$  is meaningless, reason why in Fig. 7.11 it is only shown the result for  $a = \sqrt{\frac{1}{41}}$ .

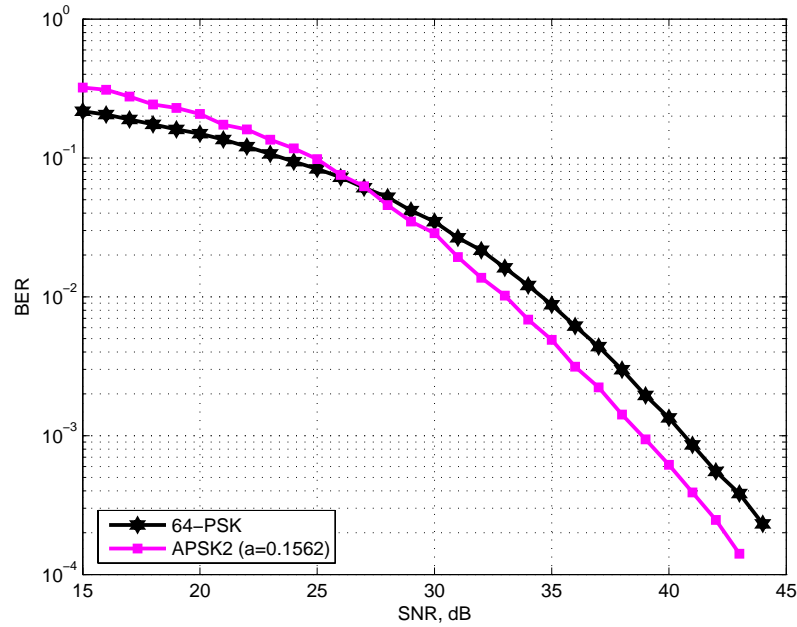


Figure 7.11: Comparison between “APSK2 PCM1” and 64-PSK for DSTBCs in an uncorrelated Rayleigh fading channel.

**“APSK3”**

Later more flexible modulation schemes were studied; the number of circles, the radii of them, the number of constellation points in each circle and also one phase shift for each circle were considered as variables to optimize. One of these modulation schemes is presented in Fig. 7.12 under the name of “APSK3”. For this specific modulation scheme the set of radii was

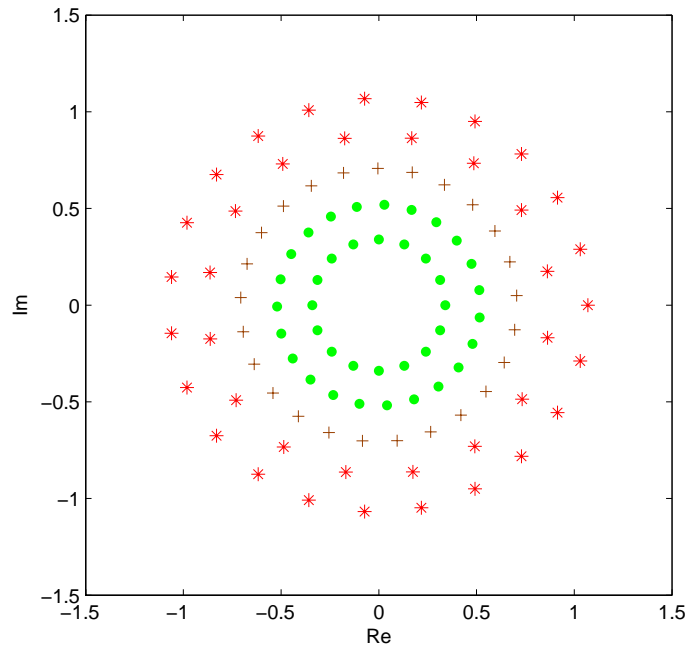


Figure 7.12: “APSK3” modulation scheme used in DSTBC.

$(0.34, 0.52, \sqrt{0.5}, 0.88, 1.07)$ , the number of points in each circle was respectively  $(16, 23, 25, 16, 23)$  and the phase shift for each circle was respectively  $(0, 0.15, 0.07, 0.2, 0)$ . Although the flexibility for placing the constellation points was quite high for this kind of modulation schemes, it was not obtained a better result than for “4A16PSK” (see Fig. 7.13).

Several different modulation schemes were tested and some of them were presented in this section. By observing the different modulation schemes presented here and the results for them, it seems clear that is not a simple task to identify which are the factors that make a modulation scheme more effective in this particular case of DSTBCs. There are some well known factors that have influence over the performance of a normal modulation scheme

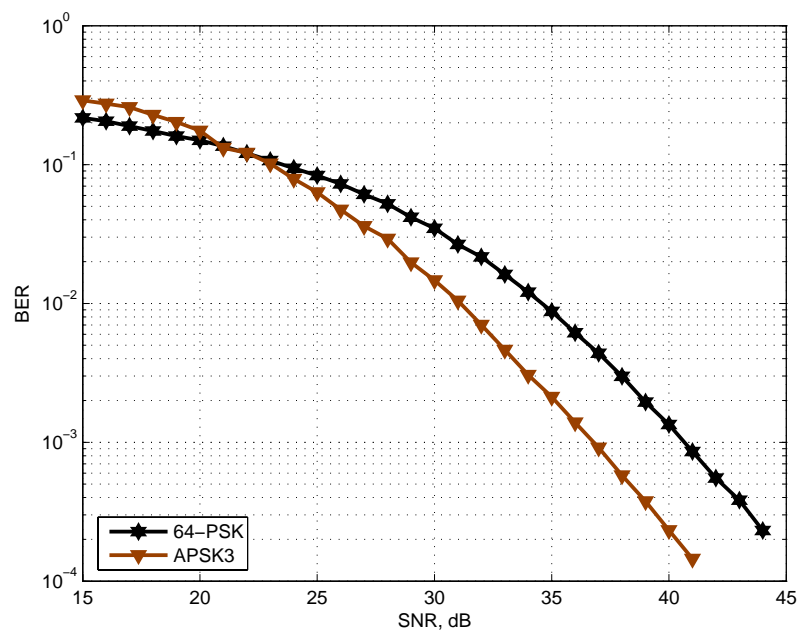


Figure 7.13: Comparison between “APSK3 PCM1” and 64-PSK for DSTBCs in an uncorrelated Rayleigh fading channel.

(e.g., distance between constellation points, power ratio between smaller and bigger constellation points in the scheme, etc.), but it is not a simple task to determine how all of them affect the performance of the system in our case. Then the simulation process is a very good alternative to look for more effective modulation schemes.

At this point it is clear that “4A16PSK” is the best of the modulation scheme presented here. Then in future sections mainly this modulation scheme will be considered.

## Power Control Mechanism in this New Class of DSTBCs

When an amplitude modulation is used in DSTBCs a PCM must be used in order to control the transmitted power, in other case the transmitted power can go to infinity or null depending on the data to transmit. Here the first PCM considered for this new class of DSTBCs is described. In the following section will be discussed the influence of the PCM over the general performance of the system.

### PCM1

The first PCM considered to be used with this new class of DSTBCs was PCM1. In this case the transmitter observes the *spectral norm* (*norm2*) of the previous transmitted block ( $\|C_{k-1}\|_2$ ).

$$\|C_{k-1}\|_2 = (\text{maximum eigenvalue } (C_{k-1}^H \cdot C_{k-1}))^{1/2}$$

Considering this value the transmitter takes the decision of using the big or small subconstellation. It can be easily demonstrated that in our case

$$\|C_{k-1}\|_2 = (|c1_{k-1}|^2 + |c2_{k-1}|^2)^{1/2}$$

If the *norm2* of the previous transmitted block is smaller than a certain limit (*maxl*) then the big subconstellation is used to modulate the bits, else the small one is used.

No redundancy is transmitted, the receiver considers both subconstellations in the demodulation process and depending on the received values, elements of  $D_k$  in (7.7), they will be recognized as points of the small or big subconstellation and demodulated.

The results obtained for the modulation schemes discussed in this section (where PCM1 was used) are summarized in Fig. 7.14.

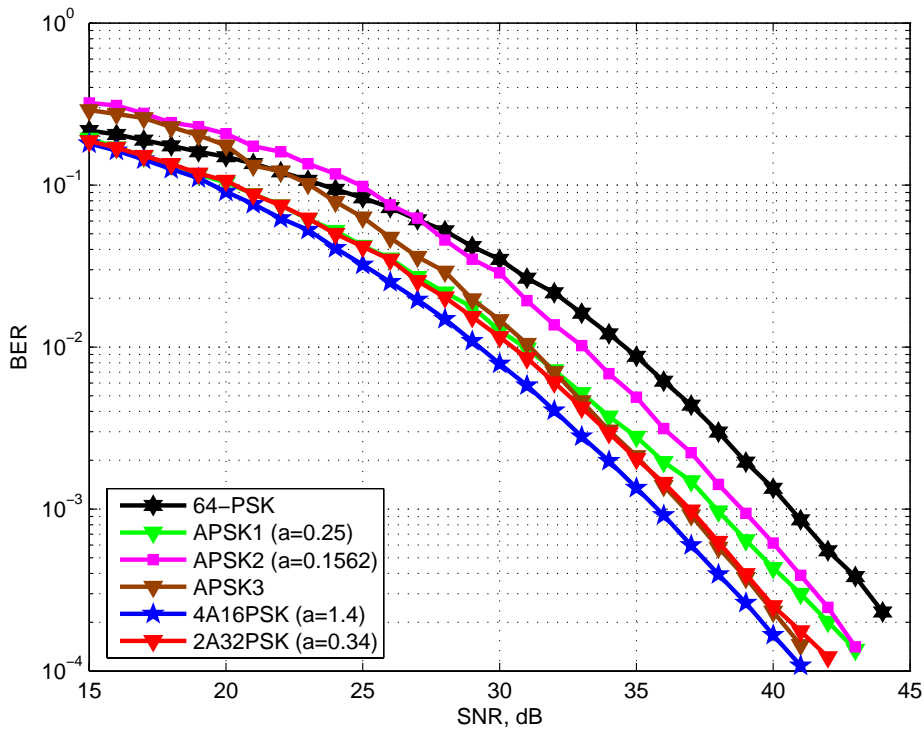


Figure 7.14: Results for all the tested APSK modulation schemes with PCM1 in an uncorrelated Rayleigh fading channel.

For the understanding of these results it is necessary to have in mind that they correspond to a system without any channel coding or any other data treatment in order to improve the BER. That is the reason why these results need a high SNR to obtain a good BER value. This model is very effective in order to compare directly (without factors to cover the differences) the performance of different modulation schemes. In Section 8.3 the performance of the proposed system will be studied in a channel coded system. Also the improvements that can be obtained by using more receive antennas will be studied.

## Proposed Technique in AWGN Channels

Initially the technique was evaluated in uncorrelated Rayleigh fading channels, because this is the channel model usually used for comparing different techniques in DSTBC research. In Fig. 7.15, the results for “4A16PSK” and “2A32PSK” with PCM1 in AWGN channels are shown.

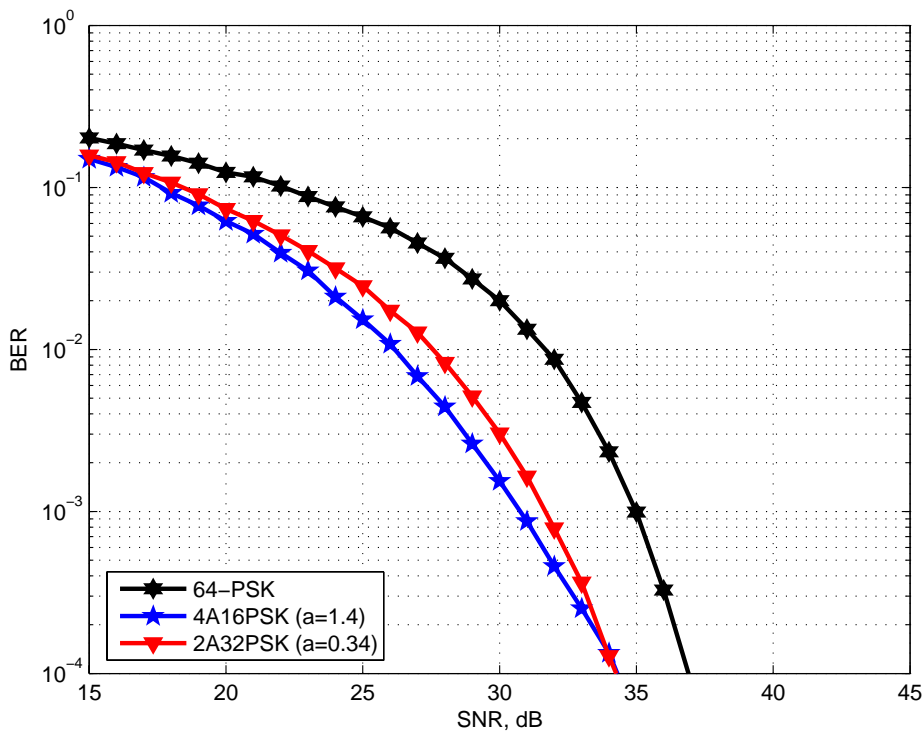


Figure 7.15: Results for 64-PSK, “4A16PSK” and “2A32PSK” with PCM1 in an AWGN channel.

The proposed new class of DSTBCs is very flexible, several APSK modulation schemes could be used with PCM1 and also with different PCMs. In the next section the influence of the PCMs over the general performance of the system is studied.

## 7.2 Influence of the PCM in this New Class of DSTBCs

Initially in page 91 PCM1 was described, the first power control mechanism used with this proposed technique. This PCM is based on observing  $\|C_{k-1}\|_2$  and then taking the decision of what subconstellation to use, the small (in order to decrease or maintain the transmit power) or the big one (for increasing or maintaining the transmit power). In this section are considered new PCM strategies. Probably the most important difference between the PCMs considered in this section and PCM1 is that now, the possible  $C_k$  that can be obtained by using the small and the big subconstellations are going to be calculated and then, the decision of transmitting the  $C_k$  matrix that better complies the defined power control strategy will be taken.

For studying the influence of the PCM in the performance of this new class of DSTBCs, two *criteria* were defined. Criterion 1 (C1) is a PCM based on controlling the  $\|C_k\|_2$ . In this case the  $C_k$  matrix which has the smallest value of  $d = (\|C_k\|_2 - \text{maxl})$  will be used, where  $\text{maxl}$  is a predefined value which was verified that does not play any perceptible role in the performance of the technique, at least while it varies in the range  $0.4 \leq \text{maxl} \leq 1$ . Criterion 2 (C2) is based on controlling  $|c1_k|^2$  and  $|c2_k|^2$ . For C2 the  $C_k$  matrix which has the smallest value of  $d = (||c1_k|^2 - \text{maxl1}| + ||c2_k|^2 - \text{maxl1}|)$  will be used.  $\text{maxl1}$  was taken as  $\text{maxl1} = \frac{\text{maxl}^2}{2}$  in order to work with similar levels of transmit power. In both cases the idea is to maintain the observed variables as close to a given value as possible.

Also two *selection procedures* were defined, selection procedure 1 (SP1) uses for  $s1_k$  and  $s2_k$  the same subconstellation (the small or the big one); while selection procedure 2 (SP2) can use different subconstellations for  $s1_k$  and  $s2_k$ .

This gives place to four new PCMs; considering as PCM1 the first used PCM, we could define PCM2 as the one obtained by the combination of C1 and SP1, PCM3 by using C1 and SP2, PCM4 by using C2 and SP1 and PCM5 by using C2 and SP2 (summarized in Table 7.1). C1 demonstrated to be more effective than C2. SP1 demonstrated to be more effective than SP2, which can sound curious at the beginning because SP2 is more flexible than SP1. SP2 achieves a narrower fluctuation of the transmitted power than SP1, but it was observed that this does not result in a better performance from a BER point of view. Considering that C1 and SP1 (PCM2) was the

more successful combination, only this case will be compared with PCM1 in the following subsections.

Table 7.1: New PCMs evaluated.

C \ SP	SP1	SP2
C1	PCM2	PCM3
C2	PCM4	PCM5

### 7.2.1 Analysis of a New PCM Scheme (PCM2)

PCM1 makes a decision about the two possible modulation symbol constellation diagrams based on the matrix norm  $\|C_{k-1}\|_2^2$ . In this subsection is shown that the performance can be slightly improved by directly controlling the complex valued symbols in the current and instantaneous transmit matrix  $C_k$ . The general objective is to keep the transmit power of  $C_k$  as close as possible to the average transmit power value. Large fluctuations of the transmit power are avoided in this case.

For PCM2 it is also decided in the modulator from which subconstellation the two modulation symbols of the information matrix  $S_k$  should be taken. In this case, there are two different possibilities to map the user bits to modulation symbols (using the small subconstellation or the big one). This results in two different transmit matrices  $C_k$ . The final decision, for PCM2, will be taken by choosing that  $C_k$  matrix which has the smallest value of  $d = (\|C_k\|_2 - \max)$ .

This new PCM scheme (PCM2) has been applied to the two APSK modulation schemes “4A16PSK” and “2A32PSK” in a DSTBC system.

#### • Result of PCM2 Applied to “4A16PSK”

Figure 7.16 shows the system performance of a pure PSK based modulation scheme without any amplitude variations (“64-PSK”) as a reference. As an example, all the modulation schemes used in this work have a BE of 6 bit/s/Hz. It is well known that in the comparison between PSK and APSK modulation techniques, the difference in performance is increased for higher BE while it is decreased for lower BE.

Other BER performance curve that can be appreciated in Fig. 7.16 is the

one that corresponds to the “4A16PSK” modulation scheme using PCM2. This BER curve shows an advantage of 6.1 dB at  $BER = 10^{-2}$  compared to the corresponding “64-PSK” modulation scheme used in DSTBC systems. It was improved by 0.6 dB at  $BER = 10^{-2}$  compared to the previous PCM (PCM1).

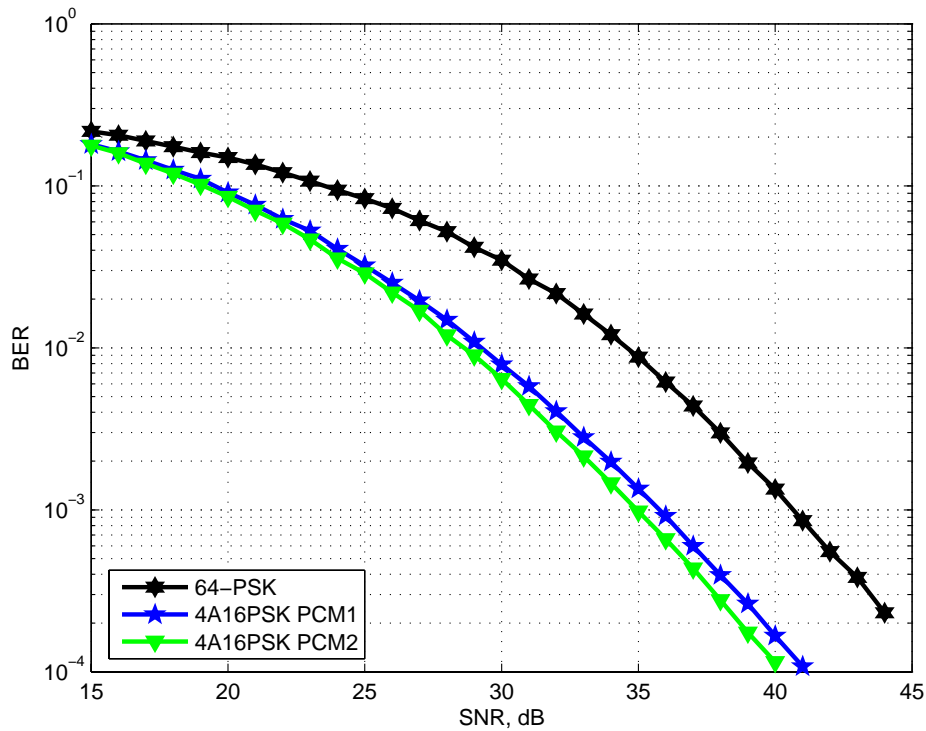


Figure 7.16: Comparison of “64-PSK” and “4A16PSK” used with different PCM techniques.

The histograms of the *spectral norm* of the  $C_k$  matrices obtained with the two different PCMs can be seen in Fig. 7.17.

7.2. INFLUENCE OF THE PCM IN THIS NEW CLASS OF DSTBCS 97

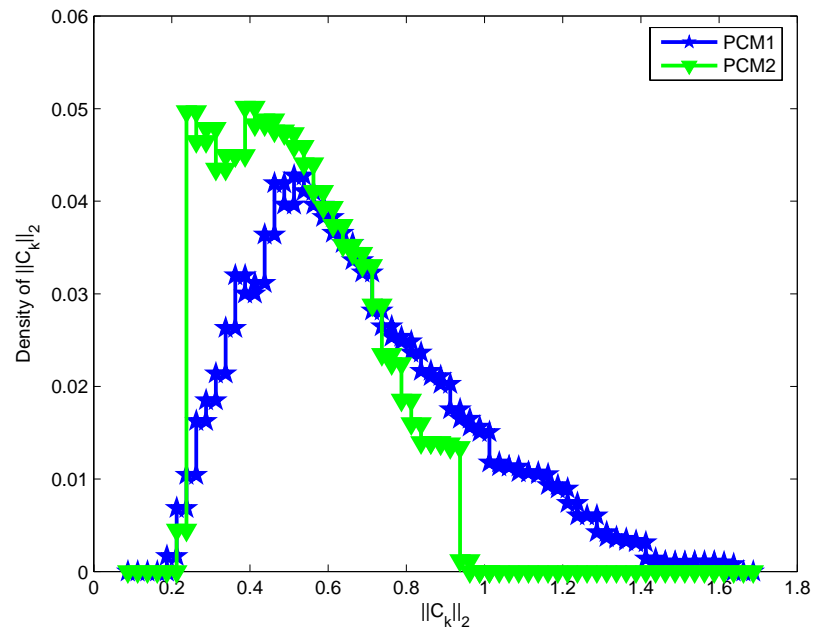


Figure 7.17: Histograms of  $\|C_k\|_2$  for “4A16PSK” used with different PCMs.

- **Result of PCM2 Applied to “2A32PSK”**

Figure 7.18 shows the BER performance for the “2A32PSK” modulation scheme under two different PCM techniques. For this particular modulation scheme the difference in performance for *PCM1* and *PCM2* is imperceptible.

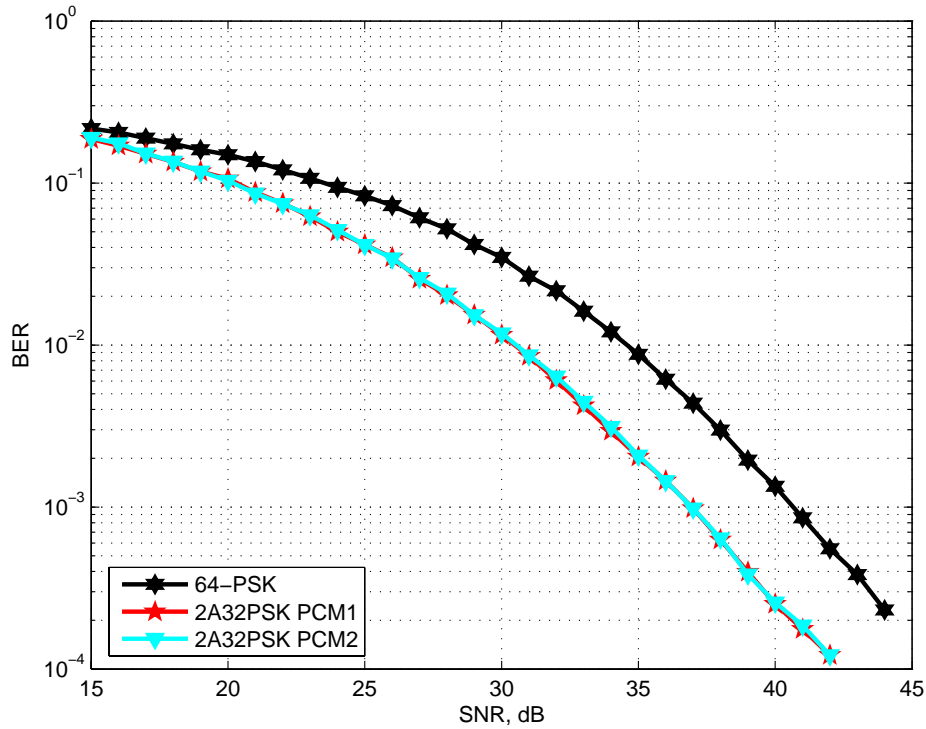


Figure 7.18: Comparison of “64-PSK” and “2A32PSK” used with different PCM techniques.

Figure 7.19 shows the histograms of  $\|C_k\|_2$  for the “2A32PSK” modulation scheme.

### 7.2.2 Conclusion about the Influence of Different PCMs

The different PCMs influence the BER performance. Better BER performance can be achieved in this new class of DSTBC systems by selecting an adequate PCM. It has been shown that an improvement in BER performance of 6.1 dB at  $BER = 10^{-2}$  can be gained by using an APSK modulation

scheme instead of a pure PSK one in DSTBC systems.

It was also shown that it is better to control the transmit power based on the instantaneous matrix  $C_k$  instead of  $C_{k-1}$ . In this case an improvement in the BER performance of 0.6 dB at  $BER = 10^{-2}$  is feasible (difference between PCM1 and PCM2 for “4A16PSK”).

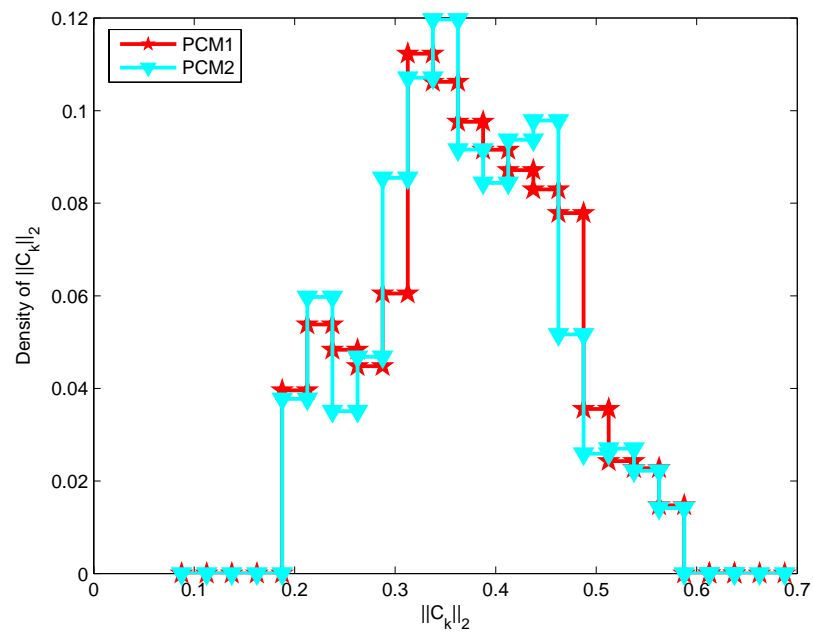


Figure 7.19: Histograms of  $\|C_k\|_2$  for "2A32PSK" used with different PCMs.

## 7.3 System Performance in WSSUS Channels

The evaluation of systems in WSSUS channels is quite appreciated because it is a more realistic model than a pure AWGN model or a Rayleigh fading model. For this reason now it will be evaluated the performance of the proposed technique under WSSUS channel condition.

Considering that the simulations are being performed for a single subcarrier ( $f_0$ ), the time variance is described as follows

$$h(\tau, t) = \frac{1}{\sqrt{P}} \cdot \sum_{p=1}^P \delta(\tau - \tau_p) \cdot e^{j(2\pi f_{D,p}t + \theta_p)} \quad (7.8)$$

by making a Fourier transform of (7.8) in the direction of  $\tau$  and using the time as discrete ( $t = nT$ ), is obtained

$$H(f, nT) = \frac{1}{\sqrt{P}} \cdot \sum_{p=1}^P e^{j2\pi f_{D,p}nT} \cdot e^{j\theta_p} \cdot e^{-j2\pi f\tau_p} \quad (7.9)$$

then by evaluating (7.9) in  $f = f_0$  the used equation is obtained

$$H(f_0, nT) = \frac{1}{\sqrt{P}} \cdot \sum_{p=1}^P e^{j2\pi f_{D,p}nT} \cdot e^{j\theta_p} \cdot e^{-j2\pi f_0\tau_p} \quad (7.10)$$

Where  $\theta_p$ ,  $\tau_p$  and  $f_{D,p}$  are obtained by using the *probability density functions* (2.36), (2.38) and (2.39) described in Section 2.5.3.1.

The set of parameters used in order to perform the simulations was inspired in WiMAX standard and are contained in Table 7.2.

In first place it was decided to maintain the assumption  $H_k = H_{k-1}$  and evaluate the performance of the system for a mobile velocity of 60 km/h. In this case a result very similar to the one obtained for Rayleigh fading channels was obtained.

In Fig. 7.21 it can be observed that the improvement by using “4A16PSK PCM2” instead of 64-PSK in DSTBC is approx. of 6.1 dB at a  $BER = 10^{-2}$ ; approximately the same value obtained in Section 7.2.1 for a Rayleigh fading channel.

Table 7.2: Simulation parameters.

Parameter	Value
Carrier Frequency	$f_c = 5 \text{ GHz}$
Bandwidth	$B = 10 \text{ MHz}$
Number of subcarriers	$N_{FFT} = 128$
Subcarrier spacing	$\Delta f = \frac{B}{N_{FFT}} = 78125 \text{ Hz}$
Symbol Duration	$T_s = 12.8 \text{ } \mu\text{s}$
Guard interval	$T_G = \frac{T_s}{8} = 1.6 \text{ } \mu\text{s}$
Symbol interval	$T_{S+G} = T_s + T_G = 14.4 \text{ } \mu\text{s}$
Number of paths	$P = 30$
Number of clusters (groups of paths)	$N_c = 1$
Maximum time delay	$\tau_{max} = 1 \text{ } \mu\text{s}$
Mobile velocity	$v = 3, 60, 120 \text{ km/h}$
Maximum Doppler shift	$f_{Dmax} = f_0 \cdot \frac{v}{c} \approx 14, 278, 556 \text{ Hz}$ using $f_0 = f_c$
Time Delay distribution	$b = \frac{\tau_{max}}{\ln(1000)} = 0.1448 \text{ } \mu\text{s}$

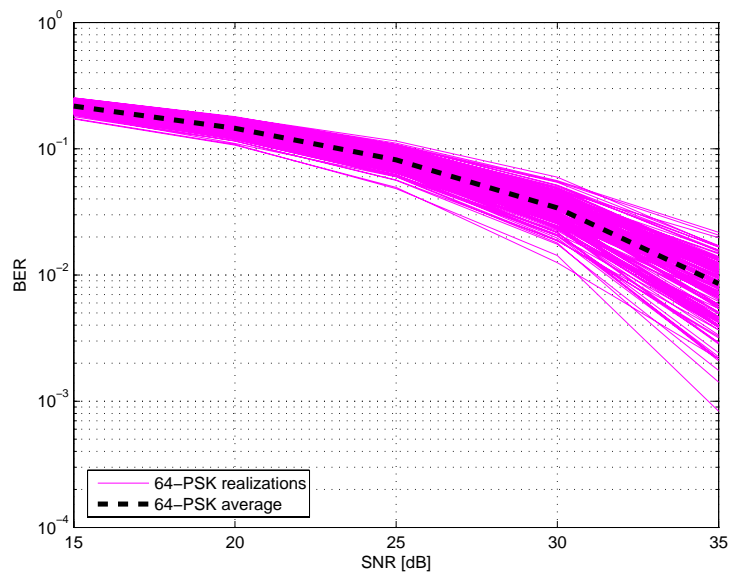


Figure 7.20: Performance of 64PSK used in DSTBC under WSSUS channels ( $H_k = H_{k-1}, v = 60 \text{ km/h}$ ).

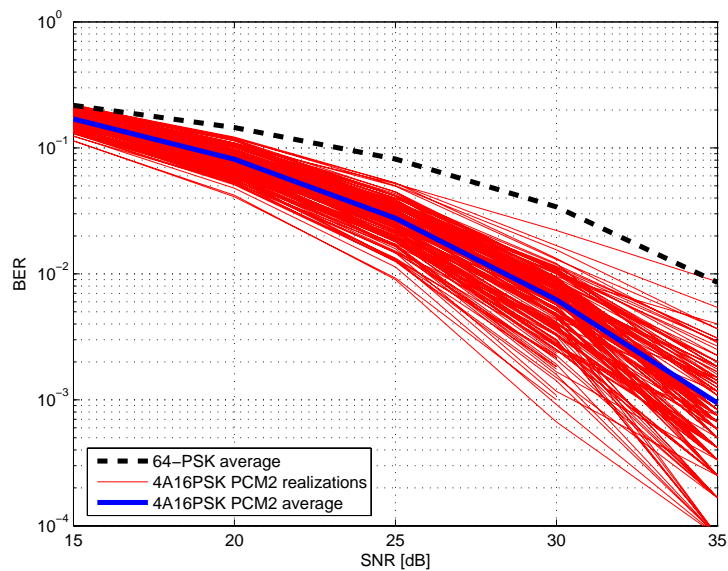


Figure 7.21: Performance of "4A16PSK PCM2" used in DSTBC under WSSUS channels ( $H_k = H_{k-1}, v = 60 \text{ km/h}$ ).

Then it was decided to work with a more realistic assumption, now for successive transmitted matrices ( $C_k$  and  $C_{k-1}$ ), successive samples of the WSSUS channel ( $H_k$  and  $H_{k-1}$ ) will be used. Then it will be valid ( $H_k \approx H_{k-1}$ ) instead of ( $H_k = H_{k-1}$ ), which is a much more realistic assumption.

By using this approach ( $H_k \approx H_{k-1}$ ), it is obtained the expected result, the performances of both systems -the one based in 64-PSK and the one based in “4A16PSK” with PCM2- are degraded. It can be observed in Figs. 7.22 and 7.23.

In Fig. 7.23 the performance of the average of 64-PSK in DSTBC with the one corresponding to “4A16PSK PCM2” in DSTBC is compared. There it can be observed that the degradation is not equal for both systems, being higher for the first one. That increases the improvement obtained by using the proposed technique instead of 64-PSK in DSTBC; now it is approx. 6.8 dB at a  $BER = 4 \times 10^{-2}$  (see Fig. 7.23) instead of approx. 5.8 dB at a  $BER = 4 \times 10^{-2}$  (see Fig. 7.21). That is an interesting result for the proposed technique; by changing to a more realistic channel model, the original improvement calculated for the Rayleigh model (and still valid for WSSUS channels under the assumption of  $H_k = H_{k-1}$ ) is increased.

Considering the question of how the performance of the proposed technique varies when the velocity of the mobile terminal is increased, the following simulations were performed. In Figs. 7.24 and 7.25 the performance for 64-PSK in DSTBC and “4A16PSK PCM2” in DSTBC were respectively evaluated for a mobile terminal velocity of 120 km/h. By comparing the average results for both techniques in Fig. 7.25 can be observed that an improvement of 9.3 dB at  $BER = 4 \times 10^{-2}$  is obtained for the proposed technique. That means that the improvement is significantly increased with the increment of the mobile terminal velocity. To verify this result new simulations at a mobile velocity of 3 km/h were performed.

In Figs. 7.26 and 7.27 the results obtained for the reference system and for the proposed system respectively when the mobile terminal velocity is 3 km/h are shown. There, it can be observed that the improvement for the proposed technique is reduced (approx. 6.0 dB at  $BER = 4 \times 10^{-2}$ ). That confirms that the improvement produced for the proposed technique is higher when the velocity of the mobile terminal is higher.

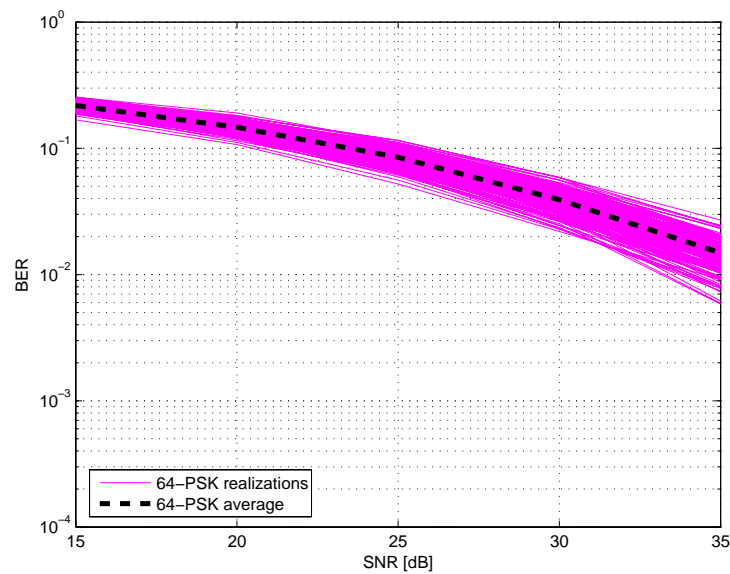


Figure 7.22: Performance of 64PSK used in DSTBC under WSSUS channels ( $H_k \approx H_{k-1}$ ,  $v = 60 \text{ km/h}$ ).

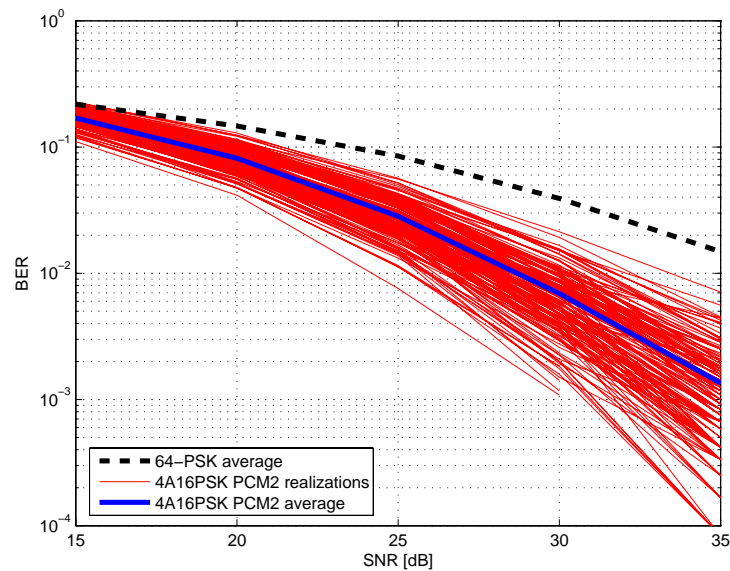


Figure 7.23: Performance of "4A16PSK PCM2" used in DSTBC under WSSUS channels ( $H_k \approx H_{k-1}$ ,  $v = 60 \text{ km/h}$ ).

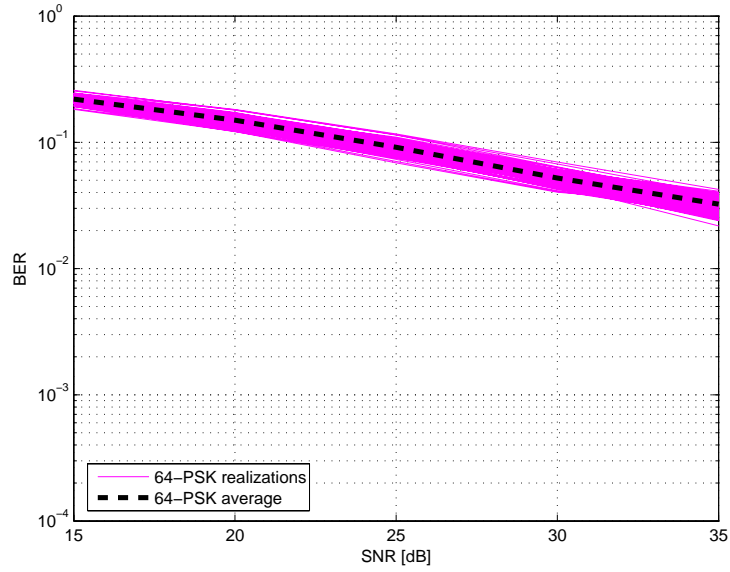


Figure 7.24: Performance of 64PSK used in DSTBC under WSSUS channels ( $H_k \approx H_{k-1}$ ,  $v = 120 \text{ km/h}$ ).

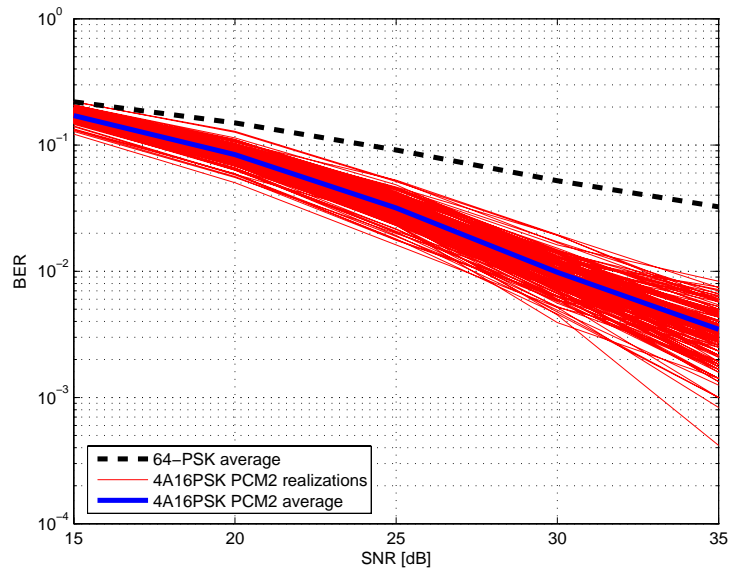


Figure 7.25: Performance of “4A16PSK PCM2” used in DSTBC under WSSUS channels ( $H_k \approx H_{k-1}$ ,  $v = 120 \text{ km/h}$ ).

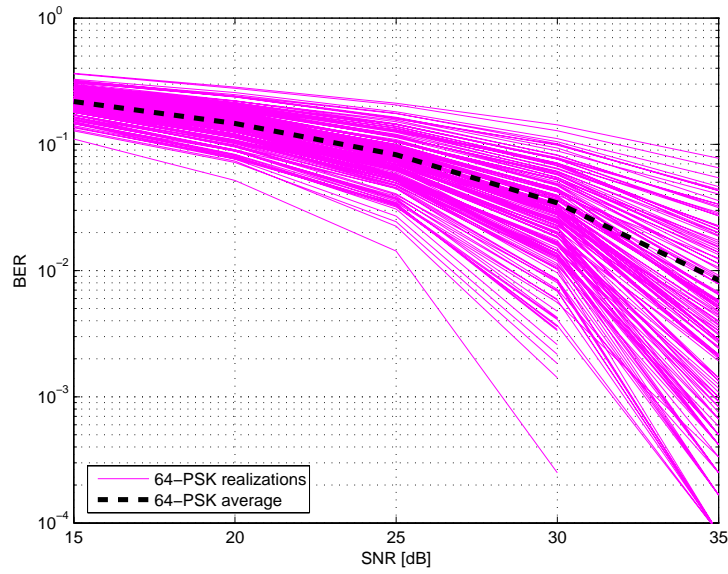


Figure 7.26: Performance of 64PSK used in DSTBC under WSSUS channels ( $H_k \approx H_{k-1}$ ,  $v = 3 \text{ km/h}$ ).

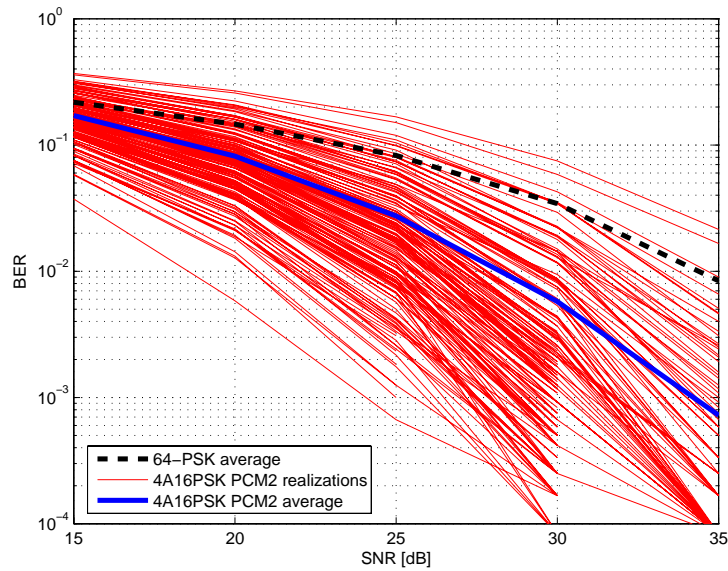


Figure 7.27: Performance of "4A16PSK PCM2" used in DSTBC under WSSUS channels ( $H_k \approx H_{k-1}$ ,  $v = 3 \text{ km/h}$ ).

In Table 7.3 in a summarized way the variation of the improvement with the velocity of the mobile terminal is shown.

Table 7.3: Improvement of the proposed technique (respect to 64-PSK) for different mobile terminal velocities in WSSUS channels with ( $H_k \approx H_{k-1}$ ).

Velocity (km/h)	Improvement (dB at $BER = 4 \times 10^{-2}$ )
3	$\approx 6.0$
60	$\approx 6.8$
120	$\approx 9.3$

Then, in this section two very important results were obtained for the proposed technique. The first one is that the original improvement is increased when a more realistic channel model is used. The second one is that the improvement is increased when the velocity of the mobile terminal is increased, which makes the proposed technique particularly useful for mobile systems, specially in high mobility scenarios. Also it can be said that the improvement is very good for low mobility scenarios, an improvement of approx. 6.4 dB can be obtained at  $BER = 10^{-2}$  for a mobile velocity of only 3 km/h (pedestrian mobility), see Fig. 7.27. Observe that the previous discussion is about the improvement in performance of “4A16PSK PCM2” with respect to 64-PSK in DSTBC, not about the absolute performance of “4A16PSK PCM2”. For sure it diminishes when the velocity of the mobile terminal is increased; but it diminishes less than for 64-PSK in DSTBC.

To verify if this behavior with respect to the velocity of the mobile terminal is a characteristic of the proposed technique shared with others APSK modulations schemes for DSTBC, or not, the study made for the proposed technique was also made for another APSK modulation technique for DSTBC called “2L-APSK” or “ $2^{2L} - APSK$ ” reported in [74] and [75].

In Fig. 7.28 the results for “2L-APSK” in a WSSUS channel as the one defined in Table 7.2, with a mobile terminal velocity of 60 km/h are shown. There it can be appreciated that exists an improvement of approximately 2.8 dB at  $BER = 4 \times 10^{-2}$  with respect to 64-PSK in DSTBC.

In Fig. 7.29 is shown that the improvement for “2L-APSK” with respect to 64-PSK in DSTBC is approximately 4.4 dB at  $BER = 4 \times 10^{-2}$  when the velocity of the mobile terminal is 120 km/h.

Finally in Fig. 7.30 can be observed that the improvement for “2L-APSK” (with respect to 64-PSK in DSTBC) is approximately 2.5 dB at  $BER = 4 \times 10^{-2}$  when the velocity of the mobile terminal is 3 km/h.

The results in Figs. 7.30, 7.28 and 7.29 show that the increment of the relative improvement (relative to 64-PSK in DSTBC) when the mobile terminal velocity is increased is also a characteristic shared for “2L-APSK” (not exclusive of “4A16PSK PCM2”). That means that the performance degradation that the techniques suffer when the mobile terminal velocity is increased is worse for 64-PSK in DSTBC than for APSK techniques as “2L-APSK” and “4A16PSK PCM2”. That is something important in favor of the use of APSK techniques. In Fig. 7.31 is graphically summarized the relative improvements of “2L-APSK” and “4A16PSK PCM2” respect to 64-PSK in DSTBC in function of the mobile terminal velocity.

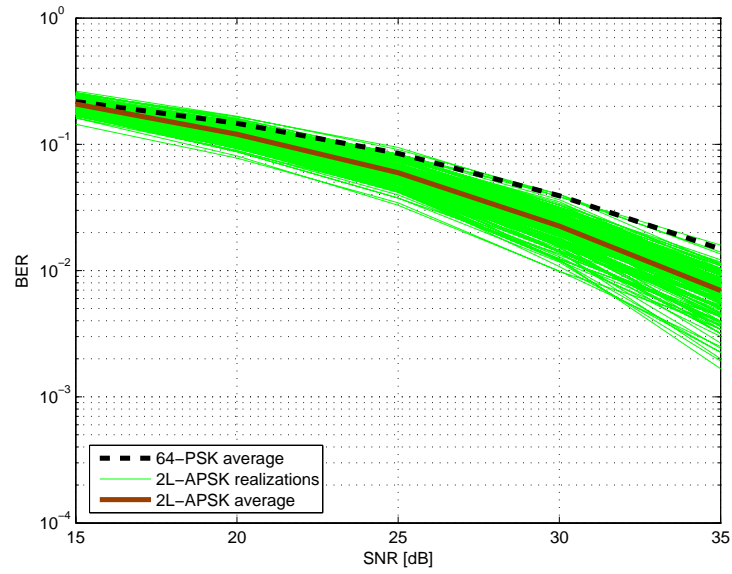


Figure 7.28: Performance of “2L-APSK” used in DSTBC under WSSUS channels ( $H_k \approx H_{k-1}$ ,  $v = 60$  km/h).

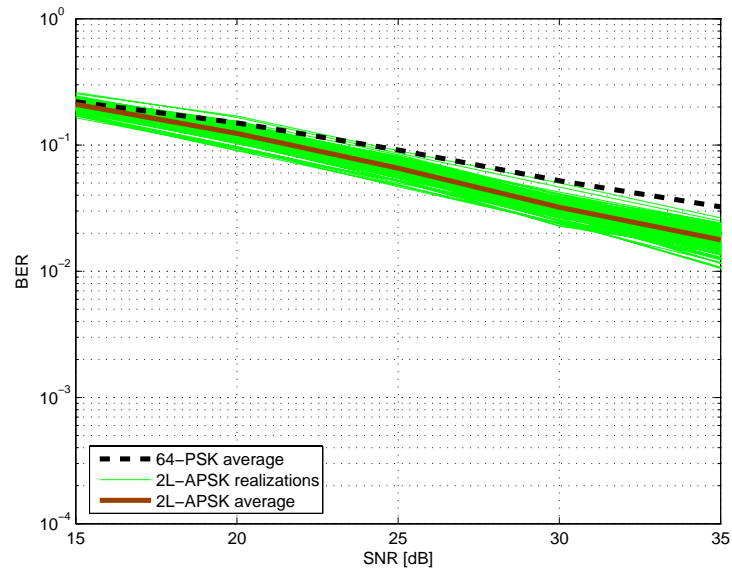


Figure 7.29: Performance of “2L-APSK” used in DSTBC under WSSUS channels ( $H_k \approx H_{k-1}$ ,  $v = 120$  km/h).

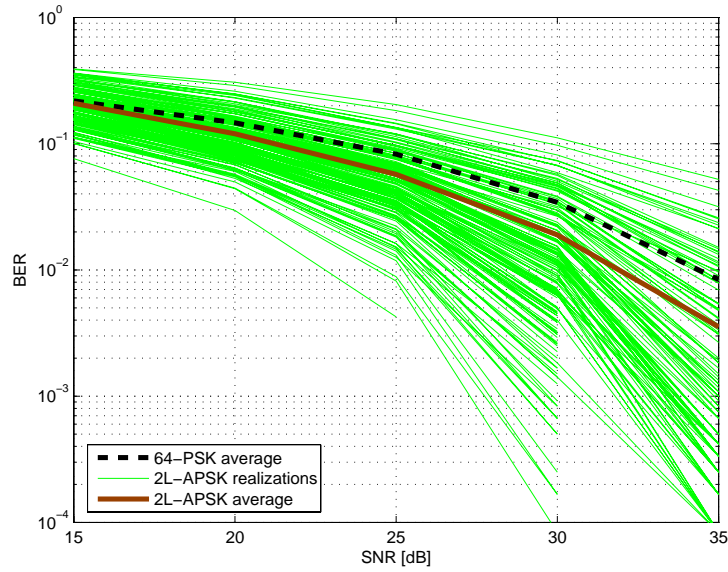


Figure 7.30: Performance of “2L-APSK” used in DSTBC under WSSUS channels ( $H_k \approx H_{k-1}, v = 3 \text{ km/h}$ ).

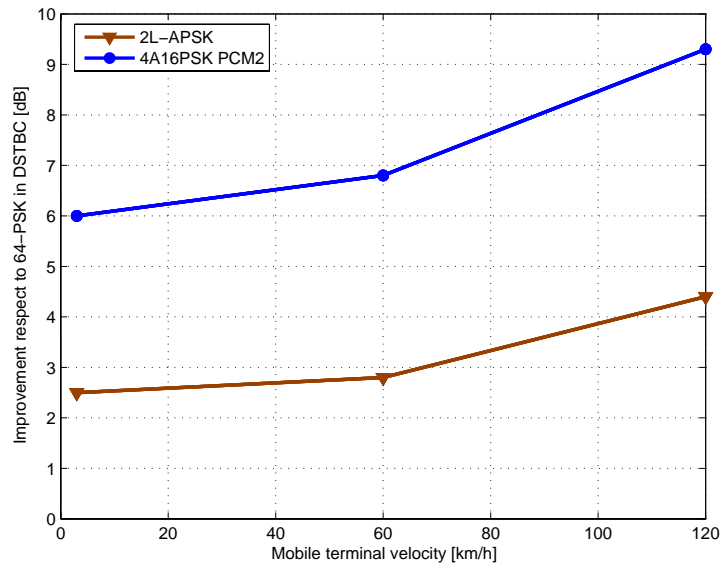


Figure 7.31: Relative improvements of “2L-APSK” and “4A16PSK PCM2” with respect to 64-PSK used in DSTBC versus mobile terminal velocity, under WSSUS channels ( $H_k \approx H_{k-1}$ ).

## 7.4 Proposed Technique with Multiple Receive Antennas

It was already discussed in Section 6.3 the advantages of using *Spatial Diversity*, i.e. MIMO systems. For the defined technique there is a very simple alternative to increase the *Spatial Diversity* order by using several antennas at the receiver side (*Receive Diversity*).

When several antennas are used in the receiver a combining technique has to be applied in order to combine the information received by each antenna. In this section we are going to explain how to apply the most well known combining techniques for the proposed system and also to show some results.

The discussion is going to be started by analyzing two well known combination techniques, *Equal Gain Combining* and *Maximum Ratio Combining*.

### *Equal Gain Combining*

This technique consists only of making an average of the  $D_k$  matrices (see (7.6) and (7.7)) obtained through each antenna, before making the demodulation. If we call to the  $D_k$  matrix obtained through the receive antenna  $i$   $D_{k,i}$ , the combination rule for *Equal Gain Combining* will be:

$$D_k = \frac{1}{M} \cdot \sum_{i=1}^M D_{k,i} \quad (7.11)$$

Where  $M$  is the number of antennas used in the receiver. Fig. 7.32 clarifies how the combination is made for the proposed technique. The “*Combination Module*” for *Equal Gain Combining* applies (7.11).

In Fig. 7.33 are shown the results of using two and three receive antennas and are also compared with the reception with a single antenna. In the three cases it was used “4A16PSK” modulation scheme under PCM2 as it was defined in Section 7.2.1. There, can be appreciated that an improvement of approximately 5 dB (at  $BER = 10^{-2}$ ) can be obtained when three receive antennas are used instead of one.

### *Maximum Ratio Combining*

In *Maximum Ratio Combining* (MRC) the criterion to make the combination is to make a weighted average of the  $D_{k,i}$  matrices obtained by the differ-

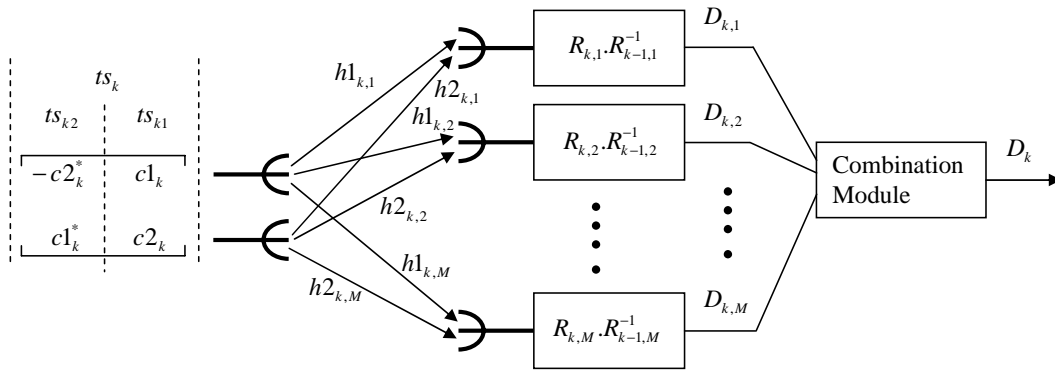


Figure 7.32: Combination system for the proposed technique with multiple receive antennas.

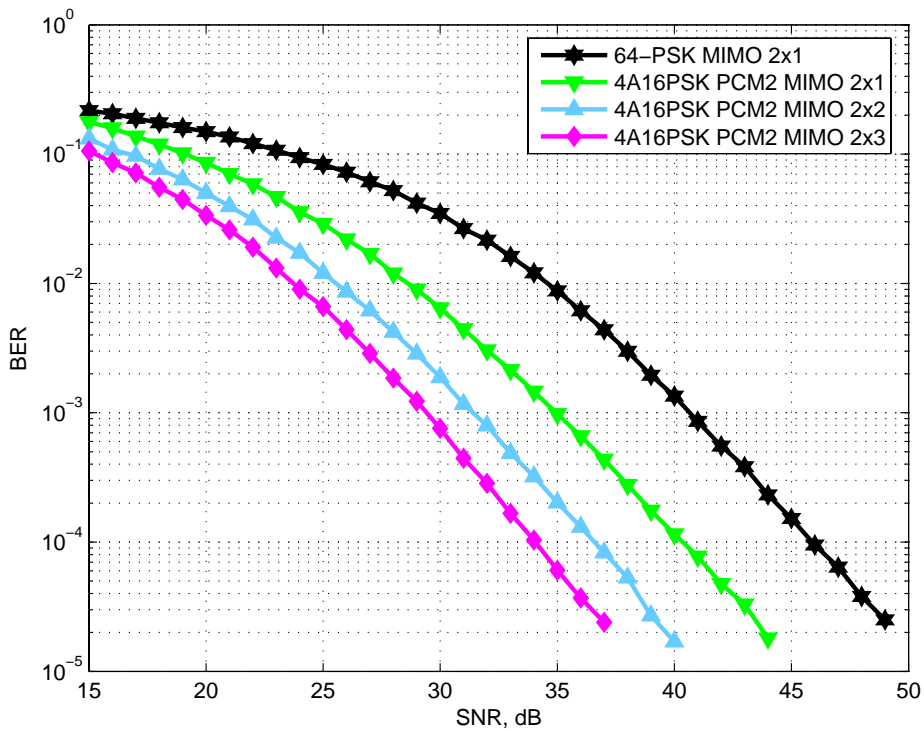


Figure 7.33: Results for the *Equal Gain Combining* technique in a multiple receive antenna system.

ent receive antennas. In Section 5.2.3 it was explained how to apply MRC for a coherent system, where the channel gain coefficients can be estimated. For DSTBC the channel gain coefficients are not available, because it is a differential technique with incoherent demodulation. In this section is proposed a way of applying a similar concept that the corresponding to MRC, for DSTBC, without adding any redundancy [76].

The proposed weighting factor ( $Wf_{k,i}$ ), for each  $D_{k,i}$  matrix, will be related with the sum of the square absolute values of the corresponding channel gain coefficients (see (7.18)). For each receive antenna  $i$ , will be considered the channel gain coefficients of the channels through which the information arrives to antenna  $i$  coming from the transmit antennas.

The weighting factor for antenna  $i$  ( $Wf_{k,i}$ ) will be

$$Wf_{k,i} = \frac{\det(R_{k,i})}{\sum_{i=1}^M \det(R_{k,i})} \quad (7.12)$$

Where  $\det(R_{k,i})$  is the *Determinant* of the matrix  $R_{k,i}$  and  $M$  is the number of receive antennas, then the combination rule will be

$$D_k = \frac{1}{\sum_{i=1}^M \det(R_{k,i})} \cdot \sum_{i=1}^M D_{k,i} \cdot \det(R_{k,i}) \quad (7.13)$$

The “*Combination Module*” in Fig. 7.32 will apply (7.13).

For an arbitrary transmit matrix  $C_k$ , the receive matrix at antenna  $i$  is

$$R_{k,i} \simeq C_k \cdot H_{k,i} \quad (7.14)$$

Using now, that the *Determinant* of a product of matrices is the product of the *Determinants* of those matrices, can be written

$$\det(R_{k,i}) \simeq \det(C_k) \cdot \det(H_{k,i}) \quad (7.15)$$

By combining (7.13) and (7.15) and eliminating the common factor  $\det(C_k)$  can be written

$$D_k \simeq \frac{1}{\sum_{i=1}^M \det(H_{k,i})} \cdot \sum_{i=1}^M D_{k,i} \cdot \det(H_{k,i}) \quad (7.16)$$

By observing the matrix  $H$  in (7.3) it is clear that

$$\det(H_{k,i}) = |h_{1k,i}|^2 + |h_{2k,i}|^2 \quad (7.17)$$

Then the weighting factors are

$$Wf_{k,i} \simeq \frac{|h_{1k,i}|^2 + |h_{2k,i}|^2}{\sum_{i=1}^M (|h_{1k,i}|^2 + |h_{2k,i}|^2)} \quad (7.18)$$

Finally it is clear that by using (7.12) as weighting factors, the  $D_{k,i}$  matrices are being weighted approximately by the channel gain coefficients of the channels through which the information arrives to antenna  $i$  coming from the transmit antennas (as shown in (7.18)).

In Fig. 7.34 the results of using two and three receive antennas with this combining technique are shown and also compared with the reception with a single antenna. For the three cases it was used “4A16PSK” modulation scheme under PCM2 as defined in Section 7.2.1. There, an improvement of approximately 7 dB (at  $BER = 10^{-2}$ ) can be observed when three receive antennas are used instead of one.

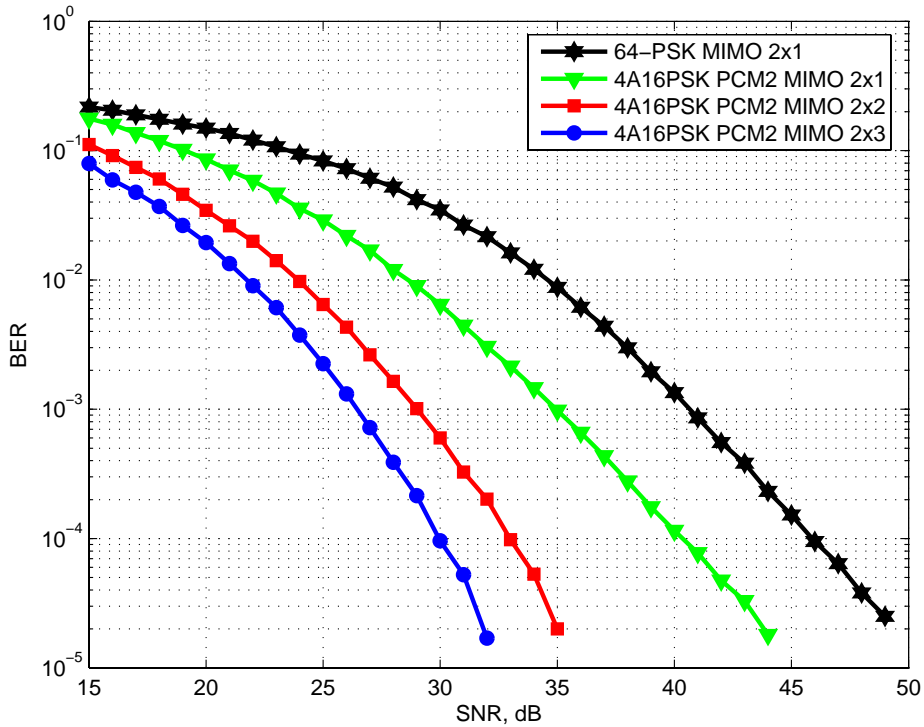


Figure 7.34: Results for the *Maximum Ratio Combining* technique in a multiple receive antenna system.

Other different methods were considered by using different weighting factors in the “*Combination Module*”, also making the combination after the demodulation. But they were not more successful than the previously explained technique.

## 7.5 Summary

In this chapter a new alternative to use APSK modulation schemes in DSTBCs is explained. By using APSK modulation schemes instead of pure PSK ones, the bit error rate is diminished for the same throughput. In order to have more freedom in the selection of APSK modulation schemes, than in previously proposed techniques, a power control mechanism (PCM) was introduced and defined. This freedom makes it feasible to look for new highly efficient modulation schemes. Then several new APSK modulation schemes were considered and evaluated. In this way “4A16PSK” was found, a new highly efficient modulation scheme for DSTBCs.

Later the optimization of the PCM was considered. The result was to find a more efficient PCM (PCM2) for “4A16PSK”. The combination “4A16PSK PCM2” was the most successful among the tested ones in this work.

Finally, “4A16PSK PCM2” was tested in different scenarios and with different number of receive antennas, showing in all these cases an excellent performance, among the best reported up to now, as far as the author knows. The relative improvement (with respect to the use of 64-PSK in DSTBC) is in some cases twice as large as in some previously proposed techniques.

# Chapter 8

## Proposed Technique in a Coded System

Channel coding allows to detect and in some cases also correct bit errors introduced in the transmission. There are several alternatives to perform channel coding, it can be performed by using *linear block codes*, *convolutional codes*, etc. In this section will be discussed one of them (convolutional coding with Viterbi decoder) and will be shown some performance results for a particular implementation of it.

### 8.1 Convolutional Encoding

#### Representation for Convolutional Encoders

The convolutional encoders are usually described by one or several of the following representations:

- *Connection representation*; basically there are two well known connection diagrams. In Figs. 8.1 and 8.2 a particular example of these representations can be seen. Also the connection can be represented by a number of polynomials, in (8.1) the corresponding polynomials for the particular case used as example are shown.
- *State diagram*; this describes the evolution of the encoding process by using a classical state diagram. See in Fig. 8.3 the state diagram corresponding to the selected example.
- *“Evolution diagram”*; these are diagrams that show the evolution of the encoding process as the movement through certain “branches” in

the diagram. In Fig. 8.4 and Fig. 8.5 the *Tree diagram* representation and the corresponding *Trellis diagram* for the example are shown.

Starting from the *Connection representation* the *State diagram* can be produced and with it the *Trellis diagram* can be drawn. Usually the *Tree diagram* is not used because it occupies much more space than *Trellis diagram*.

### ***Connection Representation***

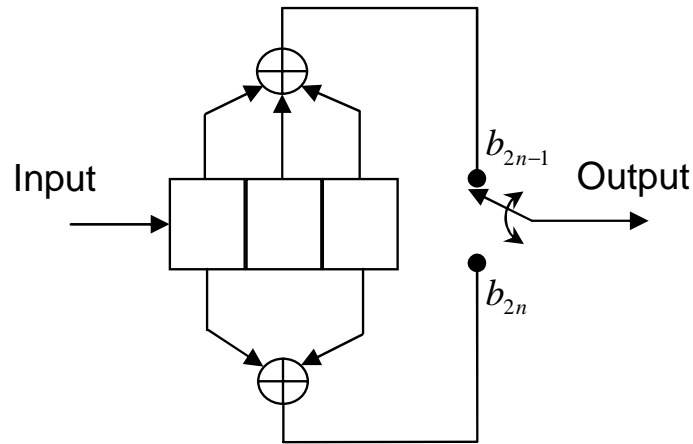


Figure 8.1: Convolutional encoder, rate  $1/2$ ,  $K = 3$ , connections  $7_8$  and  $5_8$ .

The *rate* of a convolutional encoder is the ratio between the number of inputs and the number of outputs. The factor  $K$  represents the constraint length given by the number of elements in the shift register.

The *connections* are defined by octal numbers, in this case  $7_8$  and  $5_8$ , whose binary representation are respectively  $111_2$  (indicating that the three elements of the shift register are considered in the *XOR* operation for the  $b_{2n-1}$  output) and  $101_2$  (indicating that only the first and third elements of the shift register are considered in the *XOR* operation for the  $b_{2n}$  output). *XOR* operation, is the normal logical *XOR* operation.

In the convolutional encoder described in Figs. 8.1 and 8.2 the uncoded bits go inside the encoder one by one through “Input” and the bits of the coded sequences are available in the outputs  $b_{2n-1}$  and  $b_{2n}$ . Each time that one uncoded bit goes inside the encoder, two new coded bits are available in  $b_{2n-1}$  and  $b_{2n}$ . That is the procedure to convolutional encode a sequence. Is good to observe that in Fig. 8.2 is supposed that the Input is hold by an element

of a shift register, then counting this one and the other two “D blocks” drawn in the figure, we have the same number of “memory elements” than in Fig. 8.1.

The encoder connections can also be indicated by *generator polynomials*. The following two polynomials are the correspondent ones for the convolutional encoder of the example.

$$\begin{aligned} p_1(x) &= 1 + x + x^2 \\ p_2(x) &= 1 + x^2 \end{aligned} \tag{8.1}$$

The first polynomial describes the connections for the output  $b_{2n-1}$ . The lowest order term represents the first element in the shift register (the nearest from the “Input”). If this term is 1 then the first element of the shift register is connected. The term of order 1 represents the second element in the shift register (starting from the left) and so on. Then the first polynomial indicates that all the elements of the shift register are connected. The second polynomial describes the connections for the output  $b_{2n}$ , the mechanism is equal, then it indicates that the first and third elements of the shift register are connected (the terms of order 0 and 2 are 1).

### ***State Diagram***

The *State diagram* shows the evolution of the encoding process as the variation in the state of the convolutional encoder inside a finite set of possible states. Assuming that in  $t = t_i$  one bit enters in the convolutional encoder, then the state between  $t = t_i$  and  $t = t_{i+1}$  is characterized for the content of the last two elements in the shift register in Fig. 8.1. For example if the content of the shift register in Fig. 8.1 is “000” and in  $t = t_i$  enters a “1”, then the present state (between  $t = t_i$  and  $t = t_{i+1}$ ) is “a=00” and the following state (between  $t = t_{i+1}$  and  $t = t_{i+2}$ ) will be “b=10”.

In Fig. 8.3 the *State diagram* corresponding to our example (the convolutional encoder specified in Fig. 8.1) is shown. The used notation is as follows, assume that the convolutional encoder is in the state “a=00”, then if enters one “0” to the encoder, it gives the output “00” (that is represented by “0/(0,0)”) and goes to the state “a=00”. If instead of entering one “0”, it enters one “1”, then the encoder gives the output “11” ( $b_{2n-1} = 1$  and  $b_{2n} = 1$ ) and goes to the state “b=10”; the input and the output here are represented by “1/(1,1)”. The process continues in this way for each new bit that enters to the convolutional encoder.

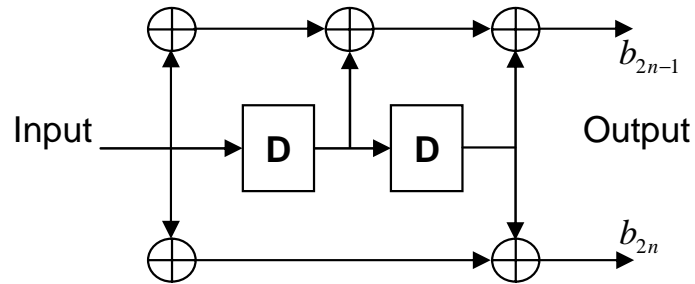


Figure 8.2: Convolutional encoder, rate  $1/2$ ,  $K = 3$ , connections  $7_8$  and  $5_8$ .

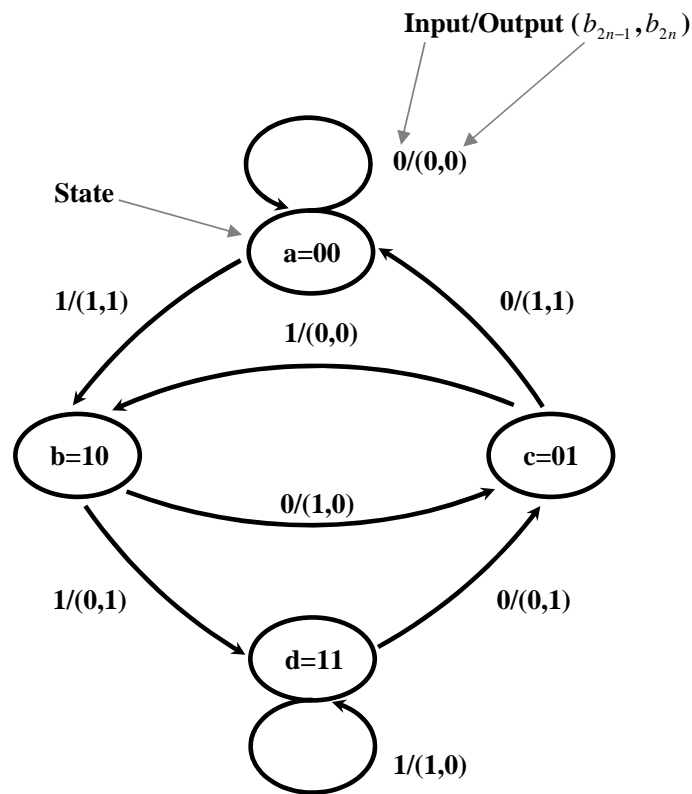


Figure 8.3: Convolutional encoder state diagram, rate  $1/2$ ,  $K = 3$ , connections  $7_8$  and  $5_8$ .

### “*Evolution Diagram*”

Due to the repetitive structure of the *Tree diagram* (Fig. 8.4) other more elegant and practical representation is possible; it is called the *Trellis diagram* (see Fig. 8.5). In the next subsection it will be explained how to use this *Trellis diagram*.

## 8.2 Viterbi Decoder

Viterbi decoder performs maximum likelihood decoding with less computational effort than “Brute Force” [7]. For “Brute Force” maximum likelihood, the number of possible paths is an exponential function of the length of the given sequence. Then for a binary sequence of length  $L$ , there will be  $2^L$  possible paths (possible sequences, each one with different probability).

In a Viterbi decoder the present state summarizes the previous evolution of the decoding process in the sense that previous states can not affect future states neither future outputs (thinking in the terminology of the state diagram). The *survivor path* (the path with higher probability) is defined each time that two possible paths join in one state. Then the *Cumulative Hamming Path Metric* (CHPM) is calculated for each path and the smallest one shows the survivor path. The CHPM evaluates the distance between the received sequence and the two possible received sequences (corresponding to each one of the two paths considered here). A deeper explanation of the process for discarding paths is given in Appendix C.

### Bit Puncturing

*Bit puncturing* is a technique to increase the data rate. It is quite well known that data rate can be changed by changing the constellation size (changing the modulation, BPSK, QPSK, QAM, etc.). But it is not the only way for achieving different data rates, puncturing allows to generate additional rates from a given convolutional code.

To explain how it works, let’s think in a convolutional code with rate  $1/2$  (1 input bit per each 2 output bits), that is the same that  $3/6$  (3 input bits per each 6 output bits); but now if it is suppressed (by puncturing) 2 bits each 6 bits at the output, that means that the final rate would be  $3/4$  (3 input bits per each 4 outputs bits).

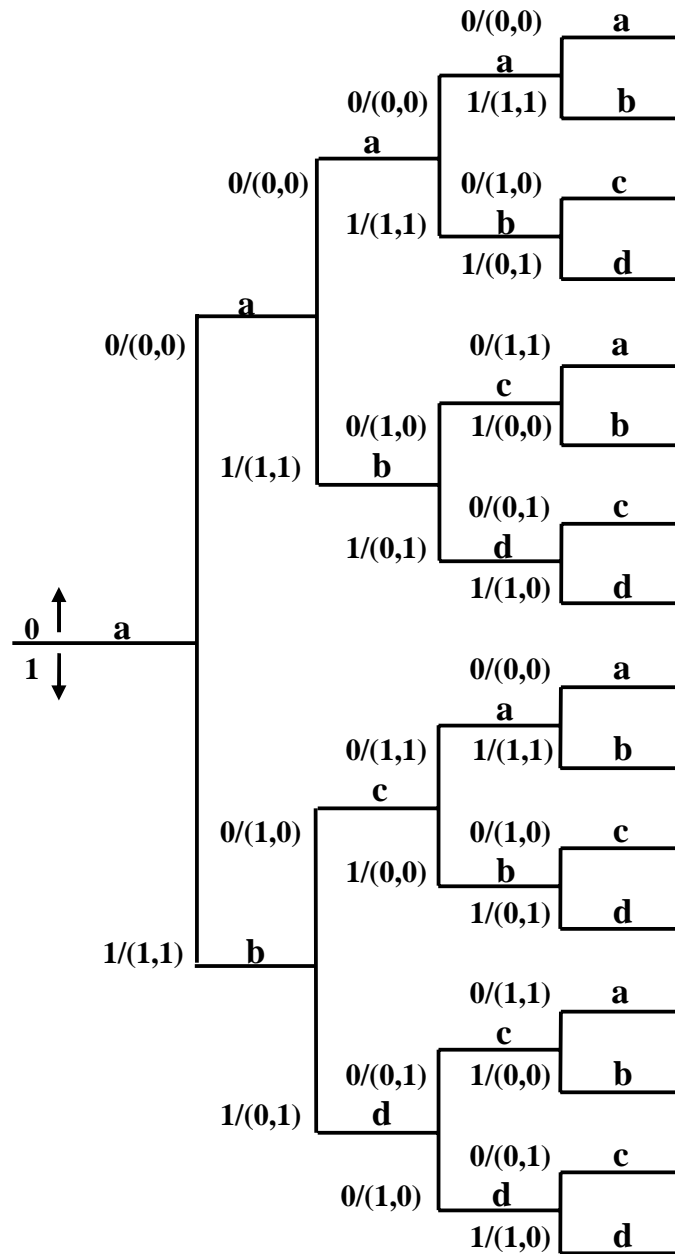


Figure 8.4: Tree representation for a convolutional encoder, rate  $1/2$ ,  $K = 3$ , connections  $7_8$  and  $5_8$ .

Which bits are suppressed is indicated by a *puncturing pattern*, e.g. it could indicate to suppress the bits four and five in each set of six bits.

This increase in rate decreases the free distance of the code; but when the convolutional code is carefully selected for the particular punctured rate, the resulting free distance is quite close to the optimum one. In the receiver, some dummy bits are inserted in the location that were punctured in the transmitter, to replace them [30].

### 8.3 Performance of the Technique in a Coded System

In this section the performance of this new class of DSTBCs in a channel coded system is studied. As channel coding technique a *convolutional encoding* with a *Viterbi decoder* was selected. These techniques were explained in the Sections 8.1 and 8.2. Some extra considerations about *Viterbi decoder*, as the time delay introduced and the complexity of the algorithm are provided in Appendix C. In particular the *convolutional encoder* considered was the one defined by the following two *generator polynomials*

$$\begin{aligned} p_1(x) &= 1 + x + x^3 + x^4 + x^6 \\ p_2(x) &= 1 + x^3 + x^4 + x^5 + x^6 \end{aligned} \quad (8.2)$$

also represented by the *connection representation* diagram specified in Fig. 8.6.

In Fig. 8.7 the results obtained for the system with *convolutional encoding* and *Viterbi decoder* are shown. There the performance with and without channel coding are compared. Also it can be seen there, that still in a coded system the performance of “4A16PSK” is much better than the corresponding to “64-PSK”. “4A16PSK PCM2” with channel coding is approximately 4.2 dB (at  $BER = 10^{-2}$ ) better than “64-PSK” used in DSTBC with channel coding.

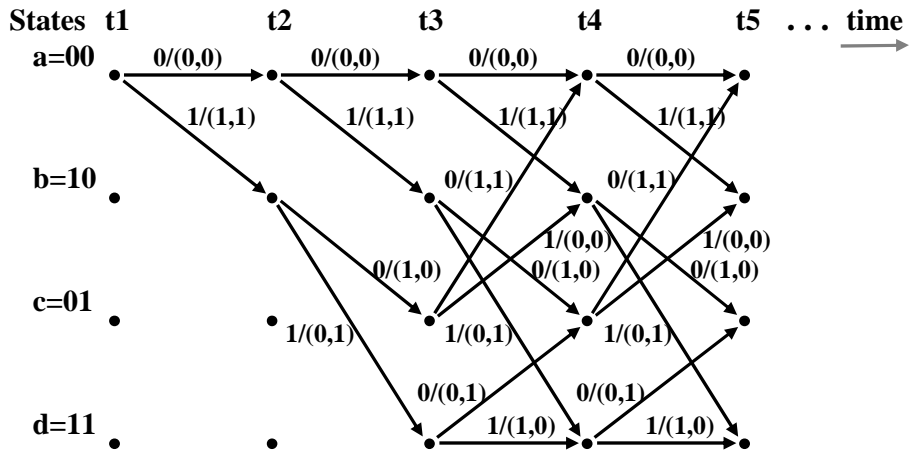


Figure 8.5: Trellis representation for a convolutional encoder, rate  $1/2$ ,  $K = 3$ , connections  $7_8$  and  $5_8$ .

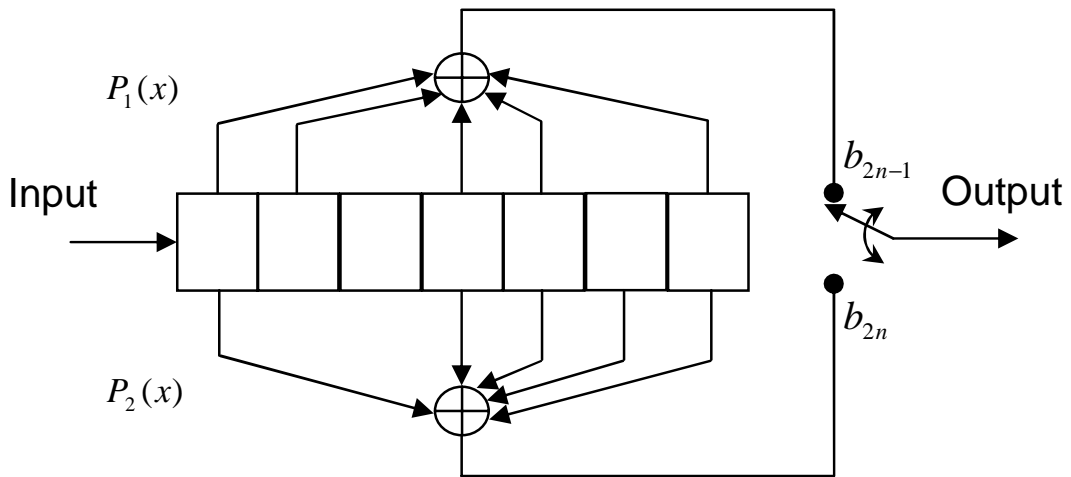


Figure 8.6: Convolutional encoder, rate  $1/2$ ,  $K = 7$ , connections  $155_8$  and  $117_8$ .

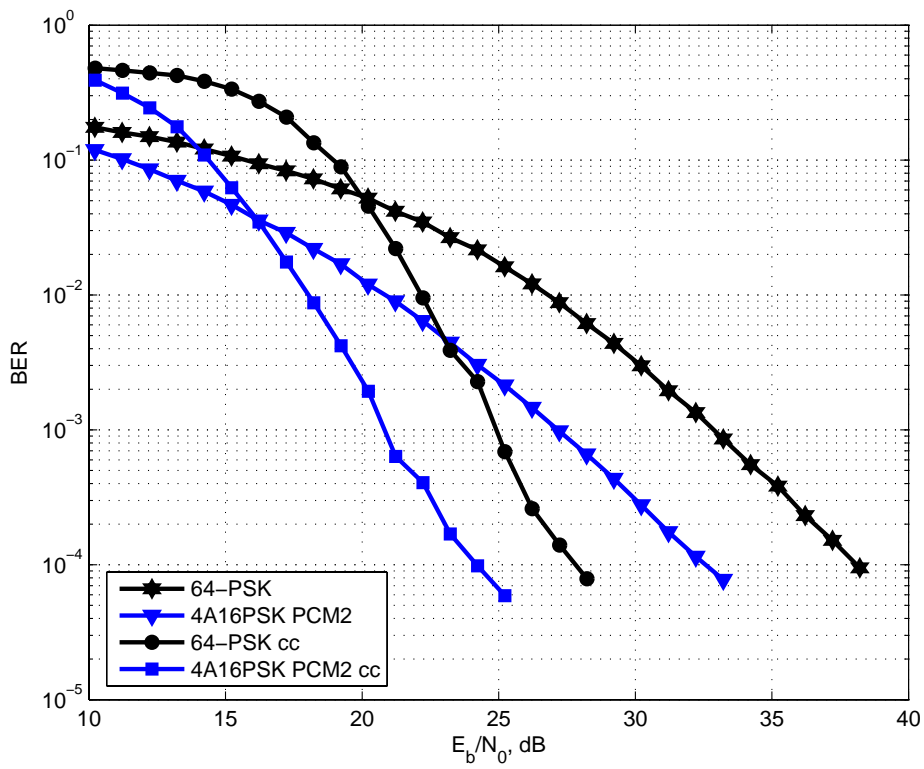


Figure 8.7: Performance of “4A16PSK PCM2” in a convolutionally coded (cc) system.

## 8.4 DSTBC, DSFBC and DSTFBC

DSTBC schemes have been considered because of its simplicity and good performance. But in order to exploit space diversity in a differential modulation scheme there are other alternatives, e.g. Differential Space Frequency Block Codes (DSFBCs) or Differential Space Time Frequency Block Codes (DSTFBCs).

In DSFBC instead of using two time slots to transmit the two rows of the  $C_k$  matrix, two neighbor subcarriers to transmit these two rows are used. In terms of an OFDM system, it means that two subcarriers of the same OFDM symbol are used instead of the same subcarrier in two consecutive OFDM symbols.

One obvious advantage of these systems is to reduce the transmission delay. DSFBCs present also advantages for channels where the time variability is high, because one  $C_k$  matrix is fully transmitted in one time slot (by using different subcarriers), that means that the condition  $H_k = H_{k-1}$  can be fulfilled just by having an unchanged channel in two consecutive time slots (considering a 2x2  $C_k$ ) instead of in four as for DSTBCs.

DSFBCs have disadvantages in channels with high frequency selectivity, because to have a good performance in this case it is necessary that the channel remains unchanged in two consecutive subcarriers (for a 2x2  $C_k$ ). That means that a similar restriction than the one in the direction of time, that has been mentioned previously, appears now in the direction of frequency. Usually one alternative to fulfill this requirement in the direction of frequency is to consider a high number of subcarriers, which results in a narrower band for each subcarrier and then less variation in the channel coefficients for neighbor subcarriers. But finally it could result in an excessive high number of subcarriers, if the channel is quite frequency selective.

The problems of this technique in frequency selective channels are still increased when four transmit antennas are used, where the channel must remain unchanged along four consecutive subcarriers. Some simulation results performed in [77] show that the restriction of constant channel coefficient over an orthogonal design (block code) is much more critical for SFBCs than for STBCs, usually needing a high number of subcarriers for the first one in order to cope with the channel frequency selectivity. While this restriction is usually easily fulfilled for STBCs.

As it was discussed previously DSTBCs have problems in channels with fast variations in time, while DSFBCs have problems in channels with high frequency selectivity. That is due to the restriction of constant channel coefficient over the block code ( $C_k$  transmit matrix). For providing more flexibility in order to handle with this restriction, the DSTFBCs were proposed.

In the case of DSTFBCs the elements of the block code can be distributed in different ways considering several subcarriers and time slots for each antenna. This option is particularly attractive when more than two transmit antennas are used. Considering the particularities of the channel (time variations and frequency selectivity) can be decided to use more time slots and less subcarriers to map the  $C_k$  elements in a mainly frequency selective channel or vice versa. In this way the degradation of the transmission can be prevented.

One advantage of DSTFBCs is to diminish the transmission delay compared with DSTBCs (advantage shared with DSFBCs). Provided that STBCs have a good performance at normal high speed for terrestrial vehicles (even using a reasonable large number of subcarriers (up to 2048) [77]), the improvement in transmission delay would be probably the more useful advantage of DSTFBCs with respect to DSTBCs. Being DSTFBCs a little bit more complex than DSTBCs and needing them some assumptions over the channel behavior in order to optimize the distribution of the block's elements in time slots and subcarriers, the second ones are still a very attractive alternative for future wireless systems.



# Chapter 9

## Summary and Conclusions

This work proposes and evaluates the use of particular modulation schemes with two subconstellations (small and big) and a power control mechanism (PCM) as an alternative for being used in DSTBC. This proposition has demonstrated to be very successful, simple and completely robust.

The proposed technique (“4A16PSK PCM2”), explained in Section 7.1, was tested in different scenarios, AWGN, uncorrelated Rayleigh fading and WS-SUS channels, showing always an excellent performance.

When this technique was tested in WSSUS channels it was found that the improvements (respect to 64-PSK in DSTBC) obtained for it are increased when the velocity of the mobile terminal is increased (considering a mobile communication). That makes the proposed technique even more convenient for high mobility scenarios (see Section 7.3). It was verified that this characteristic is also shared with another APSK technique used in DSTBC.

In order to increase the performance of the proposed technique, a receiver with multiple antennas was considered. When receive diversity is used, in order to process the information obtained through the different receive antennas is necessary to use a combining technique. In coherent systems, where channel information is available, the most successful combining technique is Maximum Ratio Combining (MRC). In DSTBCs there is no direct channel information available, consequently MRC can not be directly applied. Then, a new combining technique for DSTBCs was developed within this work. The performance of “4A16PSK PCM2” when multiple receive antennas are used demonstrated to be very good, especially when the new combining technique is used (see Fig. 7.34).

The DSTBC technique was evaluated in a coded system, showing also in this case a very good performance, see Section 8.3.

The complexity of the proposed technique is not higher than the ones corresponding to previous proposed techniques in this area, which makes this technique a quite simple and powerful option to be considered in DSTBCs. Compared with other previously proposed APSK techniques, the performance is very good, doubling in some cases the performance improvements.

The proposed DSTBC transmission technique is robust in time variant and frequency selective channels. Modulation schemes that assure a complete robustness were developed and discussed.

One important objective of this work was to study and propose a technique useful for future broadband wireless telecommunication systems. Considering the results presented in Chapter 7, the technique proposed here is a good alternative to be considered in future telecommunication systems.

The importance of MIMO techniques in broadband wireless systems was discussed. Some alternatives to apply these techniques in combination with OFDM based systems were presented. Several examples of the improvements in robustness produced by the use of multiple antennas in wireless systems were provided within this work (see Figs. 6.5, 7.33 and 7.34). Also the increase of the channel estimation effort related to MIMO techniques was discussed, as well as the convenience of avoiding it by using differential modulation techniques with incoherent demodulation. A comparative analysis of complexity and performance for coherent and incoherent demodulation techniques was also provided in this work.

Given the success of OFDM transmission technique it was important to propose a technique applicable to this multicarrier concept. The OFDM transmission technique provides an important robustness against multipath fading (as shown in Chapter 3) keeping a low level of system complexity.

When the proposed technique is considered in an OFDM based system, a differential MIMO-OFDM system is obtained, combining in this case the advantages of these techniques. By being a differential modulation technique with incoherent demodulation, channel estimation is not needed. That is particularly important for reducing the system complexity in MIMO systems, where the number of channels to estimate is equal to the product of the num-

bers of transmit and receive antennas. By being a MIMO system a lower bit error rate can be achieved for the same throughput. As an OFDM based system an excellent performance in multipath fading scenarios, a very high bandwidth efficiency and a low complexity hardware implementation can be assured. Considering all these advantages, the implementation of “4A16PSK PCM2” in DSTBC on OFDM based systems is a very attractive option for future broadband wireless telecommunication networks.



# Appendix A

## Doppler Profile

When the mobile terminal has a velocity  $\vec{v}$  then a shift in frequency is observed in the received signal. The difference between the transmitted and the received frequency is known as *Doppler Frequency* ( $f_D$ ) and it is related with the velocity of the mobile terminal as follows

$$f_D = \frac{f_0 \cdot v \cdot \cos(\varphi)}{c} \quad (\text{A.1})$$

Where  $f_0$  is the transmitted frequency,  $v$  is the velocity of the mobile (smaller or greater than 0) in reference with the direction shown in Fig. A.1 and  $c$  is the speed of light.

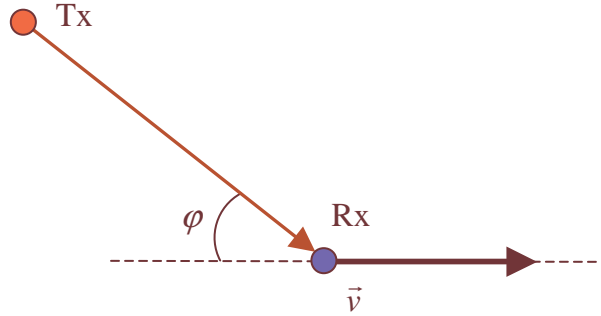


Figure A.1: Tx and mobile Rx scheme.

Observe that when the mobile terminal (Rx) moves towards the Tx then the frequency of the received signal is increased ( $f_D < 0$ ) and when the mobile terminal moves away of the Tx the frequency of the received signal is decreased ( $f_D > 0$ ).

$$f_{Dmax} = \frac{f_0 \cdot v}{c} \quad (\text{A.2})$$

The maximum frequency shift is obtained when  $\cos(\varphi) = 0$  and has the value specified in (A.2). Then,

$$f_D = f_{Dmax} \cdot \cos(\varphi) \quad (\text{A.3})$$

Now if it is assumed that the angle of arrival of the signal is uniformly distributed in  $[0, 2\pi)$  the *probability density function* (PDF) of  $f_D$  can be calculated. Remembering that for obtaining a variable  $v$  with a given *cumulative distribution function* (CDF) equal to  $C$ , we can start from an uniformly distributed variable  $u$  and make  $v = C^{-1}(u)$ . Then it can be written

$$f_D = F^{-1}(\varphi) \quad (\text{A.4})$$

where  $F$  is the CDF of  $f_D$ . Then by identifying terms in equations (A.3) and (A.4) we can write that

$$F^{-1}(\varphi) = f_{Dmax} \cdot \cos(\varphi) \quad (\text{A.5})$$

then

$$\varphi = F(f_D) = \arccos\left(\frac{f_D}{f_{Dmax}}\right) \quad (\text{A.6})$$

Where  $F(f_D)$  is the *cdf*( $f_D$ ) (CDF of  $f_D$ ), for more clarifications see Fig. A.2.

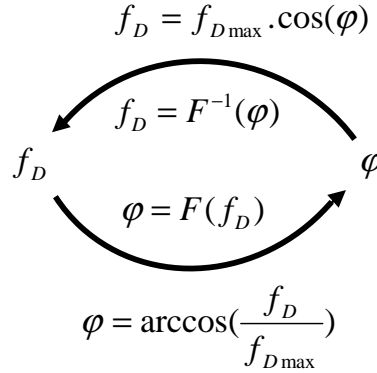


Figure A.2: CDF of  $f_D$  ( $F(f_D)$ ).

Considering that the CDF is the integral of the PDF,

$$cdf(f_D) = \int_{-\infty}^{f_D} pdf(f'_D) \cdot df'_D \quad (\text{A.7})$$

then can be obtained the PDF as

$$pdf'(f_D) = \frac{d}{df_D}(cdf(f_D)) \quad (\text{A.8})$$

then

$$\begin{aligned} pdf'(f_D) &= \frac{d}{df_D} \left( \arccos \left( \frac{f_D}{f_{Dmax}} \right) \right) = -\frac{\frac{1}{f_{Dmax}}}{\sqrt{1 - \left(\frac{f_D}{f_{Dmax}}\right)^2}} \\ &= -\frac{1}{f_{Dmax} \cdot \sqrt{1 - \left(\frac{f_D}{f_{Dmax}}\right)^2}} \end{aligned} \quad (\text{A.9})$$

But for being a PDF it has to verify that

$$\int_{-f_{Dmax}}^{f_{Dmax}} pdf(f_D) \cdot df_D \equiv 1 \quad (\text{A.10})$$

Assuming  $pdf(f_D) = k \cdot pdf'(f_D)$  then

$$\int_{-f_{Dmax}}^{f_{Dmax}} k \cdot pdf'(f_D) \cdot df_D = k \cdot [\arccos(1) - \arccos(-1)] = -k \cdot \pi = 1 \quad (\text{A.11})$$

then

$$k = -\frac{1}{\pi} \Rightarrow pdf(f_D) = \frac{1}{\pi \cdot f_{Dmax} \cdot \sqrt{1 - \left(\frac{f_D}{f_{Dmax}}\right)^2}} \quad (\text{A.12})$$

Then we can write this *probability density function* as:

$$pdf(f_D) = \begin{cases} \frac{1}{\pi \cdot f_{Dmax} \cdot \sqrt{1 - \left(\frac{f_D}{f_{Dmax}}\right)^2}} & (|f_D| < f_{Dmax}) \\ 0 & \text{in other case} \end{cases} \quad (\text{A.13})$$

This Doppler power spectra profile is known as “*Jakes Doppler Profile*” and it looks like it is shown in Fig. A.3.

Other well known profiles are: “*Rectangular Doppler Profile*”

$$pdf(f_D) = \begin{cases} \frac{1}{2 \cdot f_{Dmax}} & (|f_D| \leq f_{Dmax}) \\ 0 & \text{in other case} \end{cases} \quad (\text{A.14})$$

and “*Gauss Doppler Profile*”

$$pdf(f_D) = \frac{1}{\sqrt{2 \cdot \pi \cdot \sigma_{f_D}^2}} \cdot e^{-\frac{(f_D - \bar{f}_D)^2}{2 \cdot \sigma_{f_D}^2}} = G(\bar{f}_D, \sigma_{f_D}) \quad (\text{A.15})$$

Where  $\sigma_{f_D}$  is the standard deviation of  $f_D$  and  $\bar{f}_D$  is the mean Doppler shift. Further information in [17].

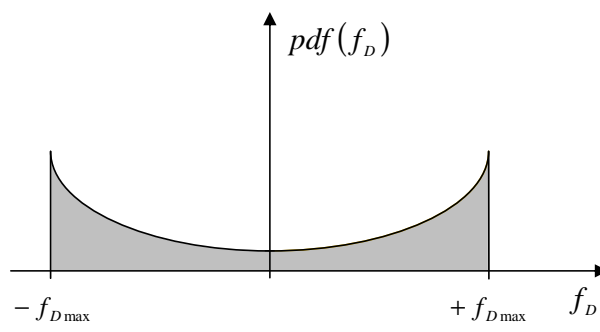


Figure A.3: *Jakes Doppler Profile.*

# Appendix B

## Channel Model Based on COST 207 Project

Different examples of  $p(\tau)$  can be found in the COST 207 specifications, used for the research and development of GSM system. In this case the *probability density function* of  $\tau$ ,  $p(\tau)$  (also called *power delay profile*) is as it was shown in (2.38). The parameters  $a$ ,  $b$  and  $\tau_{max}$  in this case were provided considering three different environments, *rural area* (RA), *typical urban* (TU) and *hilly terrain* (HT). The parameters corresponding to the different channel models for these environments considered in COST 207 are summarized in Table B.1.

Table B.1: Power delay profiles for COST 207.

Models	Power Delay Profile $p(\tau)$
RA	$p(\tau) = e^{\left(\frac{-9.2\tau}{1\mu s}\right)} \quad 0 \leq \tau < 0.7\mu s$
TU	$p(\tau) = e^{\left(\frac{-\tau}{1\mu s}\right)} \quad 0 \leq \tau < 7\mu s$
HT	$p(\tau) = \begin{cases} e^{\frac{-3.5\tau}{1\mu s}} & 0 \leq \tau < 2\mu s \\ 0.04e^{\frac{(15-\tau)}{1\mu s}} & 15\mu s \leq \tau < 20\mu s \end{cases}$



# Appendix C

## Viterbi Decoder Considerations

The process for discarding paths with lower probability (Higher CHPM) is shown in Figs. C.1 and C.2; in Fig. C.1 the CHPM for all possible paths is calculated and in Fig. C.2 the process to obtain the *survivor path* is shown. In both Figs. we are considering the Viterbi decoding process applied over a sequence encoded by the convolutional encoder used as example in Section 8.1.

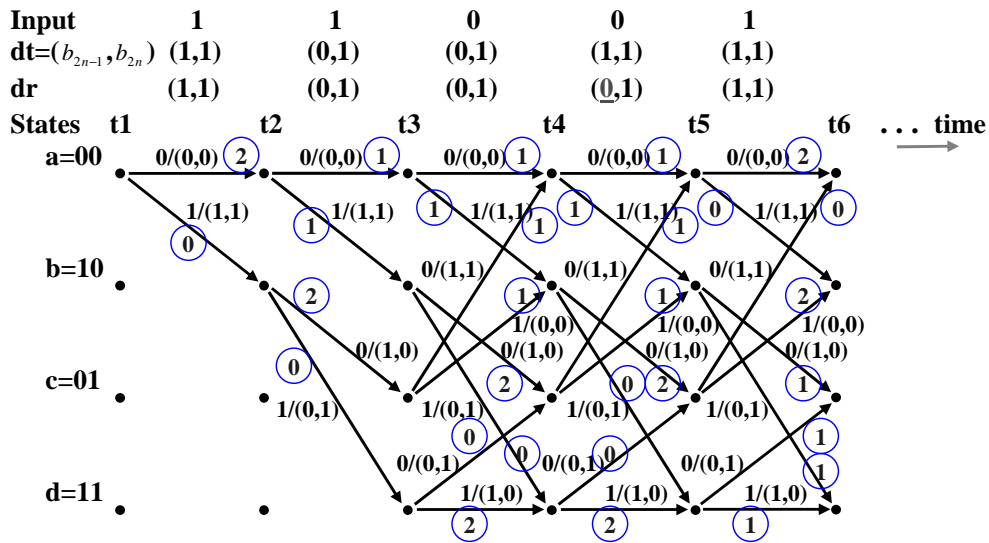


Figure C.1: CHPM calculation in the Viterbi decoding process.

In Fig. C.1, when the process arrives to  $t_5$  there is enough information to decide between two possible paths. In this way the *survivor path* is obtained.

In Fig. C.2, two paths that converge to one point (state  $a$  in  $t = t_5$ ) are shown, the CHPM for the upper path is 4 while the CHPM for the lower path is 1, then the surviving path will be the lower one. Observe that this path should have a CHPM=0; the reason why it is 1 is only because it was assumed the reception of an erroneous bit at  $t = t_4$  ( $(0, 1)$  instead of  $(1, 1)$ ).

When both paths starting from one point are discarded, also the path arriving to that point is discarded, there is no reason to maintain this path because the paths starting from that point are not *survivor paths*. That is the way for eliminating paths with lower probability in order to obtain the path with highest probability as the executed path. This process is analyzed in detail with the help of Fig. C.3.

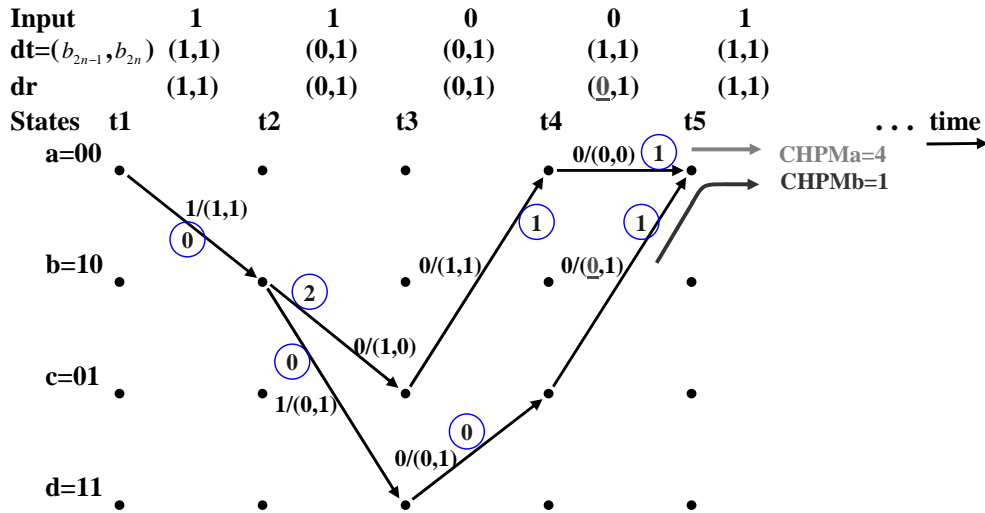


Figure C.2: Discarding of paths by comparing the CHPM in a Viterbi decoding process.

In Fig. C.3 can be observed that the first data bit received can not be decoded until the path metric computation for  $t_4$  has been processed in the trellis; only in that moment we have enough information to discard the path that goes from state  $a$  in  $t = t_1$  to state  $a$  in  $t = t_2$  ( $(a, t_1) \rightarrow (a, t_2)$ ). Only at  $t = t_4$  is clear that all the paths to which this path ( $(a, t_1) \rightarrow (a, t_2)$ ) contributes have higher CHPM than the corresponding alternative path, then this path can not be part of the executed path (*survivor path*) and is deleted. This delay in the decoding process is called *decoding delay*. For a typical Viterbi decoder implementation, this *decoding delay* can be as much as five times the constraint length (see Section 8.1); that means that in this example ( $K = 3$ )

the *decoding delay* can be as much as  $5 * K = 15$  time intervals; that is an important time delay. As it was said, when this path  $((a, t_1) \rightarrow (a, t_2))$  is deleted, all the paths that had origin in this one are deleted too, that is the difference between (c) and (d) in Fig. C.3.

Later the trellis evolution between  $t_4$  and  $t_5$  is presented in (e) and the “*survivor paths up to  $t_5$* ” are calculated (see (f)). The future evolution of the decoding process will determine which one of these “*survivor paths up to  $t_5$* ” will be finally the *survivor path*. An extended evolution of trellis diagram is presented in Fig. C.4.

Fig. C.4 shows a deeper evolution of the Viterbi decoder in the trellis diagram in order to carefully describe the Viterbi decoding algorithm. As an example for the two paths that arrive to state  $b$  in  $t = t_7$  the (minimum) CHPM is equal, then none of them can be discarded at  $t = t_7$ . But in  $t = t_8$  both will be discarded, due to the fact that the two paths coming from this point (state  $b$  in  $t = t_7$ ) will have grater CHPM than the corresponding other two paths arriving respectively to state  $c$  in  $t = t_8$  and state  $d$  in  $t = t_8$ . Once that the two paths coming from one point (in this case state  $b$  in  $t = t_7$ ) are discarded, they are also discarded the two paths arriving to this point. In this way some previously possible paths are discarded at  $t = t_8$ .

By applying this procedure of discarding paths with grater CHPM can be seen that only at  $t = t_{10}$  there is enough information to decide which was the third sent bit (at  $t = t_3$ ). Also can be observed that only at  $t = t_{11}$  the fourth sent bit can be decided. Observe that thanks to the application of this procedure the fourth sent bit is correctly decided, although one of the received bits was wrong. Also at  $t = t_{11}$  (by applying this procedure) the bits 5, 6, 7 and 8 can be decided. At  $t = t_{12}$  there is enough information to decide bit 9 but not enough to decide bit 10. At  $t = t_{13}$  bit 10 can be decided and in the next time interval bit 11 can be decided. The procedure continues in this way up to the moment in which all the received bits have been processed.

The *decoding delay* described in this appendix, which can be an important limitation for certain single carrier systems, has a minor impact when OFDM systems are considered due to the parallel processing of the information in this second case. For this reason the convenience of using this channel coding technique is related with the given application (how sensitive it is to the delay), the considered system and the expected level of SNR (see Fig. 8.7).

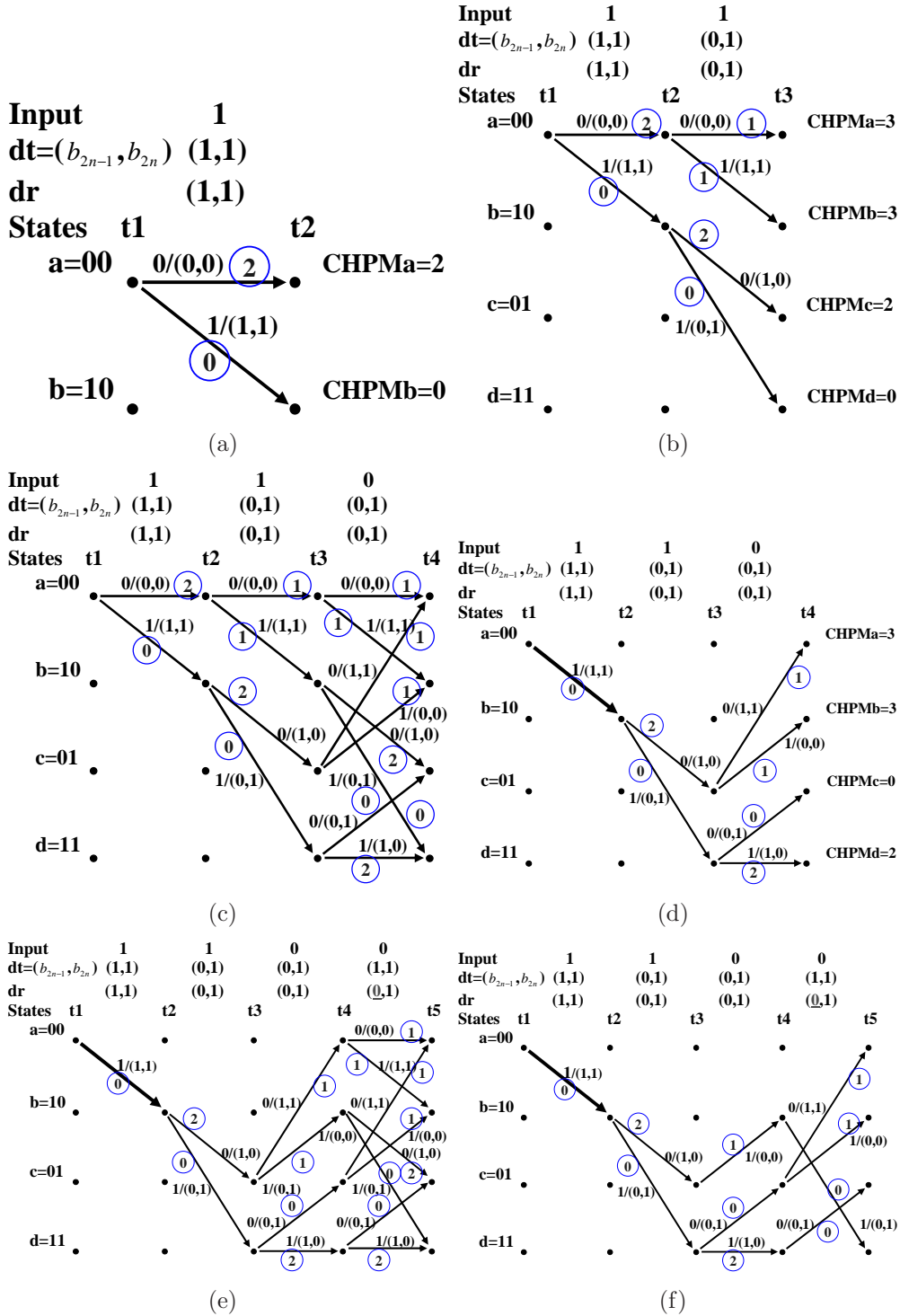


Figure C.3: Evolution of the Viterbi decoding process and *decoding delay*.





# List of Figures

1.1	Scheme of a wireless system. . . . .	2
2.1	Propagation Mechanisms. . . . .	9
2.2	$(\frac{P_r}{P_t})_{dB}$ versus $d$ for “ <i>path loss</i> ”, “ <i>path loss+shadowing</i> ” and “ <i>path loss+shadowing+multipath propagation</i> ”. . . . .	14
2.3	Multipath fading for a stationary terminal. . . . .	14
2.4	Representation of $h(\tau, t)$ . . . . .	15
2.5	Linear Time-variant systems. . . . .	19
2.6	Linear Time-variant functions. . . . .	20
2.7	Relation between ACFs for a WSSUS channel model. . . . .	21
2.8	Definition of $T_c$ and $B_c$ by using $\Phi_H(\Delta f, \Delta t)$ . . . . .	24
2.9	Examples of WSSUS channels. . . . .	26
3.1	Basic representation of an OFDM system [21]. . . . .	28
3.2	QPSK constellation. . . . .	28
3.3	Continuous time model for an OFDM system [21]. . . . .	29
3.4	Continuous time model for an OFDM transmitter. . . . .	30
3.5	Spectrum of $\phi_k(t - lT)$ . . . . .	31
3.6	Overlapping subcarrier spectra. . . . .	32
3.7	Discrete time model for an OFDM system [21]. . . . .	34
3.8	CP and FFT window in an OFDM system. . . . .	35
3.9	Simplified block diagram of a IEEE802.11a OFDM based transmitter. . . . .	36
3.10	Simplified block diagram of a IEEE802.16 OFDM based transmitter. . . . .	40
4.1	Example of a possible pilot pattern for channel estimation in an OFDM system. . . . .	43
4.2	Block diagram of differential modulation and incoherent demodulation in time direction. . . . .	49

4.3	Alternatives for the use of reference values in differential modulations for OFDM systems. . . . .	50
4.4	Comparison between coherent (ideal CSI) and incoherent 64-PSK demodulations in an uncorrelated Rayleigh fading channel. . . . .	51
5.1	Channel <i>transfer function</i> ( $H(f, t)$ ) for a given time instant ( $t = t_0$ ). . . . .	56
5.2	Water-Filling representation. . . . .	58
5.3	Receive diversity technique. . . . .	61
5.4	Transmit diversity technique. . . . .	62
6.1	Scheme of a MIMO system. . . . .	65
6.2	MIMO Channel for $N_T$ transmit antennas and $N_R$ receive antennas. . . . .	67
6.3	Representation of a MIMO system. . . . .	67
6.4	Representation of a MIMO-OFDM system. . . . .	72
6.5	Comparison between differential 64PSK modulation in a SISO case and in a 2x3 MIMO case in an uncorrelated Rayleigh fading channel. . . . .	73
7.1	General Scheme of the considered MISO system. . . . .	76
7.2	$C_k$ matrix transmitted at time slot $k$ . . . . .	77
7.3	64-PSK modulation applied to DSTBC schemes. . . . .	79
7.4	“4A16PSK” modulation scheme used in DSTBC. . . . .	80
7.5	Comparison between “4A16PSK PCM1” and 64-PSK for DSTBCs in an uncorrelated Rayleigh fading channel. . . . .	82
7.6	“2A32PSK” modulation applied to DSTBC scheme. . . . .	83
7.7	Comparison between “2A32PSK PCM1” and 64-PSK for DSTBCs in an uncorrelated Rayleigh fading channel. . . . .	84
7.8	“APSK1” modulation scheme used in DSTBC. . . . .	85
7.9	Comparison between “APSK1 PCM1” and 64-PSK for DSTBCs in an uncorrelated Rayleigh fading channel. . . . .	86
7.10	“APSK2” modulation scheme used in DSTBC. . . . .	87
7.11	Comparison between “APSK2 PCM1” and 64-PSK for DSTBCs in an uncorrelated Rayleigh fading channel. . . . .	88
7.12	“APSK3” modulation scheme used in DSTBC. . . . .	89
7.13	Comparison between “APSK3 PCM1” and 64-PSK for DSTBCs in an uncorrelated Rayleigh fading channel. . . . .	90
7.14	Results for all the tested APSK modulation schemes with PCM1 in an uncorrelated Rayleigh fading channel. . . . .	92

7.15	Results for 64-PSK, “4A16PSK” and “2A32PSK” with PCM1 in an AWGN channel. . . . .	93
7.16	Comparison of “64-PSK” and “4A16PSK” used with different PCM techniques. . . . .	96
7.17	Histograms of $\ C_k\ _2$ for “4A16PSK” used with different PCMs. . . . .	97
7.18	Comparison of “64-PSK” and “2A32PSK” used with different PCM techniques. . . . .	98
7.19	Histograms of $\ C_k\ _2$ for “2A32PSK” used with different PCMs. . . . .	100
7.20	Performance of 64PSK used in DSTBC under WSSUS channels ( $H_k = H_{k-1}, v = 60 \text{ km/h}$ ). . . . .	103
7.21	Performance of “4A16PSK PCM2” used in DSTBC under WSSUS channels ( $H_k = H_{k-1}, v = 60 \text{ km/h}$ ). . . . .	103
7.22	Performance of 64PSK used in DSTBC under WSSUS channels ( $H_k \approx H_{k-1}, v = 60 \text{ km/h}$ ). . . . .	105
7.23	Performance of “4A16PSK PCM2” used in DSTBC under WSSUS channels ( $H_k \approx H_{k-1}, v = 60 \text{ km/h}$ ). . . . .	105
7.24	Performance of 64PSK used in DSTBC under WSSUS channels ( $H_k \approx H_{k-1}, v = 120 \text{ km/h}$ ). . . . .	106
7.25	Performance of “4A16PSK PCM2” used in DSTBC under WSSUS channels ( $H_k \approx H_{k-1}, v = 120 \text{ km/h}$ ). . . . .	106
7.26	Performance of 64PSK used in DSTBC under WSSUS channels ( $H_k \approx H_{k-1}, v = 3 \text{ km/h}$ ). . . . .	107
7.27	Performance of “4A16PSK PCM2” used in DSTBC under WSSUS channels ( $H_k \approx H_{k-1}, v = 3 \text{ km/h}$ ). . . . .	107
7.28	Performance of “2L-APSK” used in DSTBC under WSSUS channels ( $H_k \approx H_{k-1}, v = 60 \text{ km/h}$ ). . . . .	110
7.29	Performance of “2L-APSK” used in DSTBC under WSSUS channels ( $H_k \approx H_{k-1}, v = 120 \text{ km/h}$ ). . . . .	110
7.30	Performance of “2L-APSK” used in DSTBC under WSSUS channels ( $H_k \approx H_{k-1}, v = 3 \text{ km/h}$ ). . . . .	111
7.31	Relative improvements of “2L-APSK” and “4A16PSK PCM2” with respect to 64-PSK used in DSTBC versus mobile terminal velocity, under WSSUS channels ( $H_k \approx H_{k-1}$ ). . . . .	111
7.32	Combination system for the proposed technique with multiple receive antennas. . . . .	113
7.33	Results for the <i>Equal Gain Combining</i> technique in a multiple receive antenna system. . . . .	113
7.34	Results for the <i>Maximum Ratio Combining</i> technique in a multiple receive antenna system. . . . .	115
8.1	Convolutional encoder, rate $1/2$ , $K = 3$ , connections $7_8$ and $5_8$ . . . . .	118

8.2	Convolutional encoder, rate $1/2$ , $K = 3$ , <i>connections</i> $7_8$ and $5_8$ .	120
8.3	Convolutional encoder state diagram, rate $1/2$ , $K = 3$ , <i>connections</i> $7_8$ and $5_8$ .	120
8.4	Tree representation for a convolutional encoder, rate $1/2$ , $K = 3$ , <i>connections</i> $7_8$ and $5_8$ .	122
8.5	Trellis representation for a convolutional encoder, rate $1/2$ , $K = 3$ , <i>connections</i> $7_8$ and $5_8$ .	124
8.6	Convolutional encoder, rate $1/2$ , $K = 7$ , <i>connections</i> $155_8$ and $117_8$ .	124
8.7	Performance of "4A16PSK PCM2" in a convolutionally coded (cc) system.	125
A.1	Tx and mobile Rx scheme.	133
A.2	CDF of $f_D$ ( $F(f_D)$ ).	134
A.3	<i>Jakes Doppler Profile</i> .	136
C.1	CHPM calculation in the Viterbi decoding process.	139
C.2	Discarding of paths by comparing the CHPM in a Viterbi decoding process.	140
C.3	Evolution of the Viterbi decoding process and <i>decoding delay</i> .	142
C.4	Example of a deeper evolution of the Viterbi decoding process.	143

# List of Tables

2.1	Path Loss Exponents for different Environments [3]. . . . .	13
6.1	Classification of MIMO techniques considering the required CSI. . . . .	66
7.1	New PCMs evaluated. . . . .	95
7.2	Simulation parameters. . . . .	102
7.3	Improvement of the proposed technique (respect to 64-PSK) for different mobile terminal velocities in WSSUS channels with $(H_k \approx H_{k-1})$ . . . . .	108
B.1	Power delay profiles for COST 207. . . . .	137



# List of Abbreviations

## A

- ACF** Autocorrelation Function.  
**APSK** Amplitude and Phase Shift Keying.

## B

- BE** Bandwidth Efficiency.  
**BER** Bit Error Rate.  
**BPSK** Binary Phase Shift Keying.

## C

- CDMA** Code Division Multiple Access.  
**CHPM** Cumulative Hamming Path Metric.  
**COST** European Co-operation in the field of Scientific and Technical research.  
**CP** Cyclic Prefix.  
**CSI** Channel State Information.

## D

- DAPSK** Differential Amplitude and Phase Shift Keying.  
**DDCE** Direct Decision Channel Estimation.  
**DFT** Discrete Fourier Transform.

<b>DLC</b>	Data Link Control.
<b>DSFBC</b>	Differential Space Frequency Block Code.
<b>DSSS</b>	Direct Sequence Spread Spectrum.
<b>DSTBC</b>	Differential Space Time Block Code.
<b>DSTFBC</b>	Differential Space Time Frequency Block Code.
<b>DVB-T</b>	Digital Video Broadcasting-Terrestrial.
<b>F</b>	
<b>FHSS</b>	Frequency Hopping Spread Spectrum.
<b>FT</b>	Fourier Transform.
<b>G</b>	
<b>GSM</b>	Global System for Mobile communication (Groupe Spéciale Mobile).
<b>H</b>	
<b>HF</b>	High Frequency.
<b>I</b>	
<b>ICI</b>	Inter Carrier Interference.
<b>IDFT</b>	Inverse Discrete Fourier Transform.
<b>ISI</b>	Inter Symbol Interference.
<b>L</b>	
<b>LA</b>	Link Adaptation.
<b>LOS</b>	Line of Sight.
<b>LTV</b>	Linear Time Variant.

**M**

- MCM** Multi Carrier Modulation.  
**MIMO** Multiple Input Multiple Output.  
**MISO** Multiple Input Single Output.  
**MRC** Maximum Ratio Combining.

**N**

- NLOS** No Line of Sight.

**O**

- OFDM** Orthogonal Frequency Division Multiplexing.

**P**

- PACE** Pilot Aided Channel Estimation.  
**PAN** Personal Area Network.  
**PCM** Power Control Mechanism.  
**PDF** Probability Density Function.  
**PDP** Power Delay Profile.  
**PER** Packet Error Rate.  
**PHY** Physical Layer.

**Q**

- QAM** Quadrature Amplitude Modulation.  
**QPSK** Quadrature Phase Shift Keying.

**R**

- Rx** Receiver.

**S**

- SFBC** Space Frequency Block Code.  
**SHF** Super High Frequency.  
**SISO** Single Input Single Output.  
**SNR** Signal to Noise Ratio.  
**SORRM** Self Organizing Radio Resource Management.  
**STBC** Space Time Block Code.

**T**

- Tx** Transmitter.

**W**

- Wi-Fi** Wireless Fidelity.  
**WiMAX** Worldwide Interoperability for Microwave Access.  
**WLAN** Wireless Local Area Network.  
**WLL** Wireless Local Loop.  
**WMAN** Wireless Metropolitan Area Network.  
**WSS** Wide Sense Stationary.  
**WSSUS** Wide Sense Stationary with Uncorrelated Scattering.

# Bibliography

- [1] C. A. Balanis, *ANTENNA THEORY, Analysis and Design*, 2nd ed. John Wiley & Sons, Inc., 1997.
- [2] Y.-B. Lin and I. Chlamtac, *Wireless and Mobile Network Architectures*. John Wiley & Sons, Inc., 2001.
- [3] T. S. Rappaport, *Wireless Communications Principles and Practice*, 2nd ed. Prentice Hall, 2002.
- [4] J. B. Johnson, “Thermal agitation of electricity in conductors,” *Phys. Rev.*, vol. 32, pp. 97–109, July 1928.
- [5] H. Nyquist, “Thermal agitation of electric charge in conductors,” *Phys. Rev.*, vol. 32, pp. 110–113, July 1928.
- [6] A. Papoulis, *Probability, Random Variables, and Stochastic Processes*. New York: McGraw-Hill Book Company, 1965.
- [7] B. Sklar, *DIGITAL COMMUNICATIONS Fundamentals and Applications*, 2nd ed. Upper Saddle River, New Jersey 07458, USA: Prentice Hall PTR, 2001.
- [8] A. Goldsmith, *Wireless Communications*. Cambridge University Press, 2005.
- [9] T. Okumura, E. Ohmori, and K. Fukuda, “Field strength and its variability in VHF and UHF land mobile service,” *Review Electrical Communication Laboratory*, vol. 16, no. 9-10, pp. 825–873, September-October 1968.
- [10] M. Hata, “Empirical formula for propagation loss in land mobile radio services,” *IEEE Trans. Vehic. Technol.*, vol. VT-29, no. 3, pp. 317–325, August 1980.

- [11] European Cooperative in the Field of Science and Technical Research EURO-COST 231, "Urban transmission loss models for mobile radio in the 900 and 1800 MHz bands," Revision 2, The Hague, Netherlands, September 1991.
- [12] J. Walfisch and H. L. Bertoni, "A theoretical model of UHF propagation in urban environments," *IEEE Trans. Antennas and Propagation*, pp. 1788–1796, October 1988.
- [13] S. Y. Seidel and T. S. Rappaport, "914 MHz path loss prediction models for indoor wireless communications in multifloored buildings," *IEEE Transactions on Antennas and Propagation*, pp. 207–217, February 1992.
- [14] A. J. Motley and J. M. P. Keenan, "Personal communication radio coverage in buildings at 900 MHz and 1700 MHz," *Electronics Letters*, pp. 763–764, June 1988.
- [15] F. C. Owen and C. D. Pudney, "Radio propagation for digital cordless telephones at 1700 MHz and 900 MHz," *Electronics Letters*, pp. 52–53, September 1988.
- [16] A. F. Toledo and A. M. D. Turkmani, "Propagation into and within buildings at 900, 1800 and 2300 MHz," in *Proc. IEEE Vehicular Technology Conference*, May 1992, pp. 633–636.
- [17] A. Hutter, "Multiple antenna equalization for mobile OFDM systems," Ph.D. dissertation, Munich University of Technology (TUM), January 2001.
- [18] P. Hoehner, "A statistical discrete-time model for the WSSUS multipath channel," *IEEE Transactions on Vehicular Technology*, vol. 41, no. 4, pp. 461–468, November 1992.
- [19] R. W. Chang, "Synthesis of band-limited orthogonal signals for multi-channel data transmission," *Bell System Technical Journal*, vol. 45, pp. 1775–1796, 1966.
- [20] S. B. Weinstein and P. M. Ebert, "Data transmission by frequency-division multiplexing using the discrete fourier transform," *IEEE Trans. Commun.*, vol. 19(5), pp. 628–634, October 1971.

- [21] O. Edfors, M. Sandell, J. J. van de Beek, D. Landström, and F. Sjöberg, “An introduction to orthogonal frequency-division multiplexing,” *Research Report TULEA 1996:16, Division of Signal Processing, Luleå University of Technology, Luleå*, September 1996, available in: <http://www.sm.luth.se/csee/sp/research/report/esb96rc.html>.
- [22] A. V. Oppenheim and R. W. Schaffer, *DISCRETE-TIME SIGNAL PROCESSING*, 2nd ed. Upper Saddle River, New Jersey 07458, USA: Prentice Hall, 1989.
- [23] IEEE Std 802.11a-1999, “Supplement to IEEE Standard for Information technology - Telecommunications and information exchange between systems - Local and metropolitan area networks - Specific requirements, Part 11: Wireless LAN Medium Access Control (MAC) and Physical Layer (PHY) specifications - High-speed Physical Layer in the 5 GHz Band,” 1999.
- [24] J. Maurer, T. Fügen, and W. Wiesbeck, “System simulations based on IEEE802.11a for inter-vehicle communications using a realistic channel model,” in *Proc. of the 2<sup>nd</sup> International Workshop on Intelligent Transportation*, Hamburg, Germany, March 15<sup>th</sup> / 16<sup>th</sup> 2005, pp. 147–151.
- [25] K. Meier, A. Lübke, and T. Thomas, “Performance tests of wireless LAN for Car-to-X communication,” in *Proc. of the 4<sup>th</sup> International Workshop on Intelligent Transportation*, Hamburg, Germany, March 20<sup>th</sup> / 21<sup>st</sup> 2007, pp. 21–24.
- [26] D. Bonacci, W. Vigneau, and F. Castanié, “A Wi-Fi network for surveillance of airport mobiles,” in *Proc. of the 3<sup>rd</sup> International Workshop on Intelligent Transportation*, Hamburg, Germany, March 14<sup>th</sup> / 15<sup>th</sup> 2006, pp. 95–100.
- [27] IEEE Std 802.16-2004, “IEEE Standard for Local and metropolitan area networks, Part 16: Air Interface for Fixed Broadband Wireless Access Systems,” October 1<sup>st</sup> 2004.
- [28] IEEE Std 802.16e-2005, “IEEE Standard for Local and metropolitan area networks, Part 16: Air Interface for Fixed and Mobile Broadband Wireless Access Systems, Amendment 2: Physical and Medium Access Control Layers for Combined Fixed and Mobile Operation in Licensed Bands and Corrigendum 1,” February 28<sup>th</sup> 2006.
- [29] S. R. Searle, *Matrix Algebra Useful for Statistics*. New York: John Wiley & Sons, 1982.

- [30] J. Heiskala and J. Terry, *OFDM Wireless LANs: A Theoretical and Practical Guide*. SAMS Publishing, 2002.
- [31] J. K. Cavers, "An analysis of pilot symbol assisted modulation for Rayleigh fading channels," *IEEE Transactions on Vehicular Technology*, vol. 40, no. 4, pp. 686–693, November 1991.
- [32] Y. Li, "Pilot-symbol-aided channel estimation for OFDM in wireless systems," *IEEE Transactions on Vehicular Technology*, vol. 49, no. 4, pp. 1207–1215, July 2000.
- [33] S. Coleri, M. Ergen, A. Puri, and A. Bahai, "Channel estimation techniques based on pilot arrangement in OFDM systems," *IEEE Transactions on Broadcasting*, vol. 48, no. 3, pp. 223–229, September 2002.
- [34] S. Olonbayar, H. Rohling, T. Giebel, and R. Grünheid, "Decision directed channel estimation in OFDM based systems," in *Proc. of the 8<sup>th</sup> International OFDM-Workshop*, Hamburg, Germany, September 24<sup>th</sup>/25<sup>th</sup> 2003, pp. 162–166.
- [35] J. Akhtman and L. Hanzo, "Sample-spaced and fractionally-spaced CIR estimation aided decision directed channel estimation for OFDM and MC-CDMA," in *Proc. of the IEEE VTC'05 Fall*, vol. 3, Dallas, USA, September 25<sup>th</sup>-28<sup>th</sup> 2005, pp. 1916–1920.
- [36] X. Deng, A. M. Haimovich, and J. Garcia-Frias, "Decision directed iterative channel estimation for MIMO systems," in *Proc. of the ICC'03, IEEE International Conference on Communications*, vol. 4, May 11<sup>th</sup> – 15<sup>th</sup> 2003, pp. 2326–2329.
- [37] A.-L. Johansson and A. Svensson, "Multistage interference cancellation with decision directed channel estimation in multirate DS/CDMA on a mobile radio channel," in *Proc. of the 5<sup>th</sup> IEEE International Conference on Universal Personal Communications*, vol. 1, September 29<sup>th</sup>-October 2<sup>nd</sup> 1996, pp. 331–335.
- [38] J. Gao and H. Liu, "Decision-directed estimation of MIMO time-varying Rayleigh fading channels," *IEEE Transactions on Wireless Communications*, vol. 4, no. 4, pp. 1412–1417, July 2005.
- [39] K. F. Lee and D. B. Williams, "Pilot-symbol-assisted channel estimation for space-time coded OFDM systems," *EURASIP Journal on Applied Signal Processing*, vol. 2002, no. 5, pp. 507–516, March 2002.

- [40] S. M. Alamouti, "A simple transmit diversity technique for wireless communications," *IEEE Journal on Selected Areas in Communications*, vol. 16, no. 8, pp. 1451–1458, October 1998.
- [41] C. Sgraja and J. Lindner, "EM-based decision-directed channel estimation for OFDM: A new interpretation," in *Proc. of the 10<sup>th</sup> International OFDM-Workshop*, Hamburg, Germany, August 31<sup>st</sup>/ September 1<sup>st</sup> 2005, pp. 139–143.
- [42] Y. G. Li and G. L. Stüber, *Orthogonal Frequency Division Multiplexing for Wireless Communications*. New York, NY 10013, USA: Springer, 2006.
- [43] S. Olonbayar, "Multiple access techniques and channel estimation in OFDM communication systems," Ph.D. dissertation, Technische Universität Hamburg-Harburg (TUHH), Department of Telecommunications, May 2006.
- [44] Y. Rong, S. A. Vorobyov, and A. B. Gershman, "On average one bit per subcarrier channel state information feedback in OFDM wireless communication systems," in *Proc. of the Global Telecommunications Conference, IEEE GLOBECOM'04*, vol. 6, Dallas, Texas, USA, November 29<sup>th</sup>/ December 3<sup>rd</sup> 2004, pp. 4011–4015.
- [45] V. Capdevielle *et al.*, "Cellular capacity enhancement thanks to link adaptation in HiperLAN/2," in *Proc. of the IST Mobile Communication Summit*, Barcelona, Spain, September 2001.
- [46] D. Qiao and S. Choi, "Goodput enhancement of IEEE 802.11a wireless LAN via link adaptation," in *IEEE International Conference on Communications*, vol. 7, Helsinki, Finland, June 11<sup>th</sup> – 14<sup>th</sup> 2001, pp. 1995–2000.
- [47] P. S. Chow, C. M. Cioffi, and J. A. C. Bingham, "A practical discrete multitone transceiver loading algorithm for data transmission over spectrally shaped channels," *IEEE Transactions on Communications*, vol. 43, no. 234, pp. 773–775, Feb-Mar-Apr 1995.
- [48] R. F. H. Fischer and J. B. Huber, "A new loading algorithm for discrete multitone transmission," in *IEEE GLOBECOM*, vol. 1, November 18<sup>th</sup>-22<sup>nd</sup> 1996, pp. 724–728.

- [49] H. Rohling and R. Grünheid, "Cross layer considerations for an adaptive ofdm-based wireless communication system," *Wireless Personal Communications*, vol. 32, no. 1, pp. 43–57, January 2005.
- [50] D. Tse and P. Viswanath, *Fundamentals of Wireless Communication*. Cambridge University Press, 2005.
- [51] A. J. Goldsmith, "Design and performance of high-speed communication systems over time-varying radio channels," Ph.D. dissertation, University of California at Berkeley, 1994.
- [52] C. Yin and H. Rohling, "Convergence manager: flexible use of wireless standards," in *Proc. of the 9<sup>th</sup> International OFDM-Workshop*, Dresden, Germany, September 15<sup>th</sup> / 16<sup>th</sup> 2004, pp. 37–41.
- [53] B. Rodríguez and H. Rohling, "Optimum use of throughput capabilities in a multi-standard transmission," in *Proc. of the 10<sup>th</sup> International OFDM-Workshop*, Hamburg, Germany, August 31<sup>st</sup> / September 1<sup>st</sup> 2005, pp. 396–400.
- [54] G. Bauch, "Design of cyclic delay diversity with adaptive coding based on mutual information," in *Proc. of the 10<sup>th</sup> International OFDM-Workshop*, Hamburg, Germany, August 31<sup>st</sup> / September 1<sup>st</sup> 2005, pp. 184–188.
- [55] L. Correia, *Mobile Broadband Multimedia Networks*. Elsevier Ltd., 2006.
- [56] G. J. Foschini and M. J. Gans, "On limits of wireless communications in a fading environment when using multiple antennas," *Wireless Personal Communications*, vol. 6, pp. 311–335, March 1998.
- [57] G. J. Foschini, "Layered space-time architecture for wireless communication in a fading environment when using multielement antennas," *Bell Labs Technical Journal*, pp. 41–59, Autumn 1996.
- [58] E. Telatar, "Capacity of multi-antenna Gaussian channels," *AT&T Bell Laboratories, Tech. Memo.*, June 1995.
- [59] G. G. Raleigh and J. M. Cioffi, "Spatio-temporal coding for wireless communication," *IEEE Transactions on Communications*, vol. 46, no. 3, pp. 357–366, March 1998.

- [60] D. Gesbert, M. Shafi, D. Shiu, P. J. Smith, and A. Naguib, "From theory to practice: An overview of MIMO space-time coded wireless systems," *IEEE Journal on Selected Areas in Communications*, vol. 21, no. 3, pp. 281–302, April 2003.
- [61] C. E. Shannon, "A mathematical theory of communication," *Bell System Technical Journal*, pp. 379–423, 623–656, 1948.
- [62] —, "Communications in the presence of noise," in *Proc. of the IRE*, 1949, pp. 10–21.
- [63] C. E. Shannon and W. Weaver, *The Mathematical Theory of Communication*. Urbana, IL: Univ. Illinois Press, 1949.
- [64] S. Haykin, *Digital Communications*. John Wiley & Sons, 1998.
- [65] V. Tarokh, H. Jafarkhani, and A. Calderbank, "Space-time block codes from orthogonal designs," *IEEE Transactions on Information Theory*, vol. 45, pp. 1456–1467, June 1999.
- [66] B. Hochwald and W. Swelden, "Differential unitary space-time modulation," *IEEE Transactions on Communications*, vol. 48, pp. 2041–2052, December 2000.
- [67] B. L. Huges, "Differential space-time modulation," *IEEE Transactions on Information Theory*, vol. 46, pp. 2567–2578, November 2000.
- [68] V. Tarokh and H. Jafarkhani, "A differential detection scheme for transmit diversity," *IEEE Journal on Selected Areas in Communications*, vol. 18, pp. 1169–1174, July 2000.
- [69] X.-G. Xia, "Differentially encoded orthogonal space-time block codes with APSK signals," *IEEE Communications Letters*, vol. 6, pp. 150–152, April 2002.
- [70] G. Bauch, "A bandwidth-efficient scheme for non-coherent transmit diversity," in *IEEE Globecom*, December 2003.
- [71] —, "Differential amplitude and unitary space-time modulation," in *Proc. of the 5<sup>th</sup> International ITG Conference on Source and Channel Coding*, Erlangen, Germany, January 14<sup>th</sup>/16<sup>th</sup> 2004.
- [72] H. Rohling and V. Engels, "Differential amplitude phase shift keying (DAPSK) - a new modulation method for DTVB," in *International Broadcasting Convention*, Hamburg, Germany, 1995, pp. 102–108.

- [73] B. Rodríguez and H. Rohling, “A new class of differential space time block codes,” in *Proc. of the 11<sup>th</sup> International OFDM-Workshop*, Hamburg, Germany, August 30<sup>th</sup> / 31<sup>st</sup> 2006, pp. 106–110.
- [74] A. Vanaev and H. Rohling, “Design of amplitude and phase modulated signals for differential space-time block codes,” *Wireless Personal Communications*, vol. 39, no. 4, pp. 401–413, December 2006.
- [75] —, “Design of differential space-time block codes for high bandwidth efficiency,” in *Proc. of the 10<sup>th</sup> International OFDM-Workshop*, Hamburg, Germany, August 31<sup>st</sup> / September 1<sup>st</sup> 2005, pp. 119–123.
- [76] B. Rodríguez and H. Rohling, “Receive diversity in DSTBC using APSK modulation schemes,” in *Proc. of the 12<sup>nd</sup> International OFDM-Workshop*, Hamburg, Germany, August 29<sup>th</sup> / 30<sup>th</sup> 2007, pp. 90–94.
- [77] G. Bauch, “Space-time block codes versus space-frequency block codes,” in *IEEE Vehicular Technology Conference*, vol. 1, April 22<sup>nd</sup> – 25<sup>th</sup> 2003, pp. 567–571.

# Index

- absorption, 11
- APSK, 75, 80
- AWGN, 10
  
- Bandwidth Efficiency, 1, 54
- Bit loading, 58
- Bit puncturing, 121
  
- Channel, 7
  - flat frequency, 16
  - frequency selective fading, 18
  - mobile radio, 13
  - multipath fading, 14
  - Rayleigh fading, 17
  - Ricean fading, 17
  - stochastic models, 20
  - time invariant, 18
- Channel Coding, 37, 117
- Channel Decoding, 37
- Channel Frequency Response, 41
- Channel Impulse Response, 41
- Channel State Information, 51, 53
- Code Division Multiplex Access, 60
- coherence bandwidth, 21, 23
- coherence time, 21, 23
- COST 207, 137
- CP, 37
- cumulative distribution function, 134
- Cumulative Hamming Path Metric, 121
- Cyclic Prefix, 27
  
- DAPSK, 76
- Data Link Control, 55
- decoding delay, 140
  
- delay-power spectral density, 22
- diffraction, 8, 11
- Direct Sequence Spread Spectrum, 59
- Diversities, 59
- Diversity
  - Delay, 59
  - Equal Gain Combining, 61
  - Frequency, 59
  - Maximum Ratio Combining, 61
  - Multiuser, 63
  - Polarization, 63
  - Receive, 60
  - Spatial, 60
  - Time, 62
  - Transmit, 60
- Doppler-power spectral density, 22
- DSFBC, 126
- DSTBC, 2, 65, 75
- DSTFBC, 126
- Dynamic Fragmentation, 54
  
- Equal Gain Combining, 112
  
- Free Space Loss, 11
- frequency correlation function, 23
- Frequency Hopping Spread Spectrum, 59
  
- Gauss Doppler Profile, 135
- IDFT, 37
- Inter Symbol Interference, 28
- Interleaving, 37
  
- Jakes Doppler Profile, 135

- large scale, 9
- large scale path loss, 11
- Line Of Sight, 16
- Linear Time Variant systems, 18
- Link Adaptation, 53
- log-normal distribution, 13
  
- Maximum Ratio Combining, 61, 112
- MIMO, 65, 66, 72
- MISO, 76
- Modulator, 37
- Multipath fading, 14
- Multiple Receive Antennas, 60
- Multiple Transmit Antennas, 62
  
- No Line Of Sight, 16
  
- PACE, 45
- Path Loss, 11
- path loss exponent, 12
- PHY mode selection, 54
- PHY modes, 54
- Power Control Mechanism, 81
- probability density function, 17, 25, 134
- propagation mechanisms, 8
  
- Rayleigh fading, 17
- Receive Diversity, 112
- Rectangular Doppler Profile, 135
- reflection, 8, 11
- Ricean factor, 17
- Ricean fading, 17
  
- scattering, 8, 11
- Scattering function, 22
- Scrambling, 36
- Selection Combining, 61
- Self Organizing Radio Resources Management, 53
- SFBC, 47
- Shadowing, 11
  
- SHF, 3
- SISO, 51, 76
- small scale, 10
- spaced time spaced frequency correlation function, 23
- STBC, 47, 75
  
- time correlation function, 23
- transfer function, 23
- transmission, 8, 11
  
- UHF, 3
  
- Water-Filling, 55
- Water-Pouring, 55
- Wi-Fi, 36
- WiMAX, 38
- WLAN, 36
- WLL, 18
- WMAN, 38

# Curriculum Vitae

Name: Benigno Rodríguez Díaz  
Date of birth: 14<sup>th</sup> September 1971  
Place of birth: Montevideo, Uruguay

## Pre-university Education

1978-1983 Primary School, Palloti School, Montevideo  
1984-1987 Secondary School, Palloti High School, Montevideo  
1988-1989 Pre-university Studies, IUDEP High School, Montevideo

## University Education

1990-1997 BSc in Electrical Engineering (6 years plan, profile: Telecommunications-Microelectronics) from the Faculty of Engineering, University of the Republic of Uruguay (UdelaR)  
1996 Microelectronics studies in Alcalá de Henares University, Madrid, Spain (“Intercampus Scholarship”)

## Postgraduate Education

2000 Course of “Design and Simulation of Microwave Monolithic Integrated Circuits (MMIC’s)” at the “The Andes’s University”, Bogotá, Colombia  
2002-2004 MSc in Electrical Engineering (area: Wireless Systems), Faculty of Engineering, UdelaR  
2005-2007 PhD in Telecommunications, Technische Universität Hamburg-Harburg (TUHH), Hamburg, Germany (“Alban Scholarship”)

## Employments

1993-1999 Research Assistant at the Physic Institute, Faculty of Engineering, UdelaR  
1997 Engineer at Carisul S.A. (NEC of Uruguay)  
1997-2004 Chief of the Engineering Department at Carisul S.A.  
Since 1998 Research Assistant at the Electrical Engineering Institute, Faculty of Engineering, UdelaR





